IDENTIFYING COASTAL PROTECTION MEASURES AT GO-CONG (TIEN GIANG PROVINCE) AND PHU-TAN (CA MAU PROVINCE)

Contents

LIST OF TABLES

LIST OF FIGURES

1. Introduction

The coastal area of the Lower Mekong Delta (LMD) is influenced by waves, tidal currents, changing sediment loads from the Mekong, and Sai Gon-Dong Nai rivers, and storm surges from the East and West Sea. In addition, human activity has an impact on erosion and deposition processes through dyke construction and drainage, agriculture, aquaculture, and fishery exploitation along the coastal areas. In recent years, the impact of upstream dams, especially on the Mekong main river, has reduced sediment feeding into the LMD and its estuary. All of these impacts have caused shore erosion along approximately two thirds of the total coastline length, and an average land loss rate of about 80 ha/year from 1990 to 2015 and 324.5 ha/year for the past ten years [4]. In the future, climate change and sea level rise will make this situation worse.

In this WP6 report, we discuss Field Studies, Lab Experiments and Numerical Modelling in separate sections.

The objectives of WP6 are:

- To select shore protection measures for the coastal zones of Go-Cong and Phu Tan.
- To check the efficiency of the selected shore protection measures for the coastal zones of Go-Cong and Phu Tan.
- To check the impact of the selected shore protection measures to the neighbouring coastal zones of Go-Cong and Phu Tan.

2. Field studies

2.1 Two in-situ survey campaigns of LMDCZ project

There were two in-situ survey campaigns of LMDCZ project for the purposes of calibration and validation of numerical models (Telemac, MIKE, Delft 3D, CROCO etc).

The project has had 2 in-situ survey campaigns. The first campaign was in October 2016 when the sediment plume extension of the Mekong estuaries is farthest offshore in the East sea. That is also the southwest monsoon season when coastal areas of the West sea are severely impacted by erosion. The second campaign was in February 2017 – at the peak of the northeast monsoon which causes severe coastal erosion in the East sea.

The survey included the following river and coastal stations:

- 2 fixed river stations in Mekong (at My Thuan) and Bassac (at Can Tho) rivers (coinciding with National Hydrology Stations) for measuring discharges (Q) and suspended sediment concentration (SSC) by ADCP.
- 2 fixed coastal stations at Go Cong and U-Minh (location was about 15 km offshore each station);
- Marine sampling stations from 2 mobile ships cruising along the East and West seas.

Measured fields at the coastal stations were:

+ Water level (hourly at the 2 fixed stations)

+ Vertical distribution of velocity

+ Vertical distribution of salinity (5 points for each vertical line)

+ Vertical distribution of sediments (5 points for each vertical line)

+ Waves (height, period and direction)

In addition, bathymetry was measured at the two study sites during each campaign: the alongshore extent at Go-Cong was 21 km and at U-Minh 25 km; the cross-shore extent was about 8 km at both sites with a sampling resolution of 1.25 km (in average). The purpose of the bathymetry survey is to validate the morphological models.

2.2 Existing shore protection measures in the LMDCZ

2.2.1 Shore protection measures in the LMDCZ

Over the years, some types of shore protection works have been built along the LMD coastline (Table 2-1). These are i) shore/dike protective embankment/revetment with concrete walls, concrete blocks, ripraps or gabions and ii) breakwaters with concrete piles, riprap, geotextile bags/geotube (Table 2-1) and recently "soft" breakwaters with local material fences (bamboo/ melaleuca piles) and filled with tree bunches in Soc Trang, Bac Lieu and Kien Giang, in the framework of GIZ projects (Figure 2-2). This "soft" type of structure is designed for wave and current attenuation so as to stimulate deposition and restore the mangrove forest.

In general, the total investments in shore protection works to prevent erosion in the LMD have been quite low, about VNĐ 1,513.4 billion, equivalent to USD 66.3 millions to date (Table 2-1).

Table 2-1 Types of coastal protection works in the LMD [4]

Province	Shore protection works' name	Length (m)	Type	Unit price (10^3 €)	Cost (M€)
Tien Giang	Go Cong GC1: Revetment	3000	Concrete block	1.85	5.56
	Go Cong -GC2: Revetment	500	Concrete block	1.85	0.93
	Go Cong -GC3: Revetment	1500	Concrete block	1.85	2.78
Tra Vinh	Hiep Thanh –HT: Revetment	1325	Concrete block	3.33	4.41
	Con Trung –CT: Revetment	750	Concrete block	2.59	1.96
Soc Trang	Vinh Chau -VC1: Revetment	380	Gabion	0.74	0.30
	Vinh Chau -VC2: Revetment	100	Gabion	0.74	0.07
	Vinh Chau -VC3 : Revetment	100	Gabion	0.74	0.07
	Mangrove rehabilitation GIZ	600	Bamboo fence	0.04	0.02
Bac Lieu	Nha Mat -NM1: Revetment	617	Concrete block	3.33	2.07
	Nha Mat -NM2: Revetment	522	Concrete block	3.33	1.74
	Geotube Breakwater at Nha Mat	1056	Geotube	0.19	0.19
	Mangrove rehabilitation -GIZ	2400	Bamboo fence	0.04	0.11
	Ganh Hao –GH: Revetment	3432	Concrete block	3.33	11.44
Ca Mau	Break water -GH	509	Concrete pile	1.48	0.74
	Break water - DM	2571	Concrete pile	1.48	3.81
	Khanh Hoi –KH: Revetment	1186	Plastic sheet, gabion	0.56	0.67
	Bien Tay –BT: Revetment	500	Concrete block	1.48	0.74
	Break water -BT	300	Concrete pile	1.48	0.44
	Break water Huong Mai-HM	6990	Concrete pile	1.48	10.37
Kien Giang	Mangrove rehabilitation KG-HĐ1	3500	Melaleuca fence	0.04	0.15
	Mangrove rehabilitation KG-HĐ2	300	Melaleuca fence	0.04	0.01
	Mangrove rehabilitation KG-HT	100	Melaleuca fence	0.04	0.00
	Vam Ray (K) Revetment	300	Concrete block	1.48	0.44
Total					**56.1**

Figure 2-1 Breakwater by riprap (at Can Gio), geotube (at Bac Lieu), and concrete piles (at Ca Mau)[4]

Figure 2-2 Foreshore erosion at Go Cong Revetment (left) and wave and current attenuation by T fences at Soc Trang and Bac Lieu provinces by GIZ projects [4]

2.2.2 Tentative solutions for structural measures in the LMDCZ

Shore protection measures from around the world have been modified and applied in the LMDDCZ.

To date, the dyke revetments have been built mostly in the serious shore erosion areas without mangrove forest belt and considered to be successful in the short term due to it can't stop erosion at foreshore such as in Go Cong district (Figure 2-2, left).

Breakwaters were rarely used in LMDDCZ (Table 2-1). Three types were applied using local bamboo/melaleuca fences, concrete pile wall and geotube. Field investigation showed that the local material fences were successful in trapping fine sediment for mangrove rehabilitation in one place (at Soc Trang) but the other (at Bac Lieu) and therefore needed to define the applicable conditions such as foreshore conditions (elevation, soil properties, sediment, current and wave height limits). Moreover, such local materials are rapidly degraded due to site environment associated with wave attack. The geotube breakwater has failed due to poor design (in Bac Lieu) and its life expectancy is doubtful. One type of geotube was the "stabiplage" of French company (Espace Pur) which was applied in Loc An – Vung Tau City, was assumed to be durable for 30 years but in fact it was destroyed after about 10 years [2,3]. In 2015 the geotube breakwater was piloted in Go Cong. Report from local government showed that accretion inside geotube could get 0.7 m thickness. However, the detail data (such as position, monitoring time…) was not accessible. Moreover, as discussing above, its longevity is the concern. The concrete pile breakwater could trap sediment but it was "too hard" for environment and costly.

Therefore, the tentative structural measures for shore protection in the LMDCZ should be a combination of sound revetments, local material fences in the middle and breakwaters for wave and current attenuation. Thanks to "hard" breakwater, local material fences can be survived longer to trap fine sediment for mangrove rehabilitation. The scale of these structures obviously are depended on the site-specific conditions of wave, current, sediment, ecologic etc.

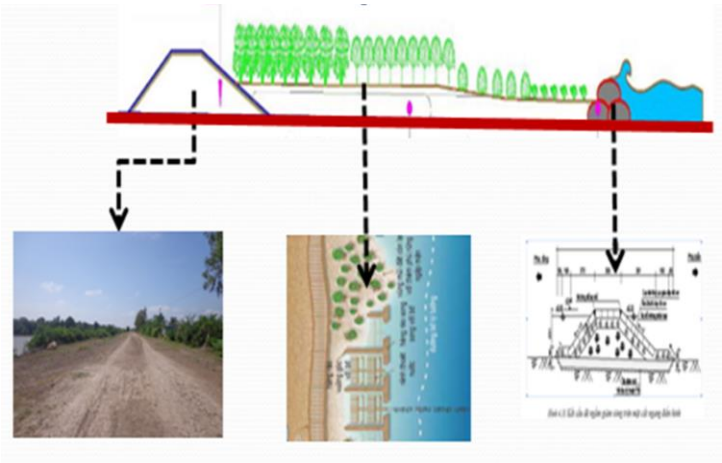

Figure 2-3 Oriented shore protection structure measures in the LMDCZ [4]

2.3 Effects of pile breakwaters in Ca Mau

2.3.1 Motivation

The concrete pile breakwaters (CB) applied in West sea of Ca Mau Province were considered “too hard” for environment and costly. Satellite image analysis showed that after this structure installation, the accretion process developed quite well but the mangrove trees could not naturally exist. Figure 2-4 presented a typical location where the CB was installed in 2014 and to 2017; nearly nothing changes for the mangrove forest belt in the concerned area (see Report [7] for more detail). Therefore we want to examine the impacts of CB to the surrounding areas. The SIWRR team investigated the west sea coast of Ca Mau in July (the middle of the SW monsoon season) at the CB areas to examine:

- The existing situation of the CB structure
- The exchange of suspended sediment concentration (SSC) through CB.
- The SSC along the cross section with and without CB.

Figure 2-4 Typical location where the CB was installed at Khanh Tien Commune, U Minh district, Ca Mau Province (Location 4), and pictures in 2014 and 2017 indicated poor natural mangrove tree development

2.3.2 Results and discussion

2.3.2.1 Field survey in July 2017

The first type of CB in Ca Mau was designed with two rows of concrete piles with inside-installed riprap fulfilling the gap between the piles (Figure 2-5). This type of CB had successfully trapped sediment. This can be recognized from the ground elevations both outside (seaward) and inside (landward) that are kept high nearly to the CB’s crest. Therefore there was no deeper place to install turbidity sensors to measure SSC outside and inside the first type of CB.

The Government of Ca Mau had realized the weakness of the first type of CB; thus has installed the better one, which is “more porous” than the first type. Figure 2-6 showed some pictures of second type of CB. To examine the SSC in and out the second type of CB, four turbidity sensors were installed as expressed in Figure 2-7. The sensor pair 1 (inside and outside) and pair 2 were perpendicular to the CB. The distance of the two sensor pairs were 4.5m. The turbidity meters were calibrated by sampling SSC at the measured site. The results of the calibration were provided in Figure 2-8.

July 13, 2017 was in the middle of SW monsoon, the SSC at the two sites be seen in Figure 2-9. At site 2 (down figure), the SSC outside CB could reach 1,100 to 2,300 mg/l, while the ones inside the CB, the SSC were lower, from 750 to 1200 mg/l. At site 1 (top figure), the SSC outside CB could reach 1,300 to 2,850 mg/l while the one inside the CB were sometimes lower or higher than the one outside. It could be explained by the field observation that there was a constriction flow that caused the erosion at the bottom and created high SSC. In general, the SSC value inside the CB was lower than the outside. The very high

value of SSC can be explained by the re-suspension process where high wave attached the muddy bottom.

Observation

The different of SSC outside and inside the CB may reflect the exchange of SSC through the type 2 of CB. This exchange was improved in comparison with the first type of CB due to its higher porosity.

Comparing to the SSC values of the two survey campaign of the LMDCZ project as well as from the satellite image analysis (<200 mg/l), the SSC near the CB was much higher (from 800-2,800 mg/l).

At the areas with no protection measures (CB), the survey team observed very high SSC in the wide area, about a thousand m from the shoreline offshore. Therefore it is necessary to examine the cross-shore distribution of SSC in the SW monsoon in Ca Mau to know the SSC distribution from the shoreline to approx. 2-3 km offshore for the numerical simulation purpose. The fact is that for the two field survey campaign of LMDCZ project the SSC samples were only taken from about 5 km offshore since the survey ship could not reach to the near-shore area and therefore SSC values were low (in general less than 200 mg/l). That is the reason for additional field survey in September 2017 (below).

Figure 2-5 Some pictures of the existing situation of the first type of CBs at Ca Mau in July, 2017.

Figure 2-6 Pictures of the existing situation of the type 2 of CBs at Ca Mau in July 2017

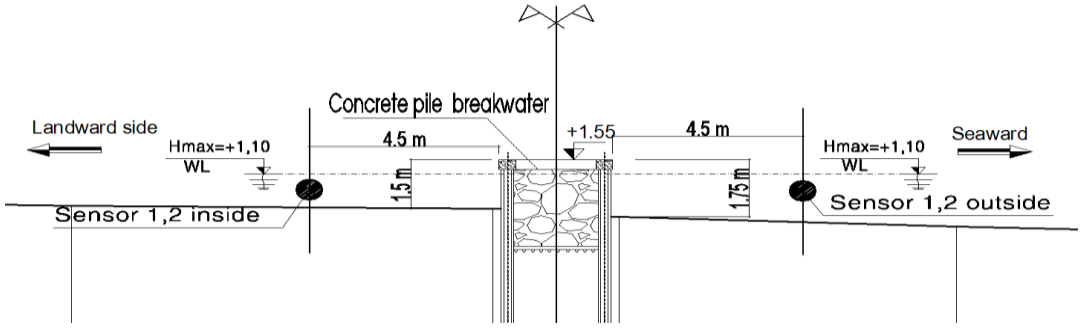

Figure 2-7 Scheme to examine the SSC exchange through CB by 4 turbidity sensors

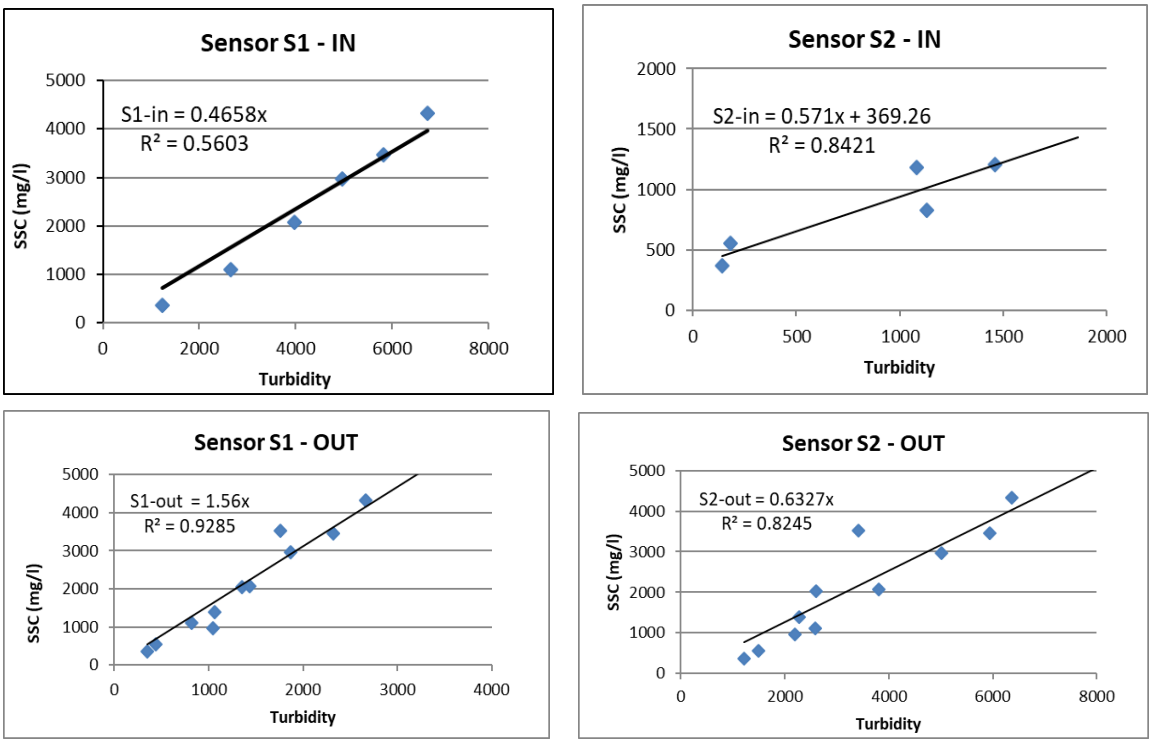

Figure 2-8 Calibration results of 4 turbidity sensors in July 2017

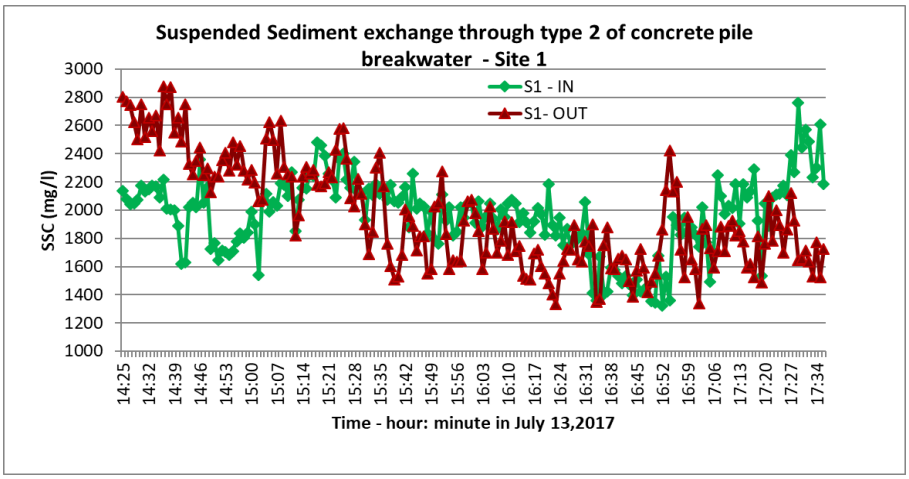

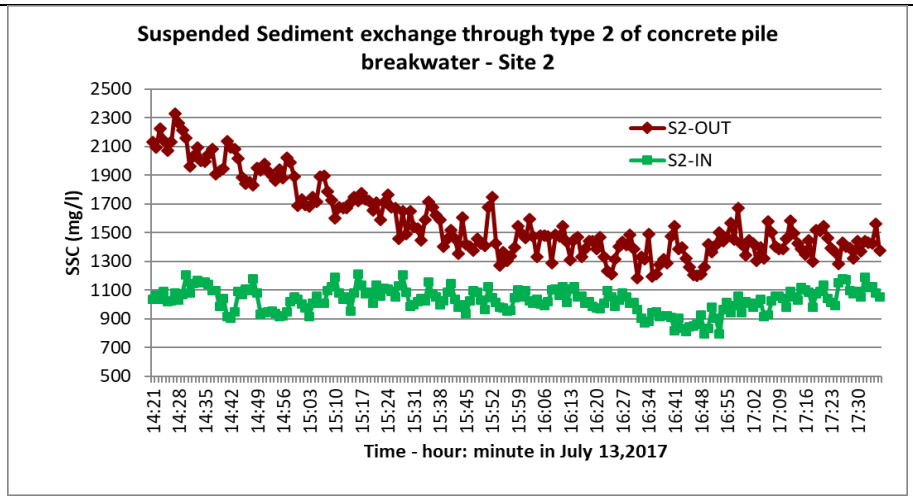

Figure 2-9 Exchange of SSC through CB type 2 in July 13, 2017

2.3.2.2 Field survey in September 2017

The field campaign took SSC samples at 3 cross-sections MC-1, MC-2 and MC-3 where MC-1 at the place of the new type of CB, MC-2 and MC-3 sections are 1600 m and 11600 m far from the end of the CB respectively, as indicated in Figure 7. The CB at the site is one of the "more porous" CB structures in Ca Mau. Figure 2-11 showed pictures of this type of CB.

The cross-shore distribution of SSC at three cross-sections on September 13th 2017 were presented in Table 2-2 to Table 2-4.

Figure 2-12 presented the SSC value versus water elevation and time. It can be recognized that the at high tide, SSCs are lower than the ones at low/ falling tide. Figure 2-13 showed the cross-shore distribution of SSCs with quite high values (300÷800 mg/l) from the shoreline to about 1600 m offshore at low/falling tide.

At the same time of sampling SSCs, four turbidity sensors were also installed (Figure 2-14) to measure the SSC out and inside the "third type" of CB structures in Ca Mau (Figure 2-11). Locations of turbidity sensors were similar to the survey on July 2017 except for the distances from the sensors to the CB were increased by 7m (the survey in July 2017, this distances were 4.5 m).

Figure 2-15 expressed the results of turbidity sensor calibrations and Figure 2-16 expressed the SSC outside and inside the CB. The results of SSC were quite similar to the the results in July 2017. That seems the exchange of SSC through CB was high due to it "porosity".

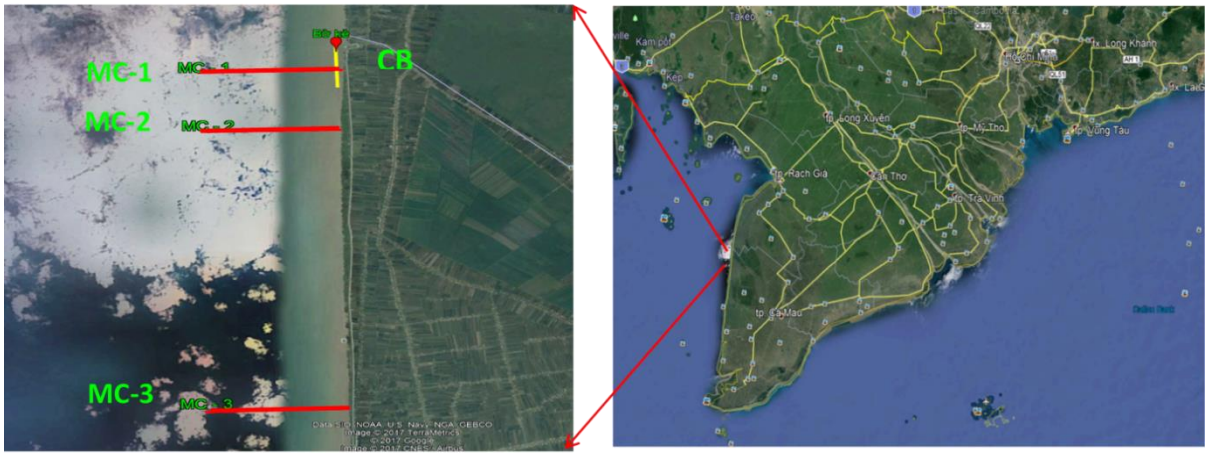

Figure 2-10 SSC measurement locations at Khanh Tien Commun – U Minh District – Ca Mau Province (9.4°N, 104.83°E) on September 13th 2017.

Figure 2-11 CB structure of Ca Mau at the survey site on September 13th 2017

Table 2-2 Cross-shore distribution of SSC at MC-1 on September 13th 2017

Cross-section	Time	Cross-shore distance (m)												
		0	50	100		200	450	700	1000	1300	1600	1900	2100	2500
MC - 1	11h - 12h : 13/9/2017	SSC (mg/l)	324	269	CB	251	164	75	12	11	6	10	4	5
MC - 1	17h - 18h : 13/9/2017					541	578	515	432	365	242	195		84

Table 2-3 Cross-shore distribution of SSCat MC-2 on September 13th 2017

Cross-section	Time	Cross-shore distance (m)												
		0	50	200	450	700	1000	1300	1600	1900	2100	2400	2600	2700
MC - 2	12h - 13h : 13/9/2017	SSC (mg/l)	113	94	117	88	77	45	34	17	13	8	8	5

Table 2-4 Cross-shore distribution of SSC at MC-3 on September 13th 2017

Cross-section	Time	Cross-shore distance (m)												
		0	70	200	450	700	1000	1300	1600	1900	2100	2400	2500	2700
MC - 3	15h - 16h : 13/9/2017	SSC (mg/l)	300	580	706	585	812	688	286	202	33	57	48	15

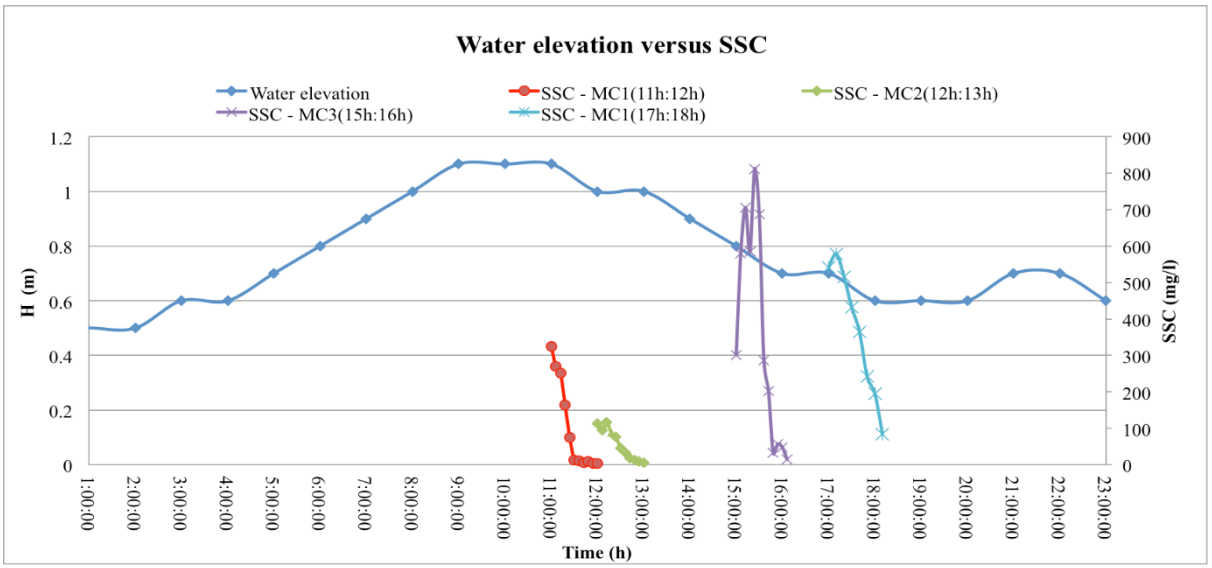

Figure 2-12 SSC at three cross-sections MC-1, MC-2 & MC-3 versus water elevation on September 13th 2017

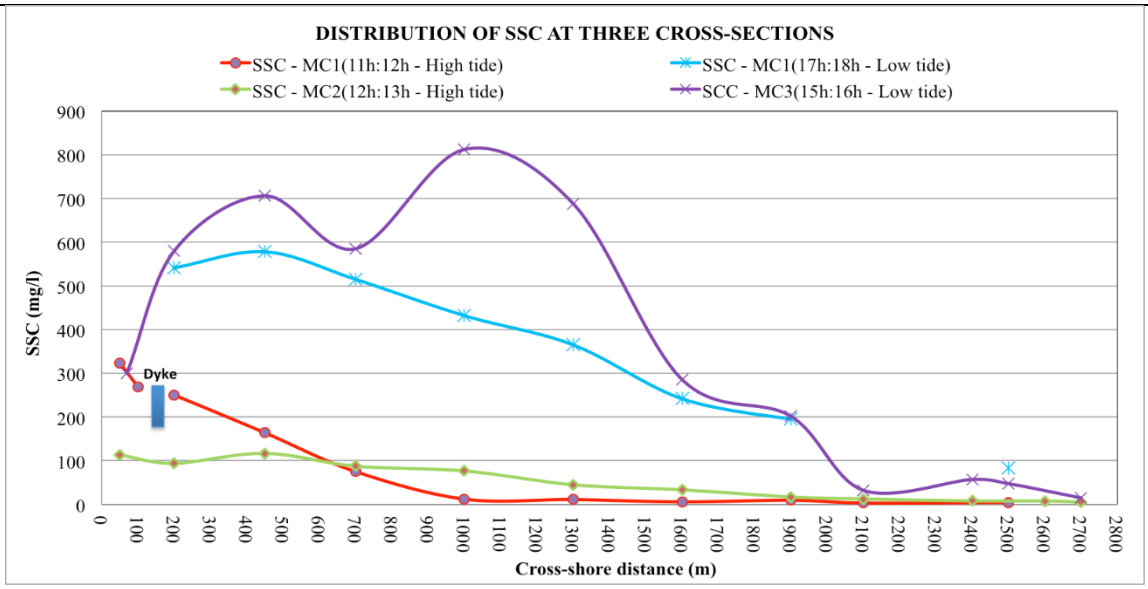

Figure 2-13 Cross-shore distribution of SSC in 11:00 to 18:00 on September 13th 2017

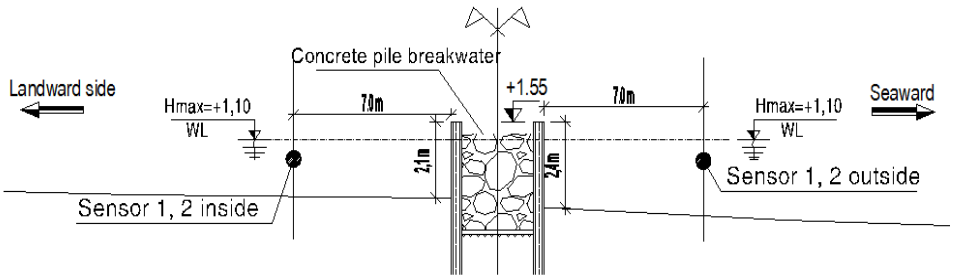

Figure 2-14 Scheme to examine the SSC exchange through CB by 4 turbidity sensors on September 13th 2017

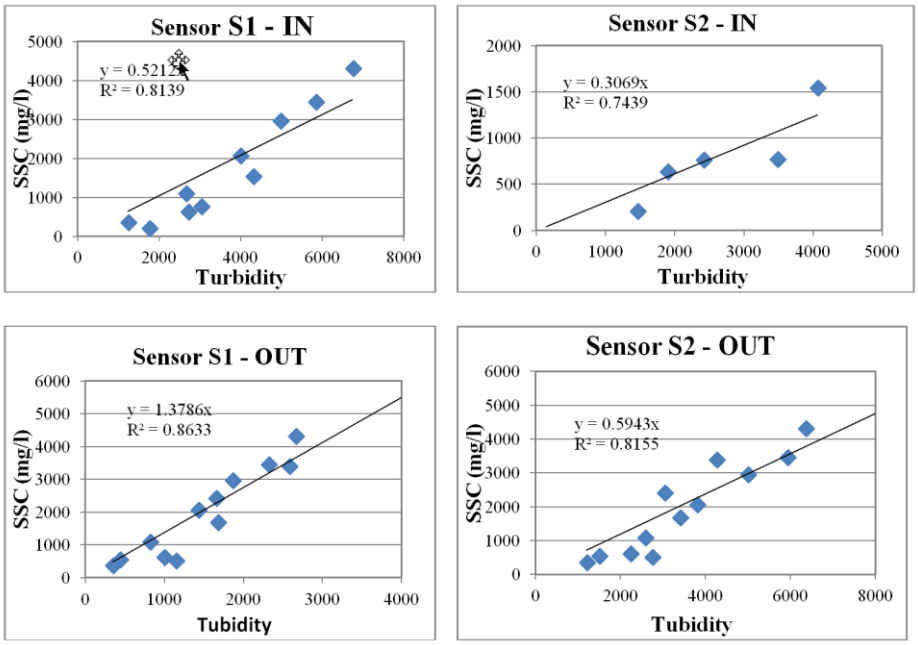

Figure 2-15 Calibration of turbidity sensors for the field survey on September 13th 2017

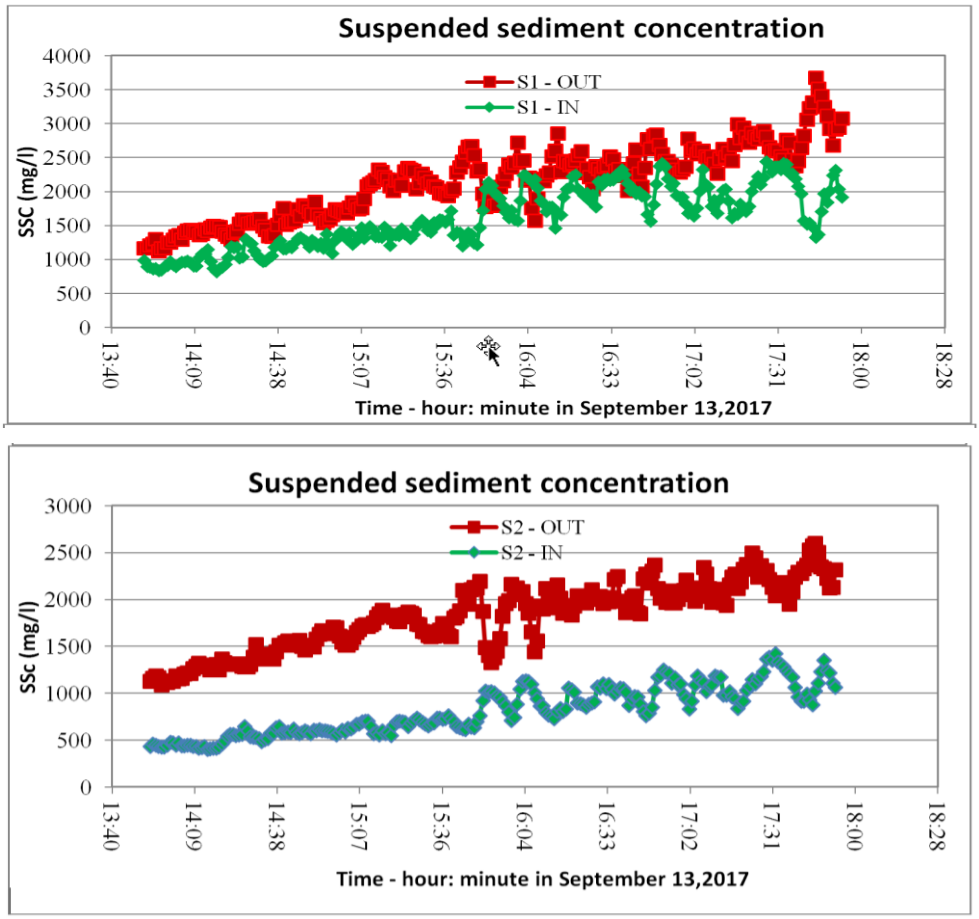

Figure 2-16 SSC outside and inside of the third type of CB on September 13th 2017

2.3.3 Conclusion and recommendation

The natural development of mangrove trees after installing the CB in the west coast of Ca Mau province was poor with the first structure type. The second and the third types of CBs were improved their porosity. The possible exchange of SSC through the two later types of CBs was improved with higher porosity and more natural development of mangrove trees is expected.

The sediment trapping efficiency of first type of CB in the west coast of Ca Mau province is very high.

The SSC values just inside and outside the CBs (about 7m) were quite high. They can reach to few thousand mg/l at low/falling tide and low water depth. The high SSC outside can be explained by re-suspension process.

The SSC in the SW monsoon at Ca Mau from the shoreline to about 1,600 m offshore were very high (300 ÷800 mg/l) in the wave breaker zone comparing to the ones from two survey campaigns of LMDCZ project and other satellite images (<200 mg/l) due to samples of the later were taken at the positions of more than 4,000 m offshore.

Additional study on the conditions for natural mangrove development for the area is necessary.

3. Physical model studies in the lab [8]

3.1 Introduction

3.1.1 Hard measure - porous breakwater

A proposed hard protective measure is considered appropriate only if it enhances local sediment balances and thus accommodates mangrove rehabilitation efforts. The applied structure should function like mangrove plants as much as possible, i.e. tide and sediment exchange, wave absorption, and efficient sediment entrapment. Besides, it should be structurally stable against design wave attack and able to withstand on a soft mud foundation of the LMD.

1. Detached (shore-parallel) breakwaters of porous elements are considered an applicable protective measure against beach erosion. This is a type of porous (hollows take up about 20% surface area) and narrow-crested structure. The idea is that the structure is sufficiently permeable so tide with fine sediment can go through and is high enough to dissipate wave energy, consequently promoting onshore sedimentation. A pilot construction has been executed at Long Hai beach. Though this was done without appropriate understanding of the structure functionality the structure has shown its high efficiency in damping waves and promoting sedimentation. However, to achieve the ultimate goal of coastal protection aspects of functional design of the structure must be realized at the first design stage. In essence, wave damping capacity, wave reflection and sediment entrapping efficiency are necessary for this design purpose. In this study the main focus is on wave transmission and reflection at this type of porous breakwater. In a 2D situation (wave flume) sediment in suspension is proportional to the wave height and wave damping capacity also reflects sediment trapping efficiency of the structure, tests on sediment trapping are therefore disregarded herein. Tests with muddy water or dye shall be carried out latter to demonstrate if the sediment exchange (or transport of sediment) through the breakwater is possible. In the literature there exist numerous studies on wave transmission at conventional types of structures such as rubble-mound breakwaters, smooth and impermeable breakwaters, etc. (see e.g. van der Meer et al., 2005 [

Van der Meer, J. W., Briganti, R., Zanuttigh, B. and Wang, B., 2005. Wave transmission and reflection at low-crested structures: Design formulae, oblique wave attack and spectral change. Coastal Engineering, 52, 915 - 929.]). However, these mostly concern with structures in relatively deep water, probably inapplicable for those with porous bodies and on very shallow foreshores considered herein. Due to drastic spectral transformation by depth-induced wave breaking, the incoming wave may interact differently with the structure, resulting in a noticeably different wave transmission (see Tuan et al., 2016 [Tuan, T.Q., Tien, N.V. and Verhagen, H.J., 2016. Wave transmission over submerged, smooth and impermeable breakwaters on a gentle and shallow foreshore. In: Proc. 9th PIANC-COPEDEC, pp. 897-905, Rio de Janeiro, BRAZIL.]). For the purpose of functional design, it is therefore required at first a quantitative understanding of wave transmission in this special circumstance. Measured laboratory data are used to derive a new empirical formulation of wave transmission at the porous breakwater on a mangrove foreshore. The result shall also be compared with some existing formulations of conventional structures.

3.1.2 Soft measures – Large-scale nourishment by near-shore sandbanks

Besides hard alternatives, soft measures following the strategy of “building with nature”, which makes use of natural processes to provide protection services for the coast and/or to support mangrove rehabilitation efforts, must be given a priority wherever possible. In this context, bamboo fences and large-scale nourishment by near-shore sandbanks are considered applicable for a mangrove mud coast. Within the scope of this laboratory study, only the latter is considered. The idea behind the large-scale nourishment is to have a wide and segmented system of sandbanks at a distance from the shore, mimicking natural submerged sandbars. A system of sandbanks is designed in such a way that it would significantly reduce the wave energy and still allow mud to be exchanged between near-shore shelf and mangroves and to be transported alongshore. Sandbanks gradually deform due to alongshore and cross-shore transport processes but simultaneously feed the coast and thus would have to be replenished at certain intervals. Because the wide-crested sandbank is like a submerged reef and the aforementioned special wave characteristics on the shallow mangrove foreshore, the wave hydrodynamics across sandbanks is rather unique. For the functional design of the nourishment, it is of interest to investigate the effect of sandbank on the near-shore wave hydrodynamics, i.e. wave transmission and spectral transformation. Moreover, the extent of sandbank profile response induced by cross-shore processes under various wave and water level conditions hints at the nourishment efficiency.

3.2 Aims and scope

In summary, scale model experiments carried out at River and Marine Hydrodynamic Laboratory of SIWRR have the following aims:

• To increase understanding of cross-shore physical processes involved, needed for the functional design purposes - Detached porous breakwater: wave transmission, reflection, transfer suspended sediment. Nourishment by sandbanks: wave transmission, spectral transformation and profile response

• To generate data for numerical validations. Note that all experiments were carried out in a wave flume, which address acrossshore processes only. Also, aspects of structural design during extreme events: wave loading, stability, etc. are beyond the scope of this study report. This report is organized as follows. The model setup and test program and experimental results for each of the tested protective measures, viz. wave transmission at porous breakwaters and the large-scale nourishment, are discussed in Section 3.3 and Section 3.3, respectively.

3.3 Wave transmission and sediment exchange at porous breakwaters

3.3.1 Wave transmission

3.3.1.1 Model setup and test program

The experiments were carried out in the wave flume at River and Marine Hydrodynamic laboratory of SIWRR (Binh Duong province, Vietnam). The facilities were constructed with all the equipment installed by HR Wallingford in 2014. The flume is 35 m long (effective), 1.2 m wide and 1.5 m high, equipped with an automated system of Active Reflection Compensation (ARC) and capable of generating both regular and irregular waves up to 0.3 m in height and 3.0 s in peak period. Reliable resistance-type wave gauges are available for measuring wave signals at sampling frequency up to 100 Hz (accuracy – 0.1 mm). Figure 3-1 illustrates the model setup for experiments. The model breakwater, 0.4m high, is founded on a mangrove foreshore with slope of 1/500. A transitional segment with slope of 1/25 is introduced between the gentle foreshore and the deep water section so that waves are well generated at the offshore boundary. Moreover, incoming waves are forced to break around the slope transition, creating wave breaking condition on the foreshore similar to that in the field. To effectively absorb the remaining wave energy, a gentle rock slope (slope 1/4) as a passive wave absorber is placed at the other end of the flume. Calibration tests without the structure show that the reflection coefficient was always less than 10%. Wave parameters in font and behind the breakwater were measured with eight capacitance wave gauges. Incident and reflected waves were separated according to the approach by Zelt and Skjelbreia (1992) using the first three-gauge array at the inflow boundary. A Hanning window was used for visualization of calculated wave spectra. A cut-off frequency of 0.025 Hz was also applied to exclude the energy part of the resonance frequency of the flume. The analysis of wave transmission involves parameters derived from the following parameters data.

Having known the wave heights in front of and behind the structure the wave transmission coefficient can be determined accordingly:

$$K_t = \frac{H_{m0,t}}{H_{m0,i}}$$

where Kt is transmission coefficient, $H_{m0,i}$ and $H_{m0,t}$ are the incident (location 1 in Figure 3-2) the transmitted wave h eight (location 2 in Figure 3-2), respectively.

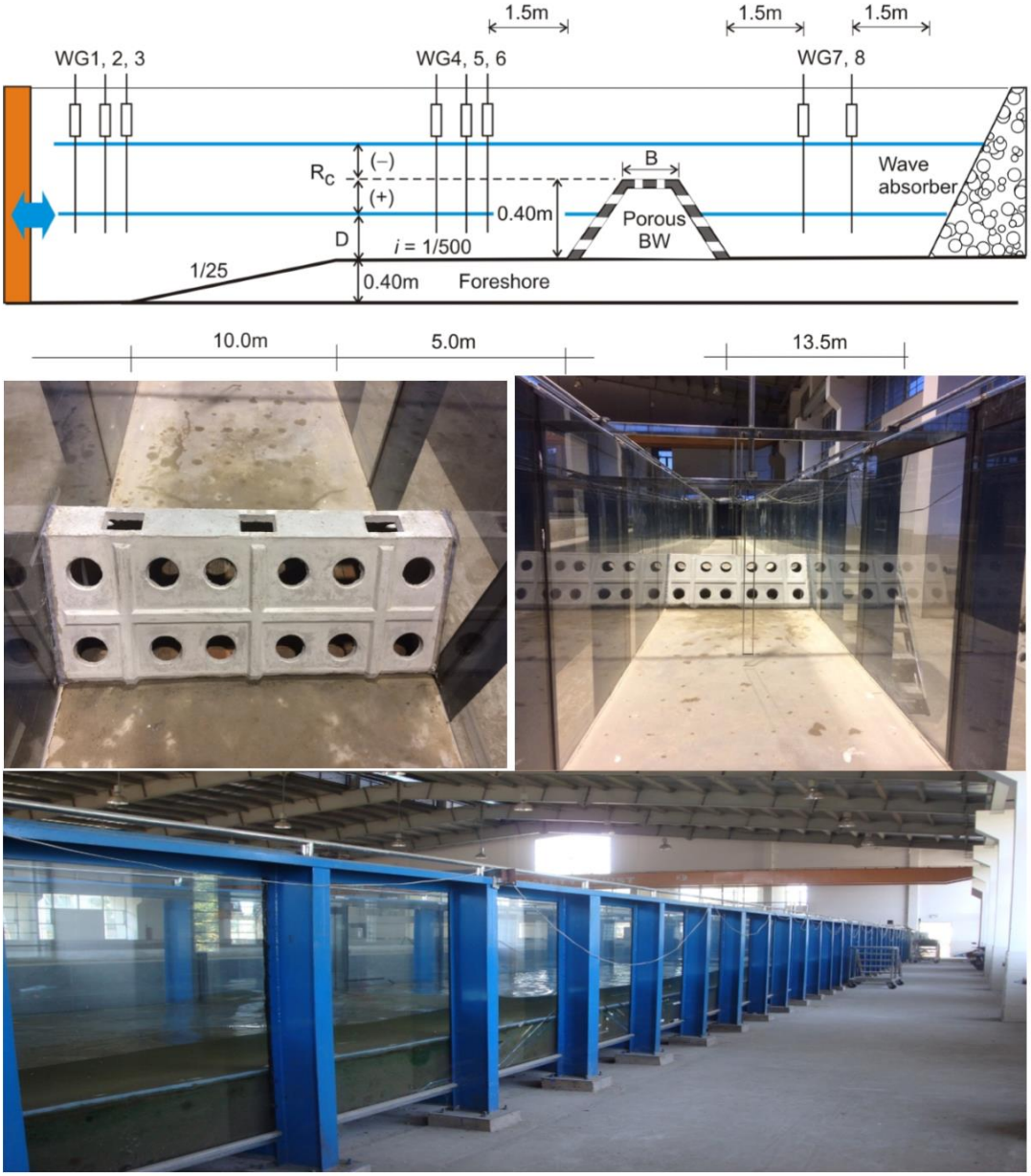

Figure 3-1 Model setup of wave transmission at porous breakwaters

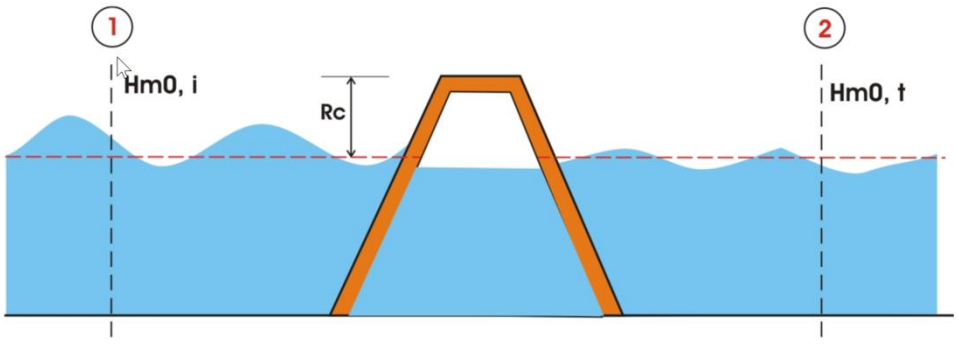

Figure 3-2 Definition sketch of wave transmission and wave reduction coefficient

The testing program as summarized in Table 3-1 consists of 60 test scenarios (including 30 base or no structure scenarios), resulting from 06 typical monsoon waves in combination with 05 water levels (both emerged and submerged) derived from typical hydraulic conditions of LWD. Note that the typical height-

period relation of monsoon waves is according to Linh and Tuan (2015) [5]. Since no measured wave spectrum on the mangrove foreshore (shallow water) is available, standard JONSWAP spectra with g = 3.30 were used for generation of tested waves at the offshore boundary. Each of the experiments lasted approximately 500.Tp to adequately produce the main frequency domain of desired wave spectra.

The scaling law for wave transmission is basically according to Froude's criteria, whereby the time scale *Nt* can be derived in connection with the length scale N_L.

$$N_t = N_L^{0.5}$$

The chosen length scale is N_L = 10 (N_t = 3.16), based on the flume capacity and the tested range of hydraulic parameters.

Table 3-1 A summary of test program on wave transmission

Test waves (Offshore boundary)	Target values		Freeboard Rc/ Depth D (m)	Model breakwaters
	H_{m0} (m)	T_p (s)		
WP6-BW-JSW1	0.10	1.79	0.20/0.20 0.10/0.30 0.00/0.40 −0.10/0.50 −0.15/0.55	No breakwater Porous breakwater
WP6-BW-JSW2	0.12	1.88		
WP6-BW-JSW3	0.15	2.00		
WP6-BW-JSW4	0.17	2.07		
WP6-BW-JSW5	0.20	2.16		
WP6-BW-JSW6	0.22	2.20		

3.3.1.2 Data analysis and results

a) Influencing parameters on wave transmission

Like other conventional breakwaters, wave transmission at porous breakwaters is generally a function of relative crest freeboard, crest width, breakwater slope, porosity/permeability, and wave characteristics. In order to arrive at an empirical formulation for wave transmission, effects on wave transmission of most influencing parameters like the relative crest freeboard and Iribarren number are analyzed with the experimental data. Other secondary parameters such as the crest width (porous breakwaters are a narrow-crested structure) and porosity, for the type of structure being considered herein, are implicitly included and thus are not present in the analysis.

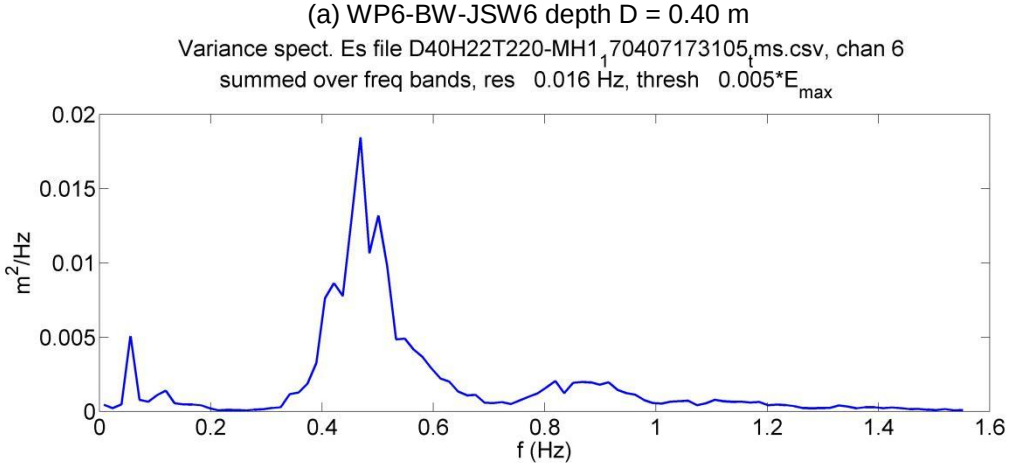

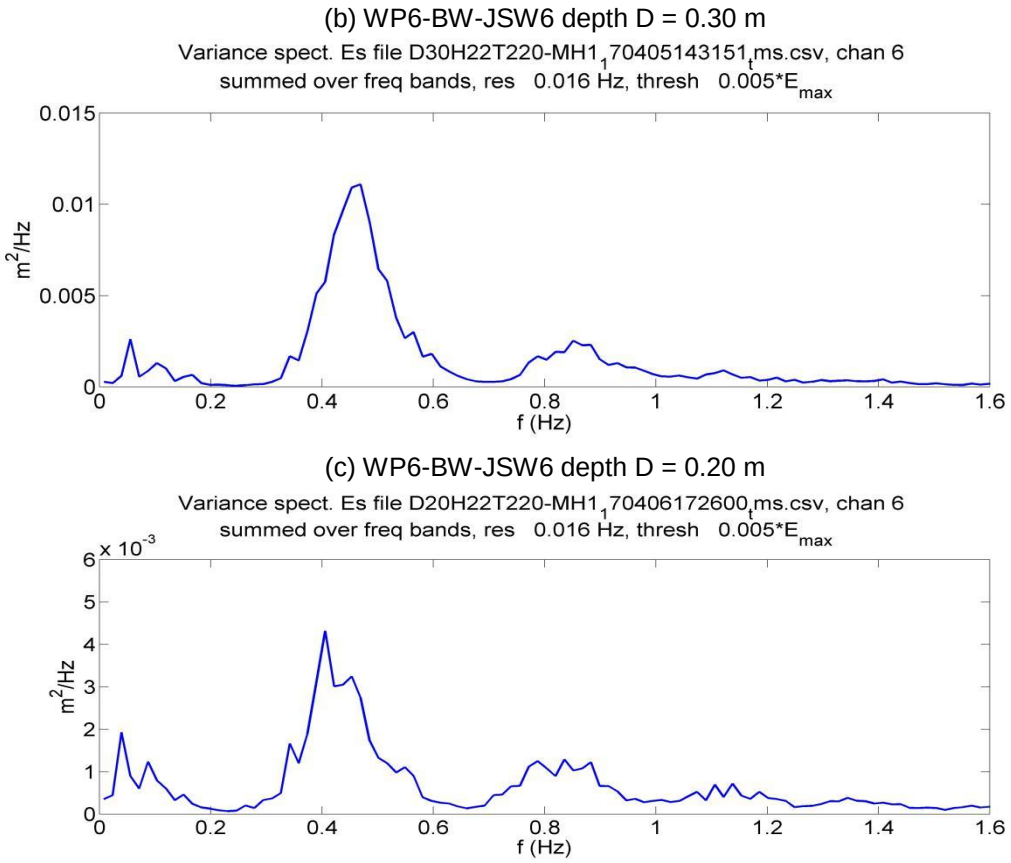

Figure 3-3 Measured shallow wave energy spectra at WG6 on the foreshore (wave WP6-BW-JSW6)

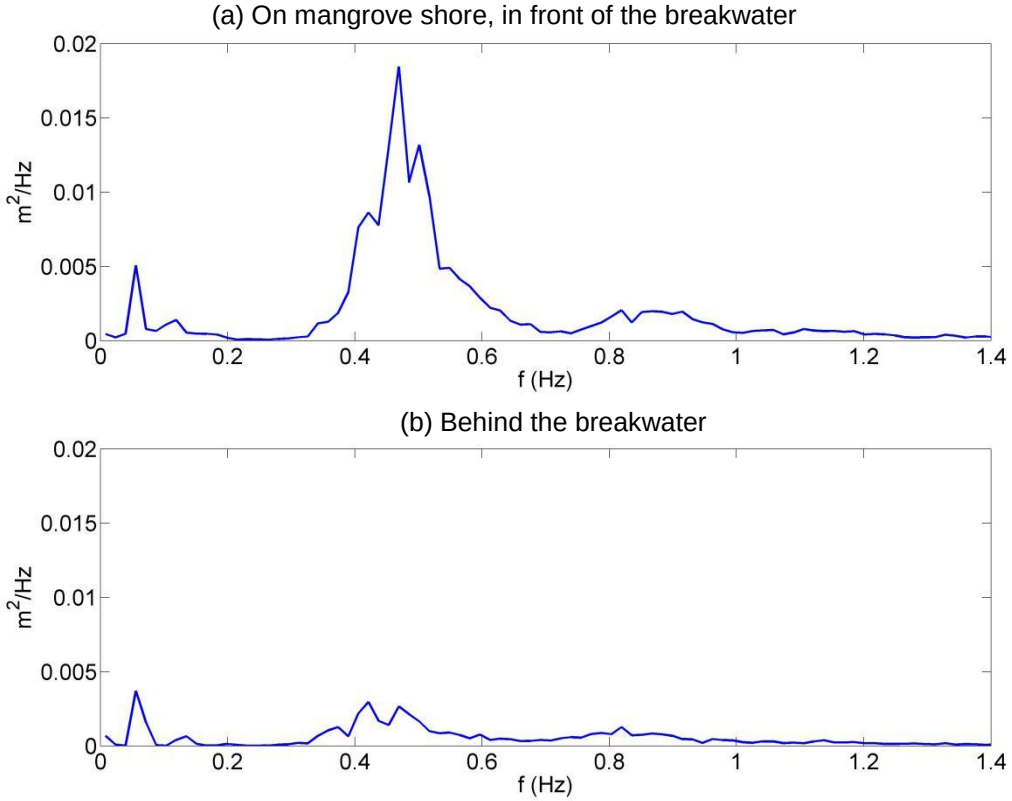

Figure 3-4 Wave energy spectra across the breakwater (test WP6-BW-JSW6-D40)

b) Relative crest freeboard Rc/Hm0

The relative crest freeboard R_c/H_{m0} always plays the most important role in wave transmission at coastal structures. Without exception, Figure 3-3-5 shows a strong dependency of the wave transmission coefficient K_t (blue points, Eq. (3)) and the wave reduction coefficient K_{re} (red points) on the crest freeboard. It follows that the transmission coefficient quickly declines in a linear trend with the increase of the relative freeboard and becomes almost constant (K_t ~ 0,30) when $R_c/H_{m0} > 0.50$. Generally speaking, wave is not much transmitted through the breakwater with high crest emergence. On the other hand, the structure is not effective in damping wave when it gets submerged, i.e. $K_t = 0.75 - 0.80$ as $R_c/H_{m0} < -0.50$.

Note that hereinafter wave transmission coefficient K_t shall be used in the analysis.

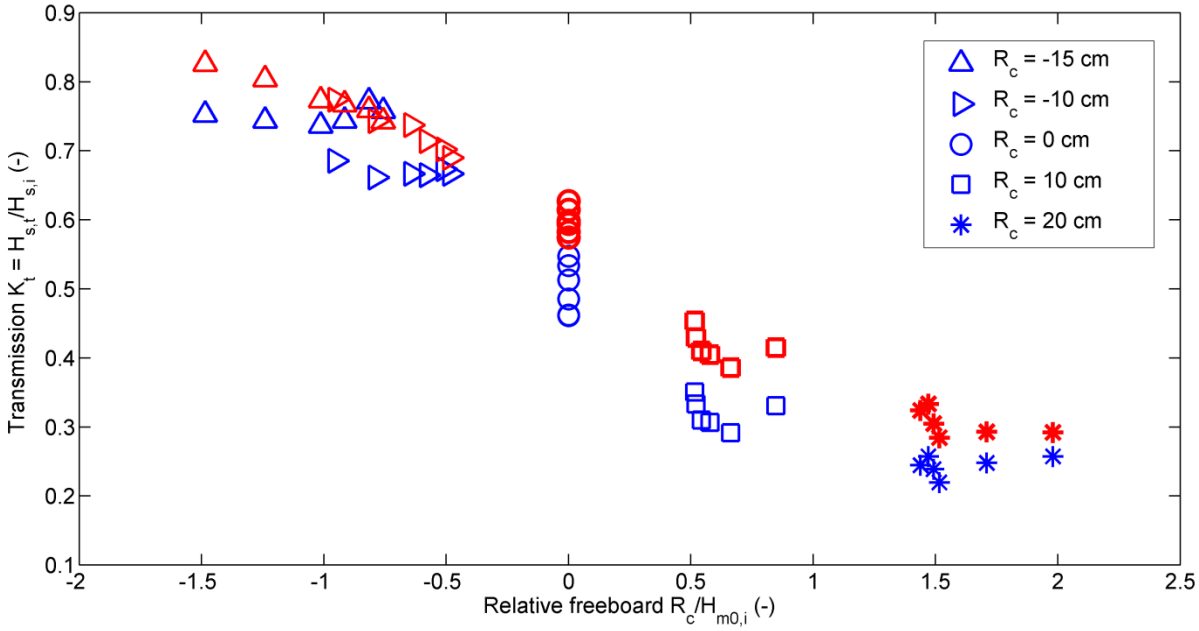

Figure 3-3-5 Effects of relative crest freeboard on wave transmission

c) Reflection

Wave reflection at a structure is a response as the result of wave-structure interaction. Though reflection is not explicitly described in wave transmission, it hints at the efficiency of energy dissipation of a structure.

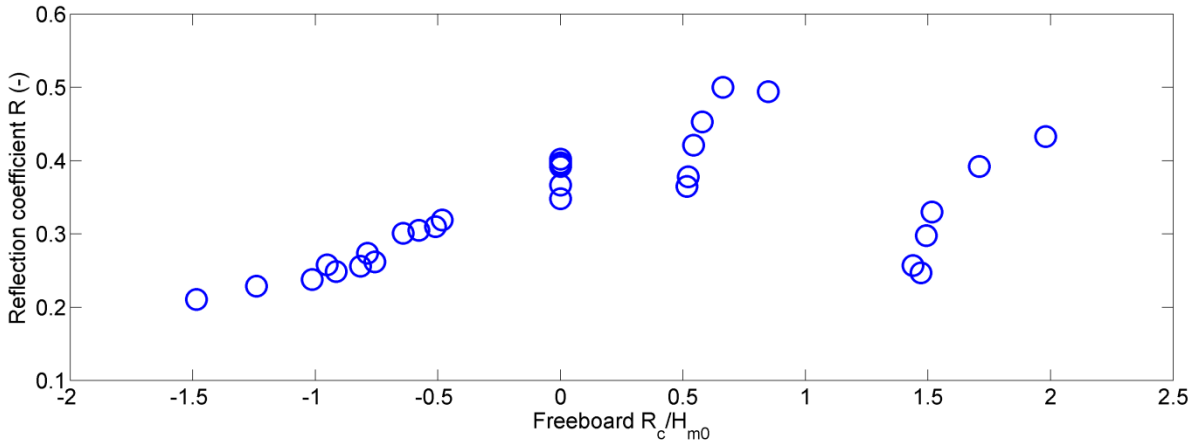

Figure 3-6 Reflection coefficient as a function of R_c/H_{m0}

The reflection coefficient plotted against the relative freeboard in Fig.8 indicates that the porous breakwater is highly reflective, particularly when the crest emerges above water (R = 0.40 ~ 0.50). Reflection generally increases with the increase of R_c/H_{m0}. This is because the structure is not sufficiently porous to absorb wave energy and so, in case of high crest emergence, most of the wave energy behind the breakwater is actually from transmitted infragravity waves and wake of wave overtopping.

It is important to realize this high reflection character in the structural design of porous breakwaters, especially care must be taken in the design of toe scour protection.

d) Empirical formulations of wave transmission

The above analysis on parameters that most influence wave transmission forms the basis for derivation of an empirical formulation. The influence of the governing parameters suggests that a similar form of the formulation by Angremond et al. (1996) can be used to derive the empirical formula for wave transmission herein. The two main considered variables are relative crest submergence R_c/H_{m0} and Iribarren number ξ_0. A general formulation of wave transmission at porous breakwaters can be expressed as follows:

$$K_t = a \cdot \frac{R_c}{H_{s,i}} + b \cdot \left(1 - e^{-c \cdot \xi_0}\right) \tag{6}$$

in which a, b, and c are empirical constants determined through regression analysis with the experimental data.

Note that compared to Angremond et al. (1996) the crest width B is not present in Eq. (6) since the porous breakwater is considered a narrow-crested type of structure (in fact its effect is implicitly included). Also, the Iribarren number ξ_0 can be determined either with T_p or $T_{m-1,0}$, depending on their availability.

Regression analysis with the experimental data results in the following two formulations of wave transmission with ξ_0 according to $T_{m-1,0}$ and T_p, respectively:

$$K_t = -0.22 \cdot \frac{R_c}{H_{s,i}} + 0.75 \cdot \left(1 - e^{-0.26 \xi_{0m-1,0}}\right) \tag{7}$$

$$K_t = -0.20 \cdot \frac{R_c}{H_{s,i}} + 0.66 \cdot \left(1 - e^{-0.39 \xi_{0p}}\right) \tag{8}$$

The above formulations are valid within the tested range of governing parameters:

$$\begin{aligned} &\frac{R_c}{H_{m0}} = -0.76 \sim 2.0 \\ &s_{0p} = 0.016 \sim 0.030 \\ &s_{0m} = 0.010 \sim 0.025 \\ &K_t = 0.22 \sim 0.77 \end{aligned} \tag{9}$$

Figure 3-7 and Figure 3-8 compare the calculated K_t according to Eq. (7) and (8) with the measured data, respectively. Agreement is generally good for both cases and slightly better with the use of $T_{m-1,0}$.

Cross-comparisons of the present study, as shown in Figure 3-9 through Figure 3-11, with existing formulations by d'Angremond et al. (1996) and van der Meer et al. (2005) for smooth and impermeable breakwaters, van der Meer et al. (2005) for rough and permeable breakwaters, and van der Meer and Daemen (1994) for narrow-crested, rough and permeable breakwaters were also made, respectively. It follows that except a satisfactory agreement is found with the formulation by van der Meer et al. (1993) for narrow-crested permeable structures, all other slightly to largely overestimate the transmission coefficient. This is in part due to the foreshore influence on the spectral transformation of the incoming wave mentioned earlier. Also, the porous breakwater considered herein appears to be closer to the type of narrow-crested, rough and permeable structure.

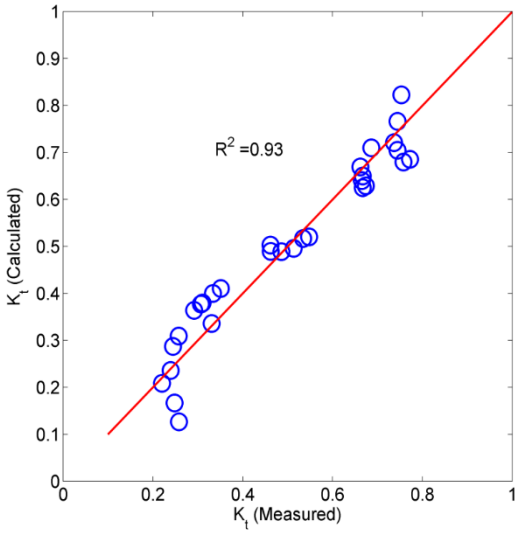

Figure 3-7 Data regression with $\xi_{m-1,0}$

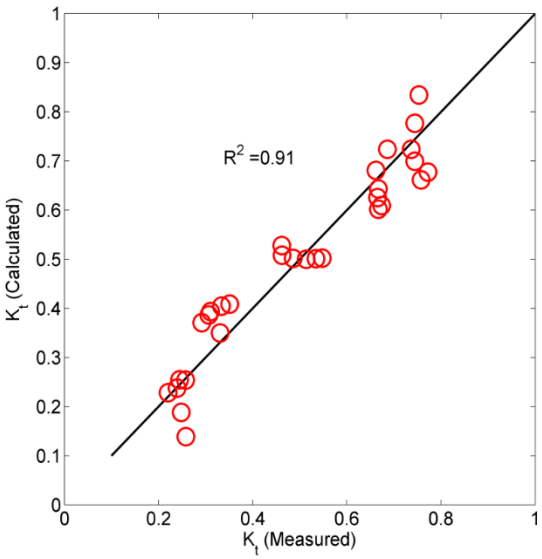

Figure 3-8 Data regression with ξ_{0p}

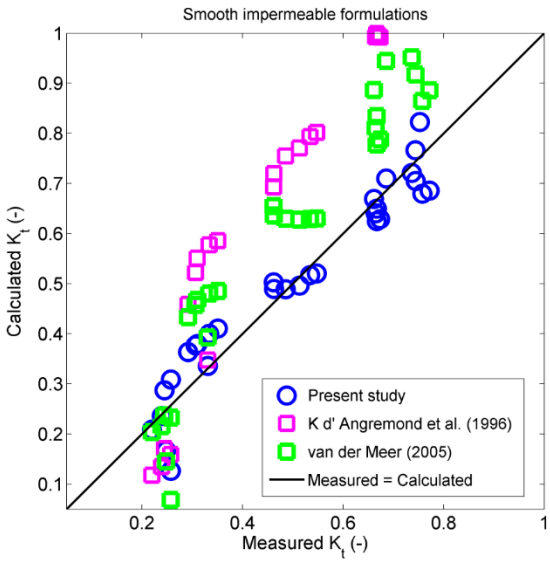

Figure 3-9 Comparison with formulations of smooth and impermeable breakwaters (Angremond et al., 1996 and van der Meer et al., 2005)

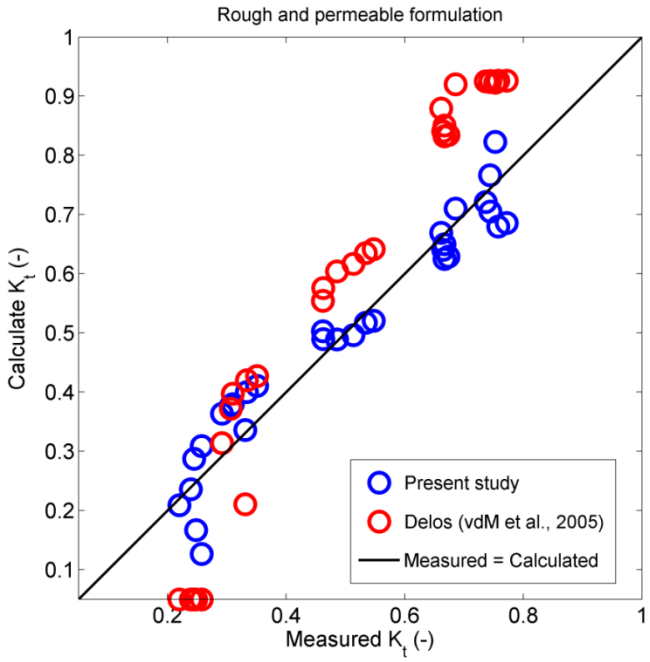

Figure 3-10 Comparison with formulations of rough and permeable breakwaters (DELOS - van der Meer et al., 2005)

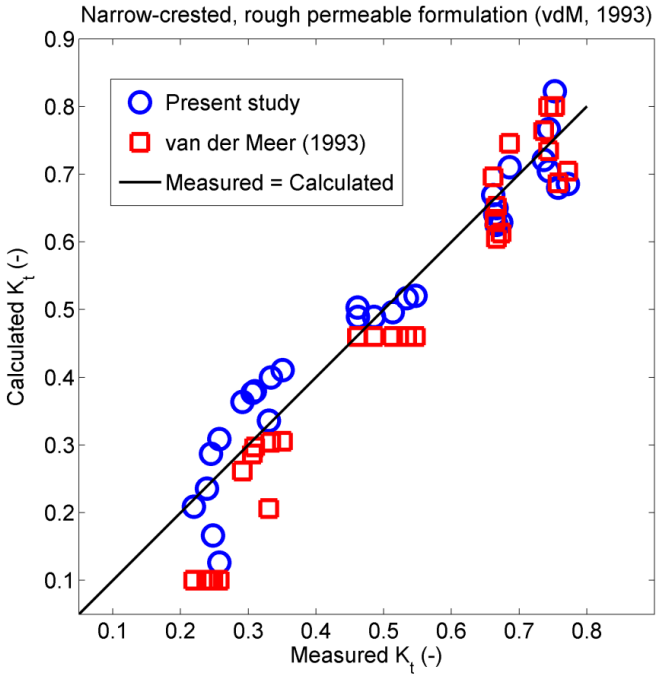

Figure 3-11 Comparison with formulations of narrow-crested, rough and permeable breakwaters (van der Meer and Daemen, 1994)

3.3.2 Sediment exchange capacity

The sediment exchange capacity for the porous coastal protection structure (Figure 3-12) was investigated, with a permeability of about 20%. This new type of structure has three main objectives (Figure 3-13):

- Reduction of the incoming wave energy to reduce coastal erosion due to a decrease of wave impacts on the mangroves and the foreshore

- Sediment transfer to accelerate sediment deposition and rehabilitation of the mangroves
- Water exchange to ensure good water quality in between the structure and the coastline

Figure 3-12 Porous Breakwater

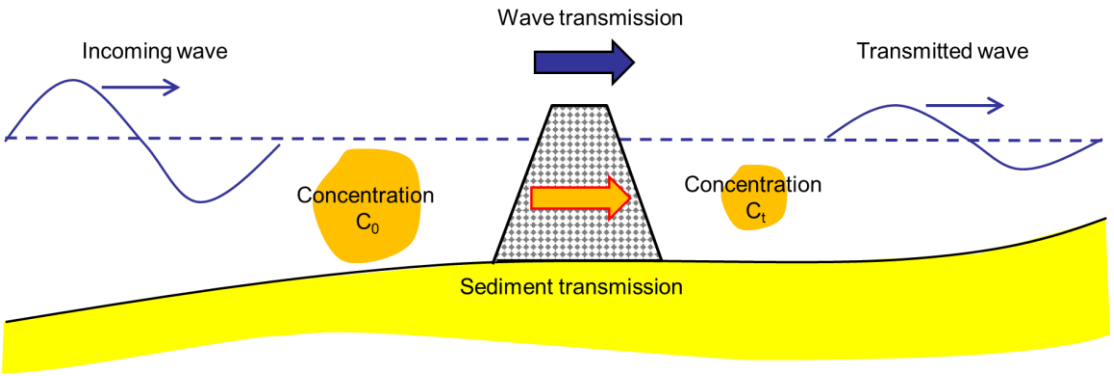

Figure 3-13. Wave and sediment transmission through a porous breakwater

In this part we discuss about the possible transfer of suspended sediment through the above porous breakwater.

3.3.2.1 Model set up and test program

The model set up is as the same as presented in part Model setup and test program and also expressed in Figure 3-14. In addition, two turbidity sensors (Figure 3-15) were place at the same cross sections as wave gauges 3 and 4 at a vertical height of about 10cm above foreshore. The turbidity sensors have sampling rate of 0.016 Hz (1 record/minute). Therefore, it is possible to measure the average change in turbidity but not the change of turbidity during individual waves.

Finally, two pressure cells were mounted to the seaward and landward front of the porous structure at a height of 3cm above the foreshore. Tests were recorded by photos and videos.

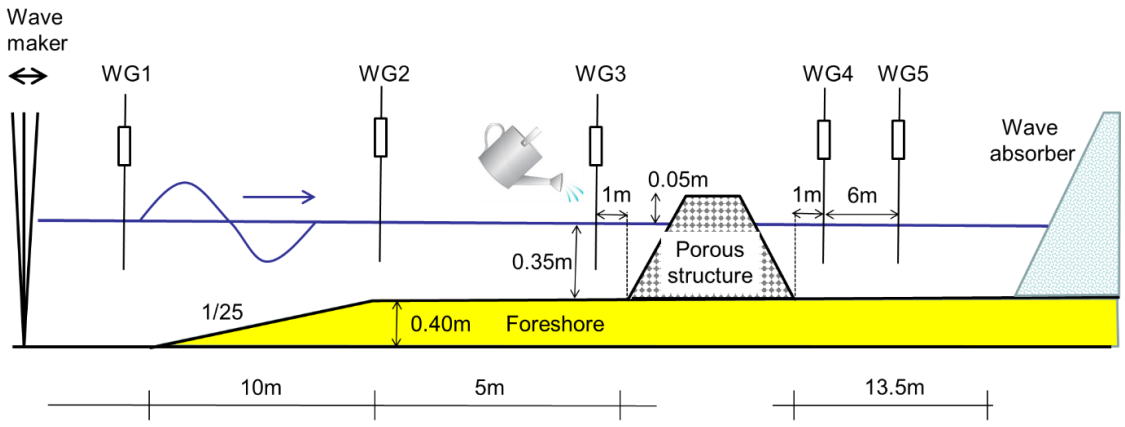

Figure 3-14 Model set-up for sediment exchange via porous breakwater

Figure 3-15 Placement of wave gauges and turbidity sensors

A representative significant wave height H_{m0} of 0.2m for a wave period of T_P=2.28 s at the wave maker was selected for the model tests due to limited time (deep water wave length L_0=8.11 m). A JONSWAP spectrum was generated. The water depth at the toe of the porous structure was selected for 3 cases with different H(m) resulting in different crest freeboard R_C (m). The main dimensionless parameters are indicated in Table 3-2.

Table 3-2 Main dimensionless parameters of 3 test cases

Parameters	Case 1	Case 2	Case 3
Wave steepness (H_{m0}/L_0)	0.025	0.025	0.025
freeboard R_C	0.05	0.10	-0.10
Depth d (m)	0.35	0.30	0.50
Relative water depth d/L_0	0.043	0.037	0.062
Relative freeboard R_C/d	0.14	0.333	-0.20

Kaolinite was selected as fine material to demonstrate the transport of fine material through the porous breakwater. A target concentration of 0.5 mg/l has been selected for the first test according to the numerical results. The kaolinite is filled into a bucket with 1.5 l of water and mixed. After the first waves, the bucket was emptied into the water at a distance of around 1 m from the porous breakwater. Thus, the target concentration should be reached in the first two meters in front of the porous breakwater. This was done under the assumption that the sediments in the field are transported from far away to the structure and are not eroded just in front of the porous breakwater.

In total, 15 tests were carried out with 3 cases as showed in Table 3-3:

Table 3-3. Tests were carried out with 3 cases of Rc

Test	Case 1: R_C=0.05 m; d=0.35 m	Case 2: R_C=0.10 m; d=0.30 m	Case 3: R_C=-0.10 m; d=0.50 m
Test 0	0 g (only wave)	0 g (only wave)	0 g (only wave)
Test 1	42 g ÷ 50mg/l	36g÷ 50mg/l	60g÷ 50mg/l
Test 2	42 g ÷ 50mg/l	36g÷ 50mg/l	60g÷ 50mg/l
Test 3	50 g ÷ 60mg/l	43g ÷ 60mg/l	71g ÷ 60mg/l
Test 4	100 g ÷ 120mg/l	86g ÷ 120mg/l	143g ÷120mg/l

It was not possible to take out the kaolinite after the tests, therefore, a stepwise increase of sediment concentration was expected from test to test.

The turbidity meters were calibrated by using the same water and the same kaolinite in buckets of 15 l volume. The turbidity was measured without any kaolinite and then after 1g, 1g and 1.5 g were put into the bucket. The results of the calibration are provided in Figure 3-16.

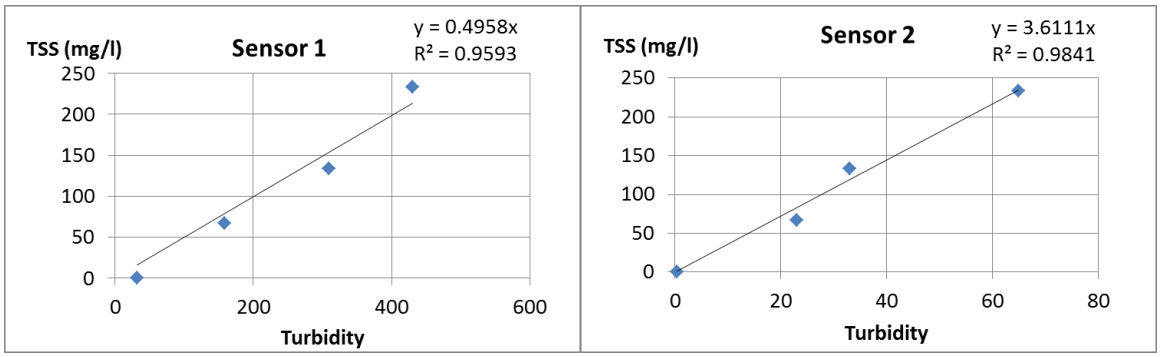

Figure 3-16. Calibration of turbidity sensors

3.3.2.2 Results and discussion

a) Wave analysis

The results of the wave analysis in frequency domain are given in Table 3-4 to Table 3-6 and in Figure 3-17 to Figure 3-19.

Table 3-4 Wave analysis for Case 1 (R_C=0.05 m; d=0.35 m)

Test	Wave	Gauge 1	Gauge 2	Gauge 3	Gauge 4	Gauge 5
1	H_{m0} [m]	0.199	0.194	0.156	0.082	0.081
	T_p [s]	2.28	2.11	1.73	2.28	2.28
2	H_{m0} [m]	0.196	0.194	0.153	0.082	0.081
	T_p [s]	2.28	2.11	2.11	2.28	2.28
3	H_{m0} [m]	0.197	0.199	0.153	0.084	0.082
	T_p [s]	1.97	1.97	1.73	2.48	2.72
4	H_{m0} [m]	0.190	0.196	0.153	0.085	0.084
	T_p [s]	2.11	2.11	1.73	2.48	2.72
Average	H_{m0} [m]	**0.196**	**0.196**	**0.154**	**0.083**	**0.082**
	T_p [s]	**2.16**	**2.08**	**1.82**	**2.38**	**2.50**

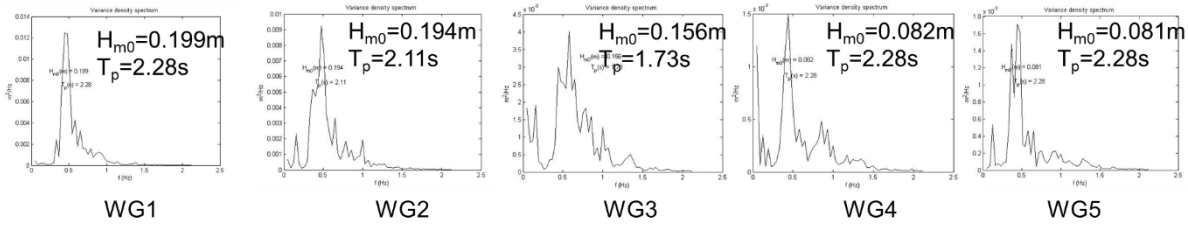

Figure 3-17 Wave spectra for WG 1 to 5 of Case 1 (R_C=0.05 m; d=0.35 m)

Table 3-5. Wave analysis for Case 2 (RC=0.10 m; d=0.30 m)

Test	Wave	Gauge 1	Gauge 2	Gauge 3	Gauge 4	Gauge 5
1	H_{m0} [m]	0.197	0.202	0.149	0.066	0.065
	T_p [s]	2.12	2.12	1.97	1.88	2.28
2	H_{m0} [m]	0.195	0.151	0.151	0.066	0.065
	T_p [s]	2.12	1.97	1.97	2.28	2.28
3	H_{m0} [m]	0.196	0.201	0.151	0.066	0.066
	T_p [s]	2.12	2.12	1.97	2.28	2.28
4	H_{m0} [m]	0.195	0.201	0.151	0.066	0.065
	T_p [s]	2.12	2.12	1.97	2.28	2.28
Average	H_{m0} [m]	**0.196**	**0.189**	**0.151**	**0.066**	**0.065**
	T_p [s]	**2.120**	**2.083**	**1.970**	**2.180**	**2.280**

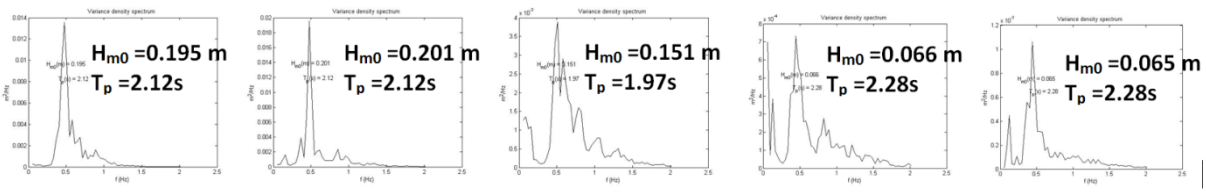

Figure 3-18. Wave spectra for WG 1 to 5 of Case 2 (RC=0.10 m; d=0.30 m)

Table 3-6. Wave analysis for Case 3 (RC=-0.10 m; d=0.50 m)

Test	Wave	Gauge 1	Gauge 2	Gauge 3	Gauge 4	Gauge 5
1	H_{m0} [m]	0.200	0.195	0.165	0.136	0.136
	T_p [s]	2.12	2.28	2.12	2.12	2.12
2	H_{m0} [m]	0.201	0.195	0.166	0.136	0.137
	T_p [s]	2.12	2.28	2.12	2.12	2.12
3	H_{m0} [m]	0.201	0.193	0.169	0.137	0.136
	T_p [s]	2.12	2.28	2.12	2.12	2.12
4	H_{m0} [m]	0.201	0.193	0.170	0.136	0.136
	T_p [s]	2.12	2.28	2.12	2.12	2.12
Average	**H_{m0} [m]**	**0.201**	**0.194**	**0.168**	**0.136**	**0.136**
	T_p [s]	**2.120**	**2.280**	**2.120**	**2.120**	**2.120**

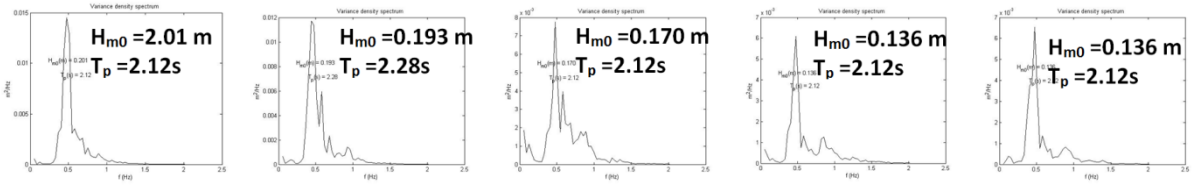

Figure 3-19. Wave spectra for WG 1 to 5 of Case 3 (RC=-0.10 m; d=0.50 m)

The wave transmission coefficient k_T can be calculated by the ratio of the transmitted ($H_{m0,t}$) and incident wave height ($H_{m0,i}$):

Therefore, the transmission coefficient k_T was calculated to be 0.42, 0.34 and 0.68 for case 1, 2 and 3 respectively.

All data are presented in Figure 3-20. In addition, the well-known formula for porous structures by Van der Meer and Daemen (1994)[11] is shown which fits very well to the new data for relative freeboards less than 1.0.

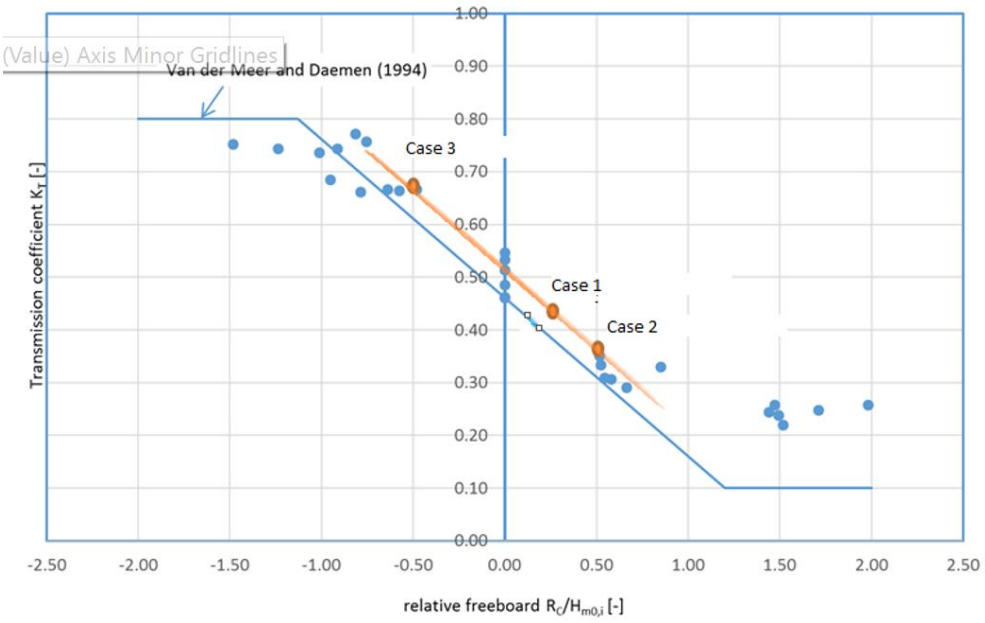

Figure 3-20. Transmission coefficient K_T as a function of relative freeboard $R_C/H_{m0,i}$

b) Sediment analysis

The observations and first results of the kaolinite ($Al_2Si_2O_5(OH)_4$) tests are given in the following section. As can be seen from Figure 3-21, the concentration of kaolinite increases during the model tests. The left side of Figure 3-21 shows the situation before any kaolinite was given into the flume. The water is clear

and the amount of fine materials is very low. After the last test, the water is milky and it was even not possible to see the instruments.

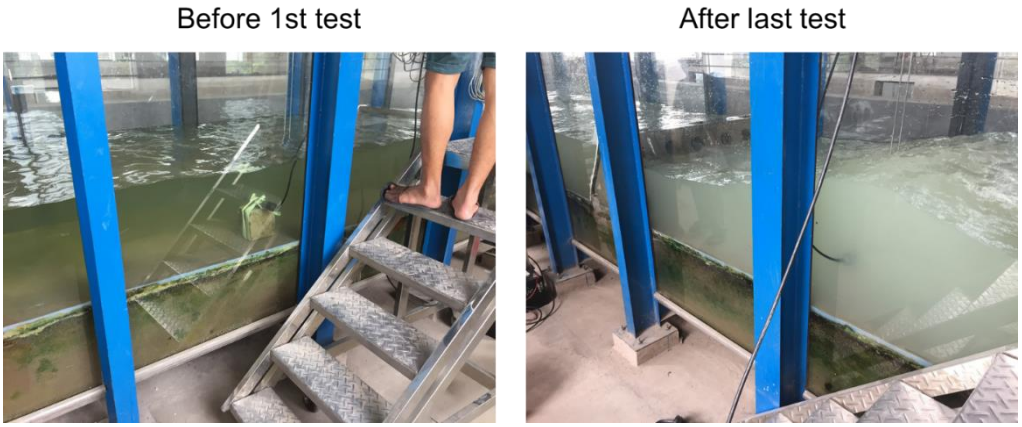

Figure 3-21 Increase of visible concentration of kaolinite between first and last test of case 1

More details about the increase of concentration can be seen in Figure 3-22, Figure 3-23 and Figure 3-24 which show the increase of concentration during the tests in the wave flume. The following observations were made:

1.) Peaks are due to input of kaolinite in flume. As already mentioned above, a bucket was emptied into the flume. Therefore, the sudden increase (peak) in sediment concentration is due to this process.

2.) Than, kaolinite is mixed due to wave turbulences during the first waves. This explains the decrease of sediment concentration after the peak.

3.) Part of Kaolinite is transported through breakwater. This can be seen in the evolution of the blue line which follows the red line.

4.) Decay between increase of concentration before and behind breakwater. This effect can be observed by comparison of the blue and red lines (in Figure 3-22, Figure 3-23 and Figure 3-24). The increase of concentration of the blue line starts after the concentration of the red line has increased.

5.) The concentration of suspension behind the breakwater is lower than before breakwater (which has been expected).

6.) Concentration behind breakwater increases with increasing concentration before breakwater. This effect can be observed especially in the steps of the blue line (in Figure 3-22, Figure 3-23 and Figure 3-24).

7.) Decrease of sediment concentration between model tests due to deposition. This effect can be best seen in the time between 14:00 and 14:30 in (in Figure 3-22. Both lines decrease).

8.) Data is accessible for calibration of numerical models. All data are stored and can be used for calibration and verification of numerical models.

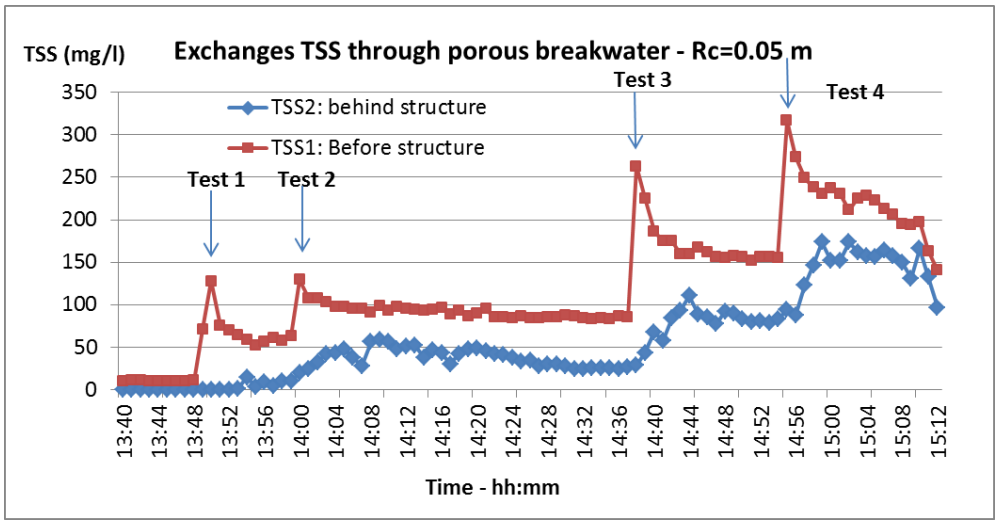

Figure 3-22. Concentration of kaolinite during the model tests with Rc= 0.05 m

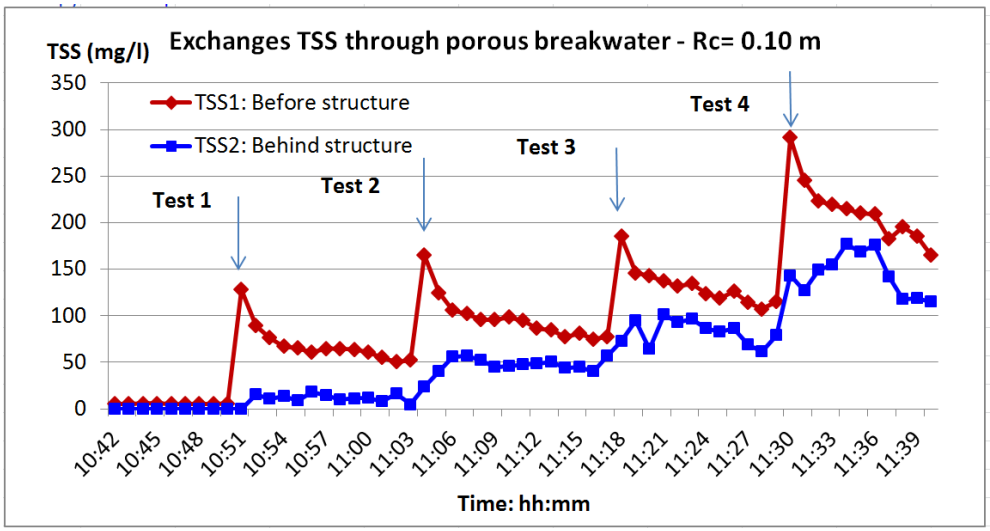

Figure 3-23. Concentration of kaolinite during the model tests with Rc= 0.10 m

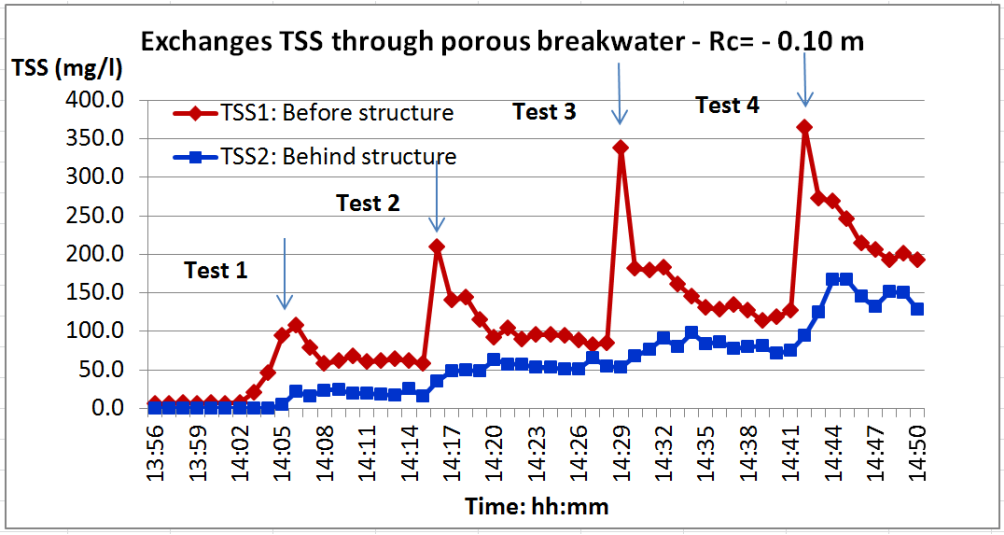

Figure 3-24. Concentration of kaolinite during the model tests with Rc= - 0.10 m

3.3.2.3 Conclusions and Outlook

A new type of porous breakwater was tested in the wave flume of SIWRR. Objective of this new type of breakwater is to reduce wave attack on mangroves and to ensure sedimentation in the sheltered area at the same time. Therefore, tests were carried out to investigate wave transmission and to compare available formulas for wave transmission with model results. In a second step, tests with kaolinite were performed to investigate the trapping efficiency of this breakwater. It is obvious from the model tests, that a part of sediments is transported through the breakwater and is deposited on the rear side of the structure. The field survey (see part Effects of pile breakwaters in Ca Mau) were indicated also the possible of sediment transfer through porous breakwaters (type 2 and type 3).

Additional model tests concerning the sediment trapping efficiency of the new type of breakwater are recommended due to the limited amount of model tests. Additional model tests are required to investigate the influence of different wave and freeboard conditions.

It has to be mentioned that the transfer of the model test results should be transferred to the field with care. Model tests were performed in a wave flume and effects such as longshore currents, oblique wave attack or tidal exchange are not taken into account. Kaolinite is very fine but due to scaling (scale factor approximately 1:10 for east coast and 1:5 for west coast) scale effects should be taken into account.

Therefore, a pilot site should be selected to test this new type of porous breakwater and to investigate the trapping efficiency.

3.3.3 Summary and Remarks on porous breakwaters

For the functional design of porous breakwaters on mangrove foreshore, a testing program consisting of 60 model experiments on wave transmission with governing parameters covering the typical range of hydraulic boundary data of LMD was carried out. Behaviour of wave spectral transformation on the shallow mangrove foreshore and across the breakwater reveals the relative importance of long-period wave energy in the wave transmission. As most short-period energy is dissipated and/or reflected back, long-period energy takes up the major part in the transmitted wave behind the breakwater.

Data analysis identifies the two most important governing variables of wave transmission at a porous breakwater which are the relative crest freeboard R_c/H_{m0} and the behaviour of waves on the dike slope expressing through Iribarren number ξ_0. The characteristic spectral period $T_{m-1,0}$ should be used instead of peak period T_p to give more emphasis on the effect of long-period waves in shallow water.

A new set of empirical formulae have been derived, allowing for a reliable determination of wave transmission at the considered porous type of breakwaters on a shallow mangrove foreshore. Cross-comparison with several existing formulations, such as by d'Angremond et al. (1996), van der Meer et al. (2005) and van der Meer and Daemen (1994) for various types of conventional breakwaters, implies that the behaviour of wave transmission considered herein is very close to that at a narrow-crested, rough and permeable breakwater.

For the purpose of functional design of porous breakwaters, it is recommended to take into account the following considerations:

- The design crest level should be above high tide (emerged structures) to be effective in damping waves. Wave is almost blocked as $R_c/H_{m0} > 0.50$.
- Because structure of this type is highly reflective, special attention must be paid to the design of toe scour protection.

Recommendations for future research include physical experiments on wave loading and structural stability so that the structure and its scour protection can be designed to withstand wave attack during extreme events.

3.4 Large-scale nourishment by near-shore sandbanks

3.4.1 Model setup and test program

Figure 3-25 illustrates the model setup for the experiments of nourishment. The model sandbank, placed on a shallow mangrove foreshore as used previously, has the crest width of B and is 0.20 m above the bed.

As usual, Froude and relative sediment fall speed similitude criteria are selected to satisfy as they are the major underlying physics behind the gravity-induced sediment transport processes (see e.g. Hughes, 1993). Also, it is customary to use the same sediment as in nature and the model is geometrically undistorted. These lead to the following scaling relations:

$$N_w = N_L^{0.5}$$
$$N_t = N_L^{0.5} \quad (10)$$

where N_w is the sediment fall speed scale.

The fall speed of sediment w_s can be estimated according to:

$$w_s = \frac{10\nu}{d_{50}}\left[\left(1+0.01\Delta g d_{50}^3 \nu^{-2}\right)^{0.5} - 1\right] \quad (11)$$

where ν is molecular fluid viscosity, Δ (= 1.65) is relative submerged density of sediment.

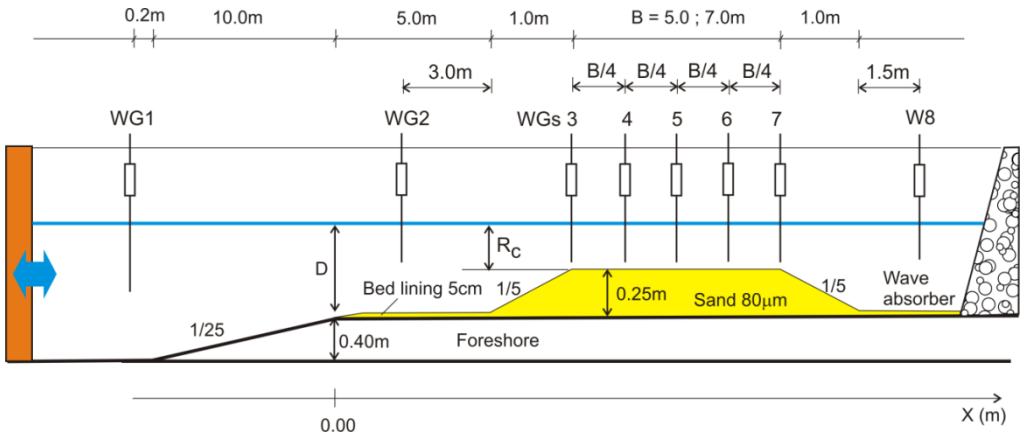

Figure 3-25 Test setup of nourishment by sandbanks

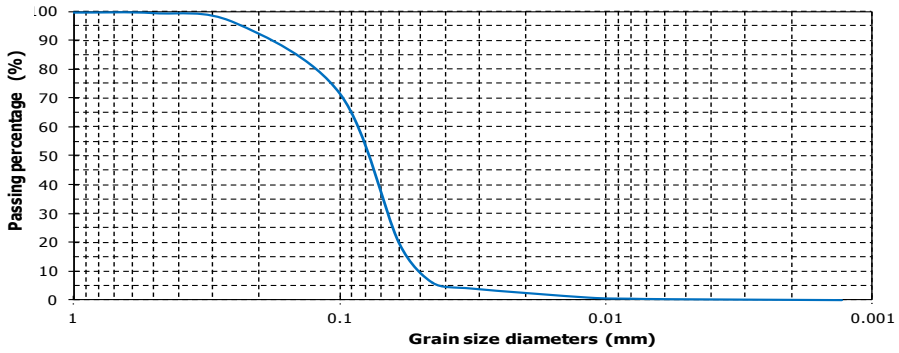

Figure 3-26 Grain size distribution of model quartz sand

The median size d_{50} of the model quartz sand is 80 μm (see Figure 3-26) and that of most available borrow sand in study area is 200 μm, which result in a model length scale N_L of about 1/20.

Wave measurements at various locations along the longitudinal axis were used to evaluate the cross-shore spectral transformation and wave damping capacity of the sandbank. To double-check the effect of high sediment concentration on the conductivity of water and thus the recorded wave signals, all wave gauges were carefully calibrated before and after each test. Averaged calibration coefficients were taken.

Simultaneous flow measurement at several locations across the sandbank would be ideal for validation of numerical models. Unfortunately, this was not possible due to lack of equipment.

The model sandbank was rebuilt after each test and sand samples at various locations were taken for determining the sand porosity as built. The average porosity was 0.430. The pre- and post-storm sandbank profiles were averaged over 3 measuring lines (two at 10 cm away from the side walls and one at the middle of the flume) with ordinary land survey equipment. To have a rough impression on the time-dependent sandbank profile response instantaneous sandbank profiles were also marked on the glass walls and measured at several intermediate time steps. The whole progress of sandbank deformation during testing was recorded with a HD video camera viewed through the glass wall. Example photos of the experiments are shown in Figure 3-27.

(a) Before testing

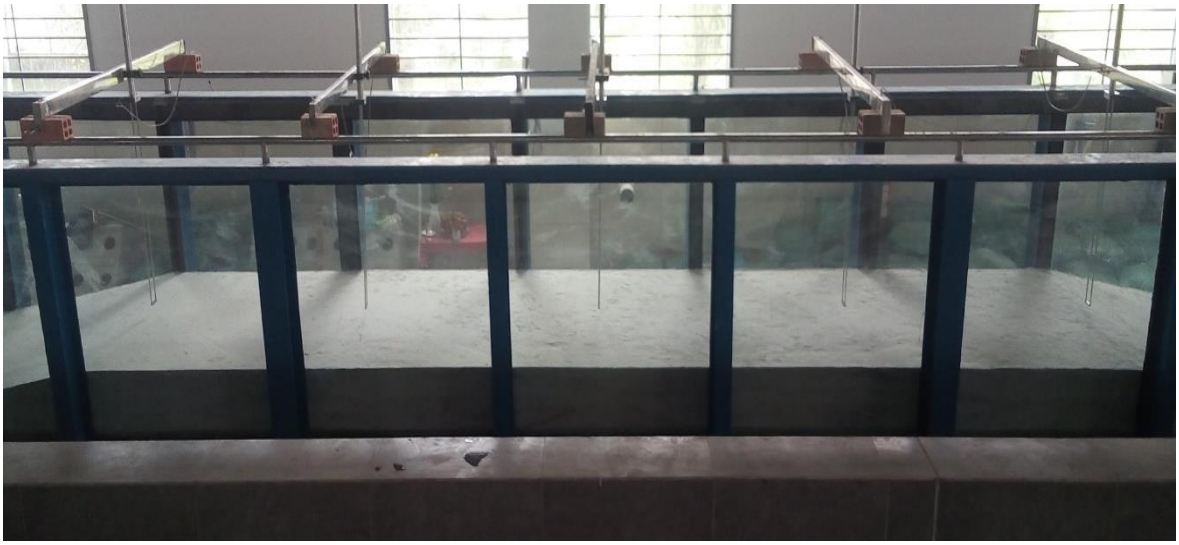

(b) During testing: severe wave breaking and high sediment concentration

(c) Sandbank deformation after testing

Figure 3-27 Photos of model experiments

The test program as summarized in Table 3-7 consists of 8 experiments, in which each of the two sandbank models (B = 5m and 7m) was tested with several (wave + water level) scenarios. Following the design philosophy of the nourishment, the model sandbank was kept sufficiently submerged so that no major bed deformation occurred during testing whilst still maintaining a high level of wave damping. The test waves at the offshore boundary, downscaled from typical monsoon waves, were standard JONSWAP. Each test lasted between 3000 and 5000 waves, depending on the actual extent of sandbank deformation.

Table 3-7 Test program of the nourishment by sandbanks

Test scenarios	Model					Prototype				
	B (m)	R_c (m)	H_{m0} (m)	T_p (s)	Dura. (min.)	B (m)	R_c (m)	H_{m0} (m)	T_p (s)	Dura. (hrs.)
WP6-NOU-B5-R05-JSW1	5.0	−0.05	0.08	1.44	120	100	−1.0	1.60	6.44	8.94
WP6-NOU-B5-R15-JSW1	5.0	−0.15	0.08	1.44	75	100	−3.0	1.60	6.44	5.59
WP6-NOU-B5-R05-JSW2	5.0	−0.05	0.10	1.53	125	100	−1.0	2.00	6.84	9.32
WP6-NOU-B5-R10-JSW2	5.0	−0.10	0.10	1.53	80	100	−2.0	2.00	6.84	5.96
WP6-NOU-B5-R15-JSW2	5.0	−0.15	0.10	1.53	125	100	−3.0	2.00	6.84	9.32
WP6-NOU-B7-R10-JSW2	7.0	−0.10	0.10	1.53	125	140	−2.0	2.00	6.84	9.32
WP6-NOU-B7-R10-JSW3	7.0	−0.10	0.12	1.61	134	140	−2.0	2.40	7.20	9.99
WP6-NOU-B7-R10-JSW4	7.0	−0.10	0.14	1.69	141	140	−2.0	2.80	7.56	10.51

Note: Wave parameters are desired values at offshore boundary (WG1)

3.4.2 Data analysis and results

3.4.2.1 Spectral transformation and wave transmission

Following the same procedure of wave analysis as mentioned in Data analysis and results, wave spectra at measured locations across the sandbank are determined. In a mobile bed experiment, one may wish to know the time-varying wave heights. However, it is observed herein that major bed changes mostly took place during the first 500-1000 waves, after which wave regime across the bank became relatively stable. An example of time variation of wave transmission from test scenario WP6-NOU-B5-R05-JSW2 with noticeable bank deformation during the first 1000 waves (50 min.) is shown in Figure 3-28. It follows that the transmitted wave height (at WG8) becomes almost constant after 50 minutes (slightly decreased as the bank crest marginally elevated by on-shore sand deposition). Therefore, for the purpose of evaluation of wave transmission discussed herein we advocate a practical and probably more appropriate approach that is to determine the wave heights once the bank profile has become relatively stable (after approximately the first 1000 waves).

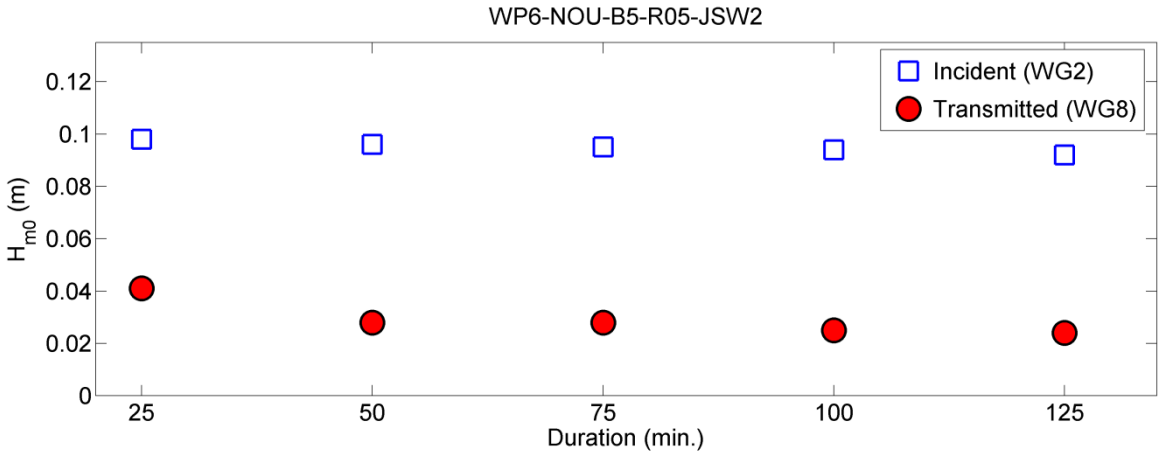

Figure 3-28 Time-varying wave transmission: WP6-NOU-B5-R05-JSW2

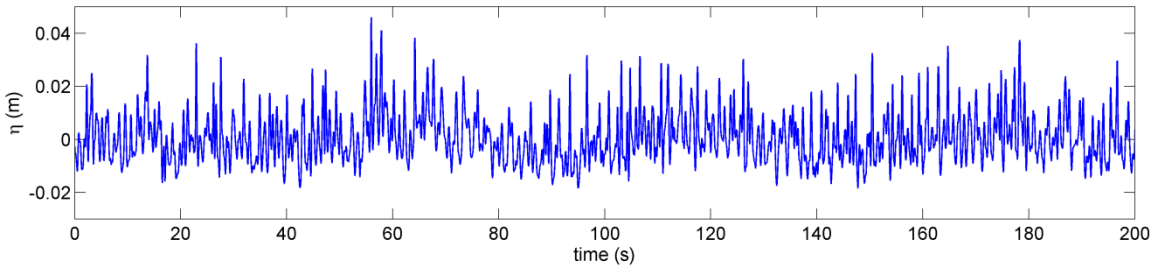

Figure 3-29 Wave signal with presence of IG waves: WG7- WP6-NOU-B7-R10-JSW3

The wave hydrodynamics over the sandbank resembles that over a shallow reef due to a similarity in geometrical conditions. Figure 18 shows the presence of IG waves in a recorded wave signal, an important character of the sandbank wave hydrodynamics. Severe wave breaking near the outer slope (see e.g. Figure 3-30) and triad wave-wave interaction cause drastic spectral transformation across the sandbank. As high-frequency waves quickly dissipates within the first wave length low-frequency waves become increasingly important as wave propagates over the sandbank and wave energy is gradually shifted toward the infra-gravity band (see Figure 3-31). Obviously, the spectral evolution toward low-frequency band increases as the water depth (R_c) over the sandbank decreases.

Figure 3-30 Severe wave breaking at the sandbank outer slope

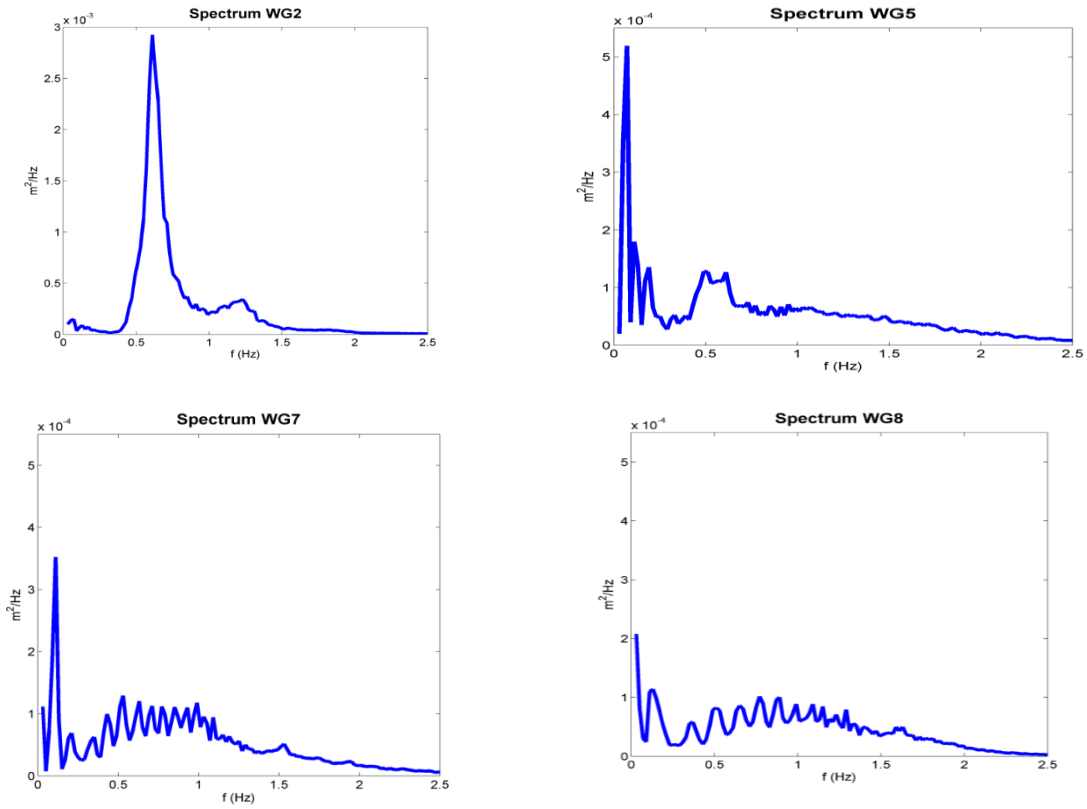

Figure 3-31 WP6-NOU-B7-R10-JSW3: Drastic spectral transformation across the sandbank: WG2, WG5, WG7, and WG8

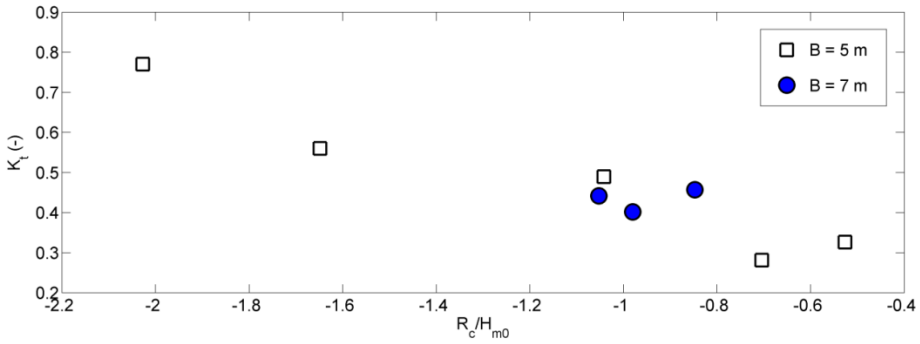

Figure 3-32 Effects of relative submergence and bank crest width

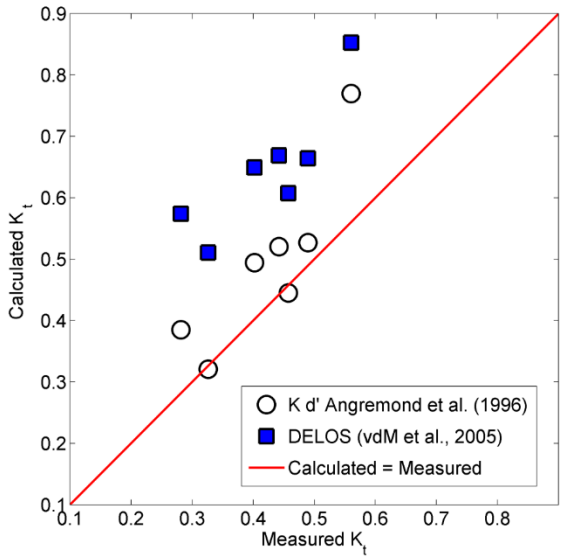

Figure 3-33 Experimental data of wave transmission at sandbanks in comparison with existing formulations of smooth and impermeable structures

For the functional design of the sandbank, it is important to evaluate the wave damping capacity of the sandbank. Table 3-8 summarizes the measured wave heights H_{m0} across the bank and the associated wave transmission coefficient. Note that wave parameters given in the table are determined once the bank profile has become relatively stable (after approximately 1000 waves). Unfortunately, due to the effect of high sediment concentration together with the shallow water depth over the crest, especially during passage of IG waves, the recorded signals from the on-crest wave gauges (WG3 through WG7) were mostly out-of-range.

Generally speaking, wide sandbanks are highly effective in damping waves. Figure 3-32 delineates the dependency of wave transmission on the major governing parameters. Similar to other type of structures, wave transmission over a wide sandbank addressed herein depends strongly on the relative submerged depth (R_c/H_{m0}) and somewhat weaker on the relative bank width (B/H_{m0} or B/L). However, Figure 3-33 shows significant overestimations of wave transmission, in comparison with the experimental data, by the existing formulations of smooth and impermeable structures by Angremond et al. (1996) and DELOS (van der Meer et al., 2005). This can be explained by the fact that none of these formulations are valid for such a wide crest structure (B/H_{m0} ~ 50 - 70 or B/L ~ 2.0). The DELOS approach does not even account for the crest width and thus gives the largest discrepancy. More importantly, as mentioned earlier, most of the energy of short-period waves is dissipated within the first wave length or so and thus the energy behind the bank is largely of long-period waves. Therefore, it is generally insufficient to describe wave transmission over a wide sandbank in this case solely by short-period wave characteristics. For instance, inclusion of the spectral period $T_{m-1,0}$ (also given in Table 3-8), which gives more emphasis on the behaviour of waves in shallow water, should be considered.

Table 3-8 Measured wave heights across the sandbank

Test scenarios	WG2			Initial geometry				On-crest gauges H_{m0} (m)				WG8		
	H_{m0} (m)	T_p (s)	$T_{m-1,0}$ (s)	B (m)	R_c (m)	R_c/H_{m0}	B/H_{m0}	WG3	WG5	WG6	WG7	H_{m0} (m)	$T_{m-1,0}$ (s)	K_t (-)
WP6-NOU-B5-R05-JSW1	0.071	1.41	1.44	5	-0.05	-0.70	70.4					0.020	11.1	0.275
WP6-NOU-B5-R15-JSW1	0.074	1.41	1.42	5	-0.15	-2.03	67.6		0.062			0.057	1.52	0.770
WP6-NOU-B5-R05-JSW2	0.095	1.57	1.57	5	-0.05	-0.53	52.6					0.031	10.0	0.326
WP6-NOU-B5-R10-JSW2	0.096	1.57	1.55	5	-0.10	-1.04	52.1	0.074			0.045	0.047	2.05	0.490
WP6-NOU-B5-R15-JSW2	0.091	1.57	1.57	5	-0.15	-1.66	55.3		0.058		0.053	0.051	2.00	0.564
WP6-NOU-B7-R10-JSW2	0.095	1.57	1.54	7	-0.10	-1.05	73.7				0.044	0.042	1.81	0.442
WP6-NOU-B7-R10-JSW3	0.102	1.64	1.63	7	-0.10	-0.99	69.0		0.047		0.045	0.041	2.15	0.404
WP6-NOU-B7-R10-JSW4	0.118	1.70	1.70	7	-0.10	-0.85	59.3	0.085				0.054	3.23	0.458

Wave parameters are determined once the bank profile has become relatively stable (after approx. 1000 waves)

K_t is based on wave heights behind (WG8) and in front (WG2) of sandbank

3.4.2.2 Sandbank profile response

Besides the wave damping capacity, the extent of sandbank profile deformation to attack by cross-shore processes is an indicator of the nourishment efficiency.

Figure 3-34 through Figure 3-41 show the time-dependent bank profile response for each of the test scenarios, respectively. It is generally observed that major bank deformation took place within the first 1000 waves, after which the bank profile was relatively stable with a slow evolution rate. Profile changes mostly occurred on the outer bank slope with the typical storm-induced erosion-accretion pattern, the inner slope remained relatively intact. In cases of low crest submergence, i.e. $-R_c/H_{m0} < 1.0$, the bank crest was even slightly elevated due to onshore transport and deposition (see e.g.Figure 3-34 to Figure 3-36).

Within the tested conditions, it appears that the sandbank did not undergo major profile deformation. There was no clear difference in the extent of profile deformation between the two cases of bank crest width. The overall dimensions of the sandbank were more or less unchanged during wave attacks, which helped maintain wave transmission as it was initially designed.

3.4.3 Summary and Remarks on large-scale nourishment

Eight mobile-bed experiments on the large-scale nourishment by sandbanks were carried out to increase understanding of the physical processes involved. The test program covers several typical monsoon wave and sandbank geometric conditions.

The wave hydrodynamics at the sandbank is typically governed by drastic spectral transformation through the processes of dissipation of short-period waves and generation of IG waves. Because short-period energy is mostly dissipated within a distance less than the bank crest width, long-period energy is dominant in the transmitted wave spectra behind the bank. The wide sandbank appears to generally effective in damping waves with small relative crest submergence (i.e. $-R_c/H_{m0} < 1.0$). None of the existing formulations of wave transmission at conventional structures are reliable for such a wide sandbank crest and more importantly as the effect of IG waves is not included. For the functional design on wave transmission, the approach by Angremond et al. (1996) for smooth and impermeable structures can be used as a first approximation. For more reliable prediction of wave transmission an appropriate numerical model validated with the experimental data can be used.

Generally speaking, the sandbank profile response to the cross-shore attack by monsoon waves appears to be rather mild, even in cases of small crest submergence. It can be concluded that the cross-shore processes are generally important for consideration of the sandbank wave damping capacity rather than that of the design nourishment volume. The weak and slow profile deformation together with high wave damping capacity also suggest that the nourishment by near-shore sandbanks can be a viable solution.

Before coming up with a design for the nourishment, extensive numerical morphological studies are necessary to incorporate some important effects such as 3D bathymetry, long-shore transport processes, spatial layout, etc. Experimental data on the wave hydrodynamics and profile evolution should be used for numerical validations.

WP6-NOU-B5-R05-JSW1: $R_c/H_{m0} = -0.70$; $B/H_{m0} = 70.4$; $K_t = 0.275$

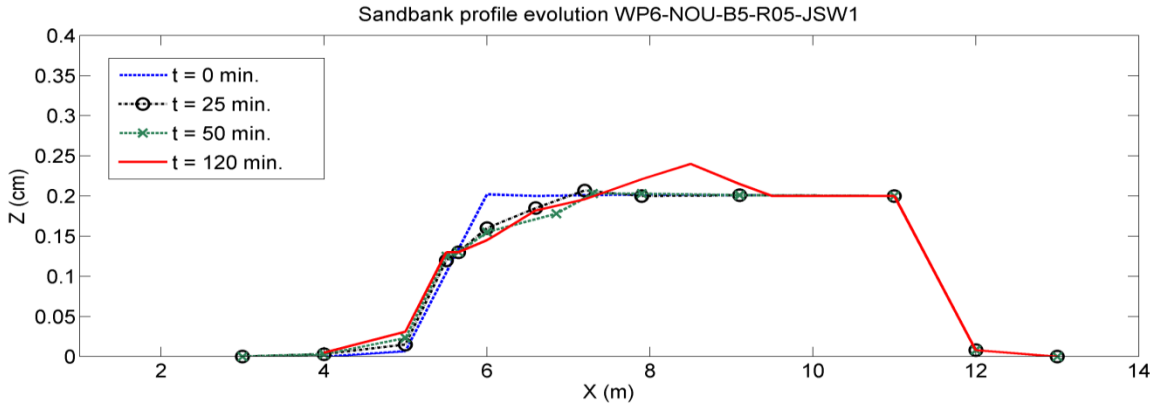

Figure 3-34 Sandbank profile response - Scenario WP6-NOU-B5-R05-JSW1

WP6-NOU-B5-R15-JSW1: $R_c/H_{m0} = -2.03$; $B/H_{m0} = 67.6$; $K_t = 0.77$

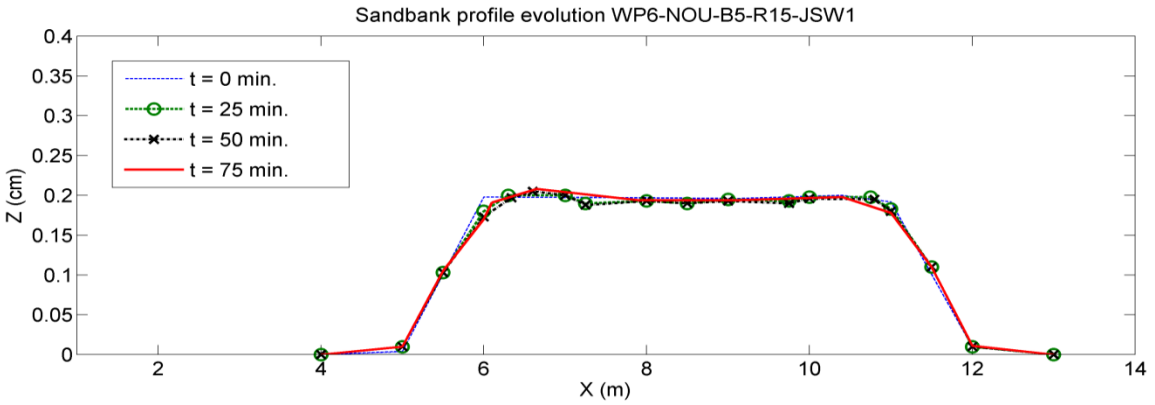

Figure 3-35 Sandbank profile response - Scenario WP6-NOU-B5-R15-JSW1

WP6-NOU-B5-R05-JSW2: $R_c/H_{m0} = -0.53$; $B/H_{m0} = 52.6$; $K_t = 0.326$

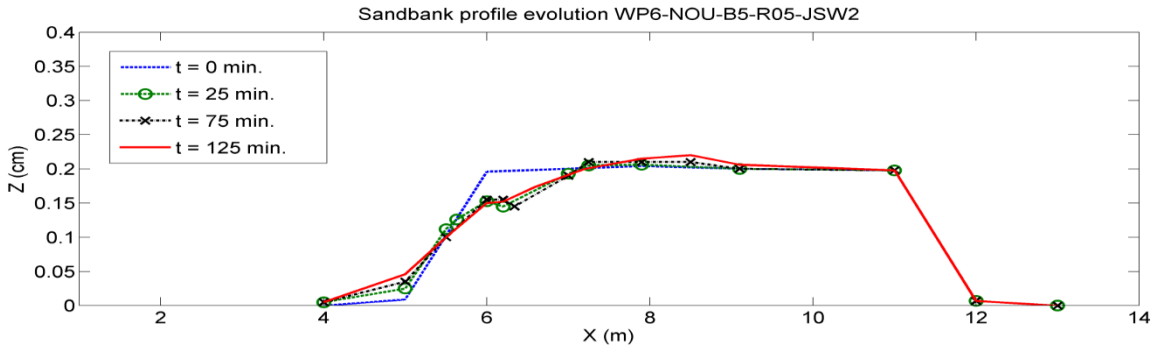

Figure 3-36 Sandbank profile response - Scenario WP6-NOU-B5-R05-JSW2

WP6-NOU-B5-R10-JSW2: $R_c/H_{m0} = -1.04$; $B/H_{m0} = 52.1$; $K_t = 0.49$

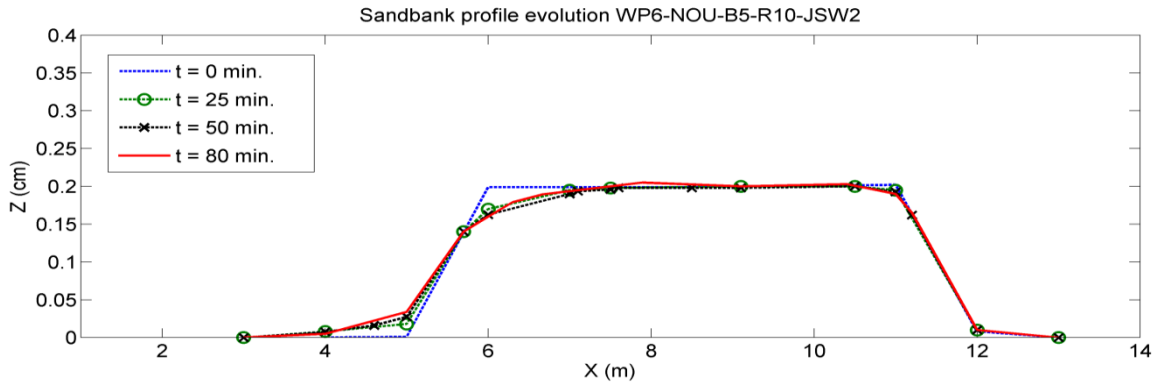

Figure 3-37 Sandbank profile response - Scenario WP6-NOU-B5-R10-JSW2

WP6-NOU-B5-R15-JSW2: $R_c/H_{m0} = -1.66$; $B/H_{m0} = 55.2$; $K_t = 0.564$

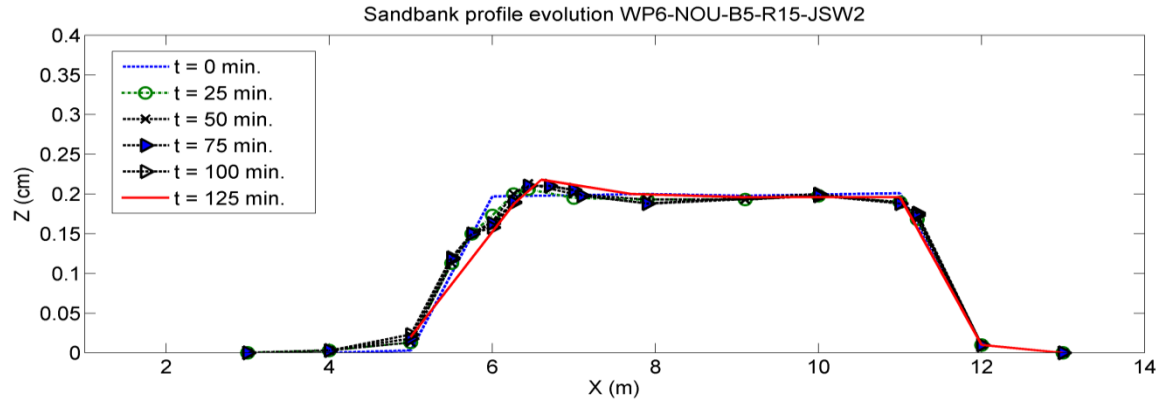

Figure 3-38 Sandbank profile response - Scenario WP6-NOU-B5-R15-JSW2

WP6-NOU-B7-R10-JSW2: $R_c/H_{m0} = -1.05$; $B/H_{m0} = 73.7$; $K_t = 0.442$;

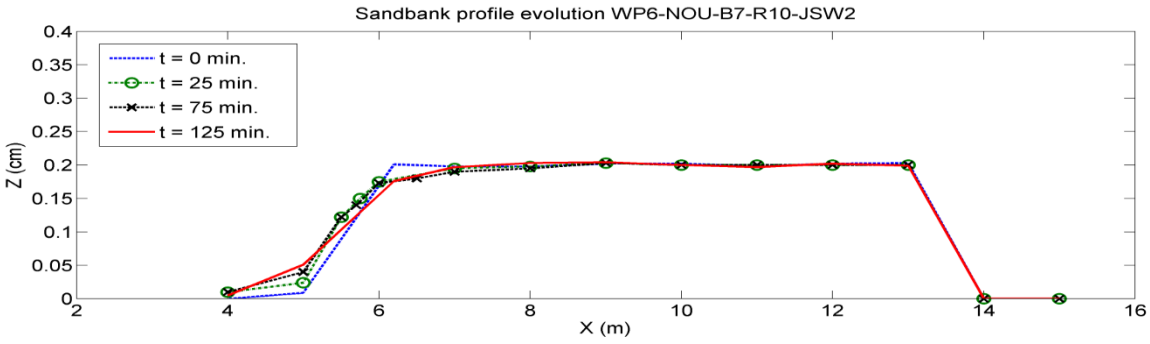

Figure 3-39 Sandbank profile response - Scenario WP6-NOU-B7-R10-JSW2

WP6-NOU-B7-R10-JSW3: $R_c/H_{m0} = -0.99$; $B/H_{m0} = 69.0$; $K_t = 0.404$

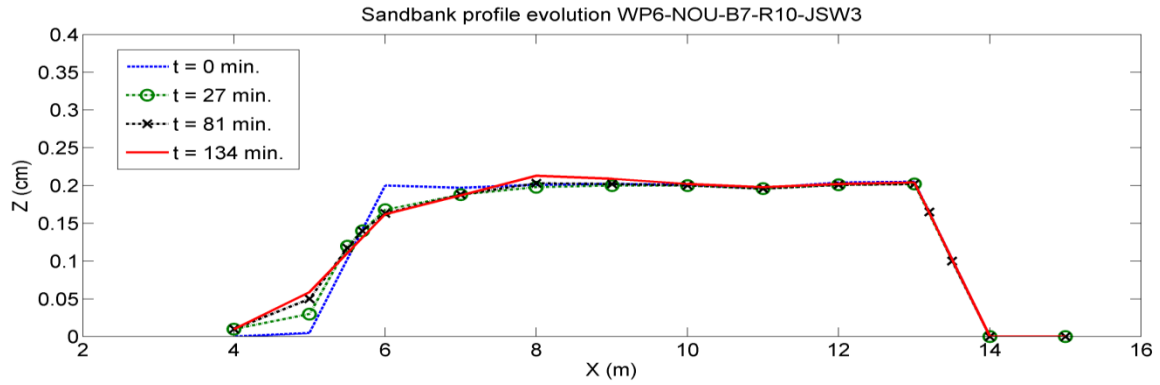

Figure 3-40 Sandbank profile response - Scenario WP6-NOU-B7-R10-JSW3

WP6-NOU-B7-R10-JSW4: $R_c/H_{m0} = -0.85$; $B/H_{m0} = 59.3$; $K_t = 0.458$

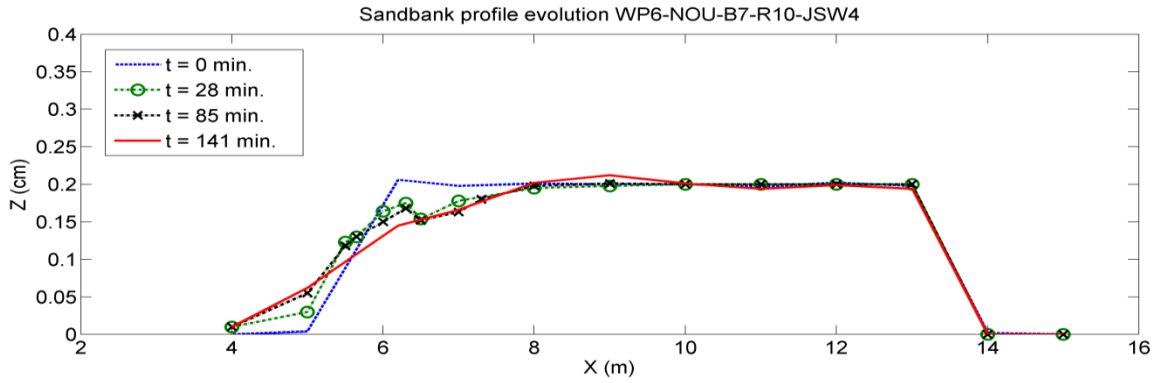

Figure 3-41 Sandbank profile response - Scenario WP6-NOU-B7-R10-JSW4

4. Numerical modelling to simulate the impact of Protection measures

To study the impact of protection measures, two set of MIKE21 and Telemac2D have been applied with parameters described in Table 4-1.

Table 4-1 Parameters of MIKE21 and Telemac2D models application

Site	Model	Domain	Number of element	Maximum size (m)	Minimum size (m)	Computing Time/month (CPU-64 processors)/ (hour)
Go Cong	MIKE21	Regional	64,608	50,000	2000	10
		Local	74,739	2000	500	9
		Study	48,077	500	10	60
	Telemac2D	Regional	65,198	57,000	733	12
		Local	223,988	7,900	16	16
		Study	101,216	2,600	8	18
Phu Tan	MIKE21	Regional	64,608	50,000	2000	10
		Local	74,739	2000	500	9
		Study	31,702	1000	8	24
	Telemac2D	Regional	124,000	10,000	200	
		Local	124,000	10,000	200	
		Study	87,000	2000	3_8	

4.1 At Go Cong, Tien Giang province

4.1.1 MIKE21 models

With the nesting methodology, from the the regional model (with 64,608 elements and the minimum edge length of 2km) to local model (with 74,739 elements and the minimum edge length of 500 m at the shore area and 15m in the river mouth) and study model (with 48,077 elements and the minimum edge length of 10m). These models were discussing in WP4 and WP5 where all of the models were calibrated/ validated with the project in-situ survey data in the SW monsoon 2016 and NE monsoon 2017 and other available data, including satellite from finished projects. This part we discuss the impact of protection measures in the study models.

4.1.1.1 Breakwater impacts

a) Breakwater configuration at Go Cong

One of the protection measures at Go Cong is T breakwater and its configuration is presented in. Table 4-2 and Figure 4-1.

Table 4-2 T Breakwater configurations

No	SCENARIOS	Senario description	BREAKWATER CONFIGURATION				Note
			Lengh (Ls)(m)	Distance from shoreline (Y)(m)	Gap between two breakwaters (Lg)(m)	Crest elevation of breakwaters (m)	
1	KB0	Baseline					
2	KB1	T shape breakwaters	600	300	30	2.2	The crest elevation of cross shore breakwaters is +0.5 m
3	KB2	T shape breakwaters	600	300	50	2.2	
4	KB3	T shape breakwaters	600	300	70	2.2	

The mesh of the study area model is an unstructured mesh with the triangular element occupying most of the sea area but with the quadrilateral part in most of the rivers. To assess the impact of the protection measures in the area of Go Cong, the net areas are divided very smoothly with a grid step of about 10m ÷ 15m (Figure 4-1).

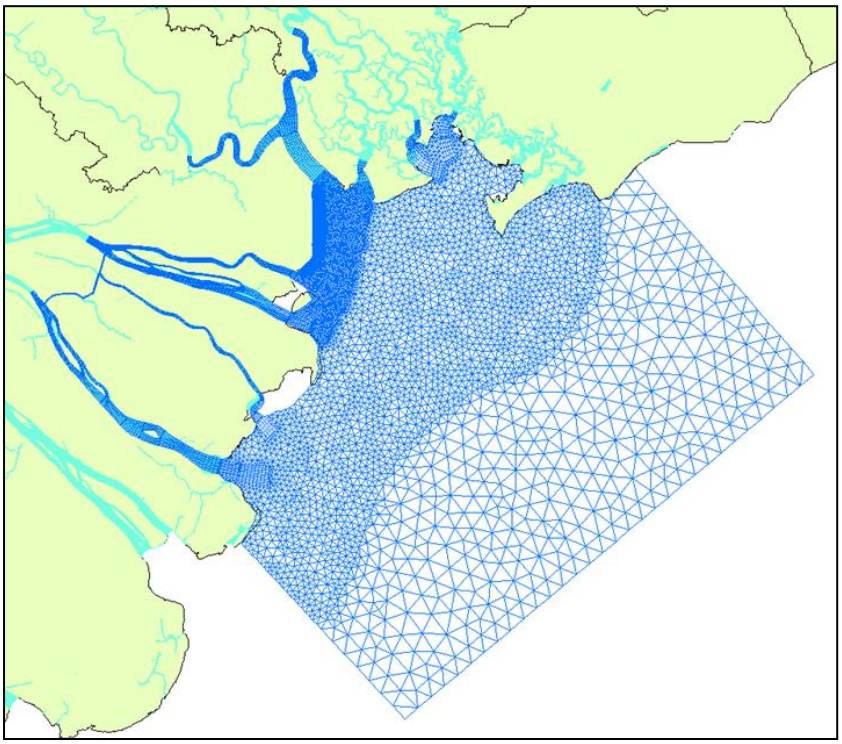

Figure 4-1 Detail meshes of the study area

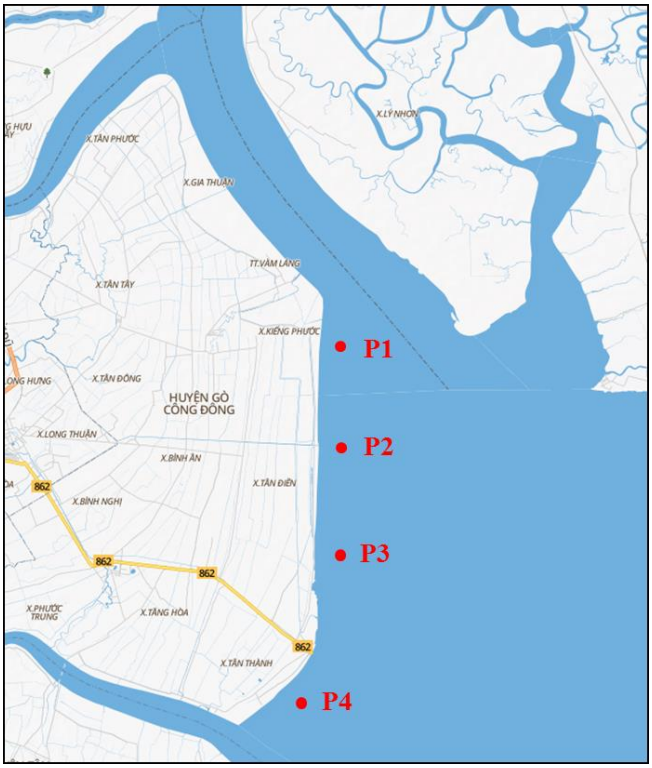

Figure 4-2 Locations for analyze impacts of breakwater in the study area

b) Breakwaters impact on flow

Figure 4-3 and Figure 4-4 illustrates the efficiency of breakwaters in reducing the flow velocity. It can be seen that the breakwaters has significantly reduced the velocity at P1 in terms of both the intensity and the duration of the high velocity. All scenarios increase the flow rate of less than 0.1 m/s to over 90% for both northeast and southwest monsoon. The difference between the scenarios can be seen by flow percentage less than 0.1 m/s reduced as the distance between the two breakwaters increases.

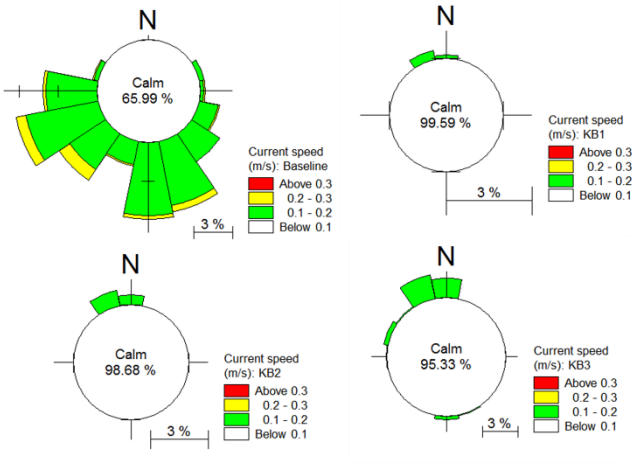

Figure 4-3 Current roses at P1 in the Northeast monsoon (25/12/2013÷ 5/2/2014) of Baseline (KB0), KB1, KB2, KB3 scenarios

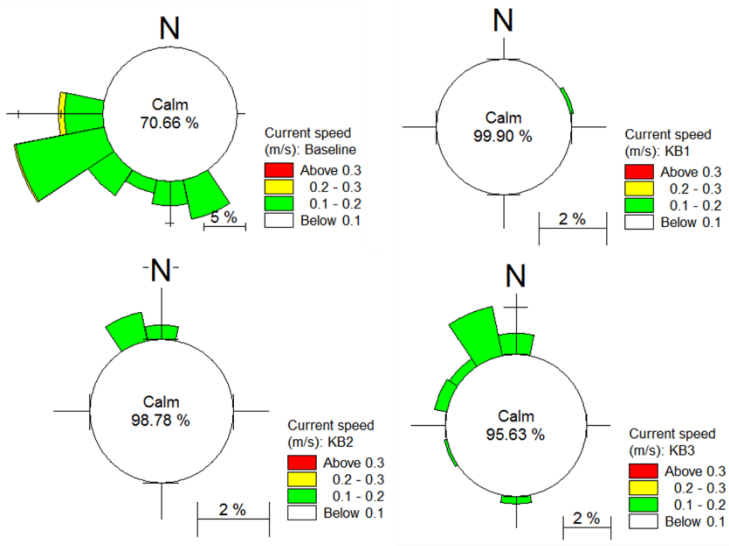

Figure 4-4 Current roses at P1 in the Southwest monsoon (25/8/2014÷ 5/10/2014) of Baseline (KB0), KB1, KB2, KB3 scenarios

c) Breakwaters impact on waves

In order to consider the effect of wave reduction between T-shaped breakwaters, sections as shown in Figure 4-5 are presented for analysis. The distance between the cross section 1 and section 2 is 50 m. The effect of wave reduction between the scenarios in sections 1, 2 and 3 is shown in Figure 4-6 to Figure 4-8. Dramatic change between the baseline (KB0) scenario and protection scenarios can be recognised. The wave heights at the section 1, 2 in the northeast monsoon of KB0 are about 1 ÷ 1.2m. After protection by breakwaters, the wave heights between the two breakwaters are reduced to less than 0.6m. It must be noted that in the spectral wave

model used diffraction is not included, so in reality the energy behind the gap will be spread more laterally.

The effect of wave reduction between scenarios are different. The smaller gap between the breakwaters (Lg), the better the wave reduction effect. In this study, the reduction effect of KB3 (Lg = 30m) was highest compared to Lg = 50m (KB2) and Lg = 70m (KB3). However, considering the significant wave height in section 3 (Figure 4-8), with KB3 (Lg = 70m) wave height higher than 0.6m was about 50m from breakwater landward. Therefore, in order to achieve the target of wave reduction of Hs<0.6 m, Lg should not be higher than 70m if not using additional measures to combine such as bamboo fence for wave reduction inside the breakwater.

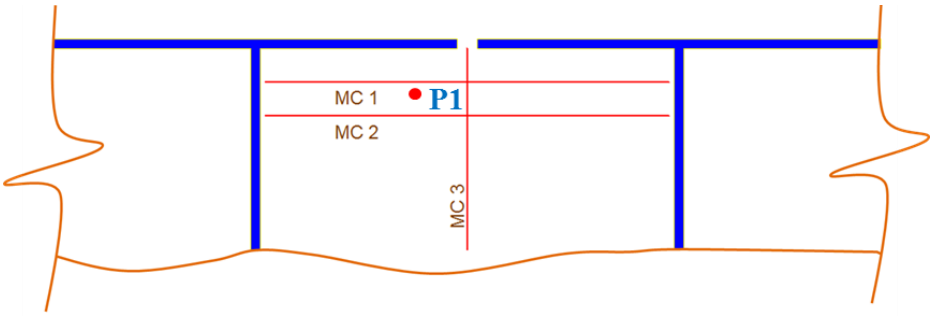

Figure 4-5 Cross-sectional locations to check the impact of T-shaped breakwaters

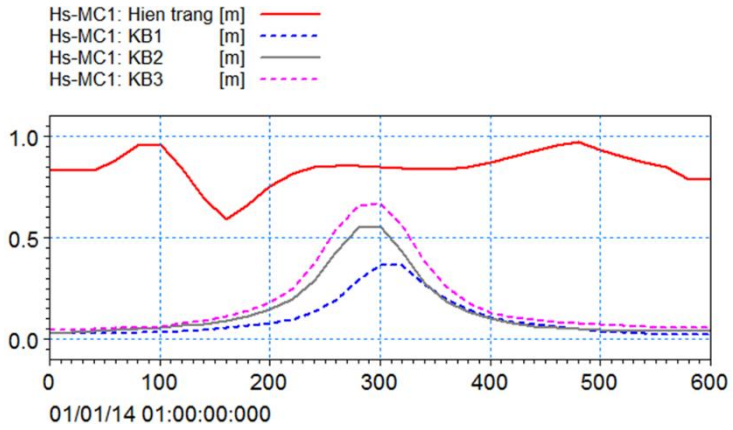

Figure 4-6 Wave heights at section 1 of KB0, KB1, KB2 and KB3 scenarios

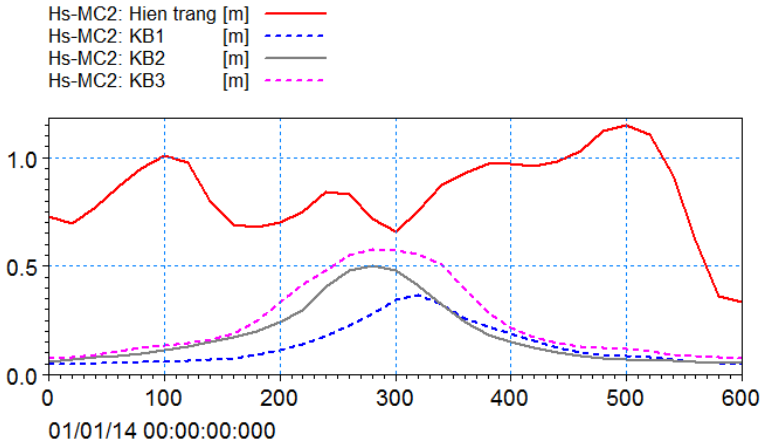

Figure 4-7 Wave heights at section 2 of KB0, KB1, KB2 and KB3 scenarios

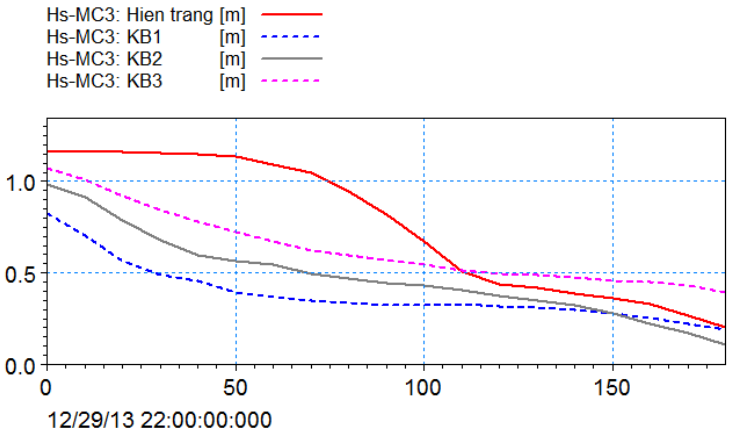

Figure 4-8 Wave heights at section 3 of KB0, KB1, KB2 and KB3 scenarios

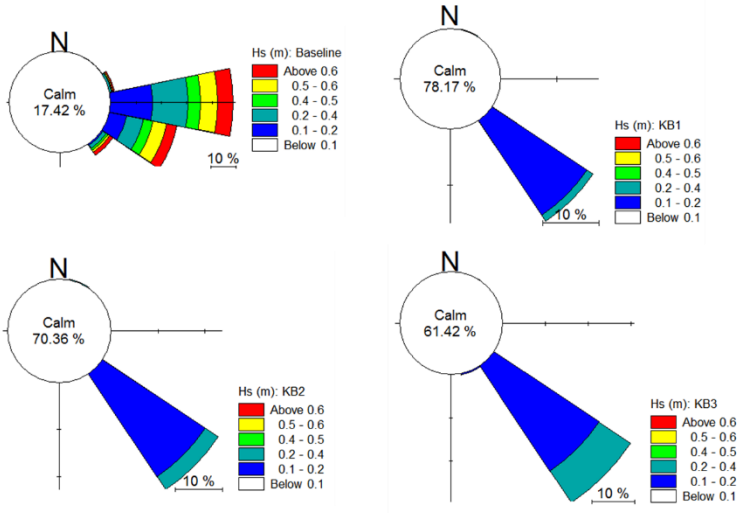

Figure 4-9 Significant wave roses in the Northeast monsoon (25/12/2014 ÷ 5/2/2014) at P1 for KB0, KB1, KB2 and KB3 scenarios

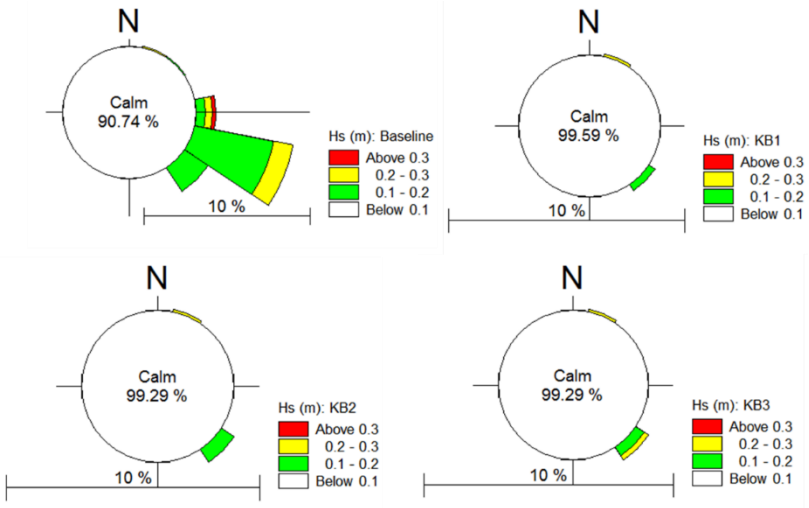

Figure 4-10 Significant wave roses in the Southwest monsoon (25/8/2014 ÷ 5/10/2014) at P1 for KB0, KB1, KB2 and KB3 scenarios

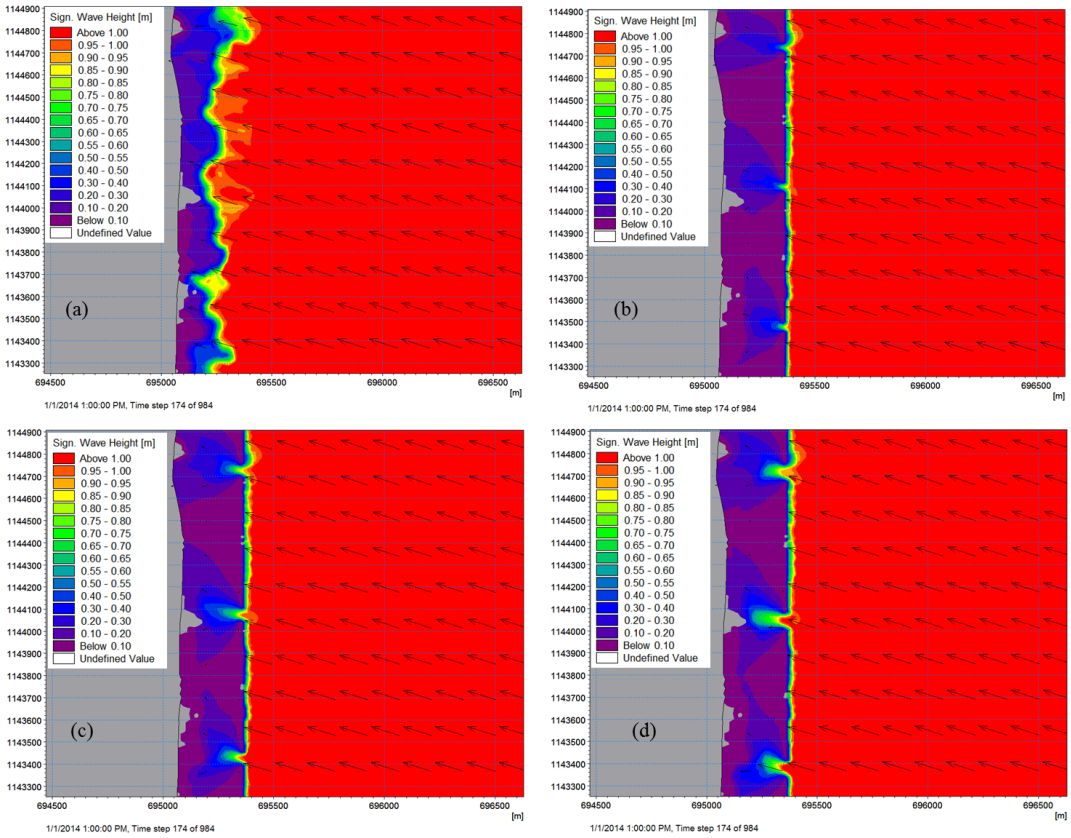

Figure 4-11 The North East monsoon wave fields between scenarios ((a) Baseline (KB0), (b) KB1, (c) KB2, (d) KB3)

d) Breakwaters impact on morphology

The morphological change with KB0 ÷ KB3 scenarios after 1 month of simulation of the Northeast monsoon (25/12/2013 ÷ 5/2/2014) were presented in *Figure 4-12* . Even during the Northeast monsoon, the breakwater impacts are quite clear. The difference between the gap of two breakwaters (Lg) is not much.

The accretion impact is clearer after 1 month of simulation of the southwest monsoon (25/8/2014 ÷ 5/10/2014) as expressed in *Figure 4-13*.

For erosion and accretion analysis, the study area is separated into two areas (*Figure 4-14*). Area 1 is from the shoreline to 2km offshore and length of 15.5 km. Area 2 is the rest of the study area. To analyse the impacts of breakwater, the net volume (V accr. – V ero.), average accretion thickness over the whole area 1 and the maximum erosion thickness (normally at the gap area) are considered. ***In general, the appropriate scenario is the one of high accretion of combined net volume for the two typical NE and SW months and low erosion thickness.*** The calculation results of erosion and accretion volume, after 1 month in the NE and SW monsoon are presented in *Table 4-3* and Table 4-4. *Table 4-5* combined the NE and SW monsoon results.

Due to the impacts in the whole area (2) is not significant, only the area 1 is considered in detail. The effect of accretion in Area 1 combining 2 months in the NE and SW monsoons in KB0, KB1, KB2 and KB3 are -0.087, 0.2996, 0.2891 and 0.2913 Mm3 respectively (equivalent to -0.003, 0.01, 0.009, 0.009 m respectively). For the average erosion in the gaps, they are -0.196, -0.653, -0.618 and -0.566 respectively. From these data, it can be seen that KB1 (with gap of 30 m) is better than among other scenarios in total accretion. It means that wave attenuation impact is the most important factor. All scenarios have erosion in the gap areas but not much different. However, in term of erosion at the gaps, KB3 is better than others. Therefore, KB1 and KB3 are the options.

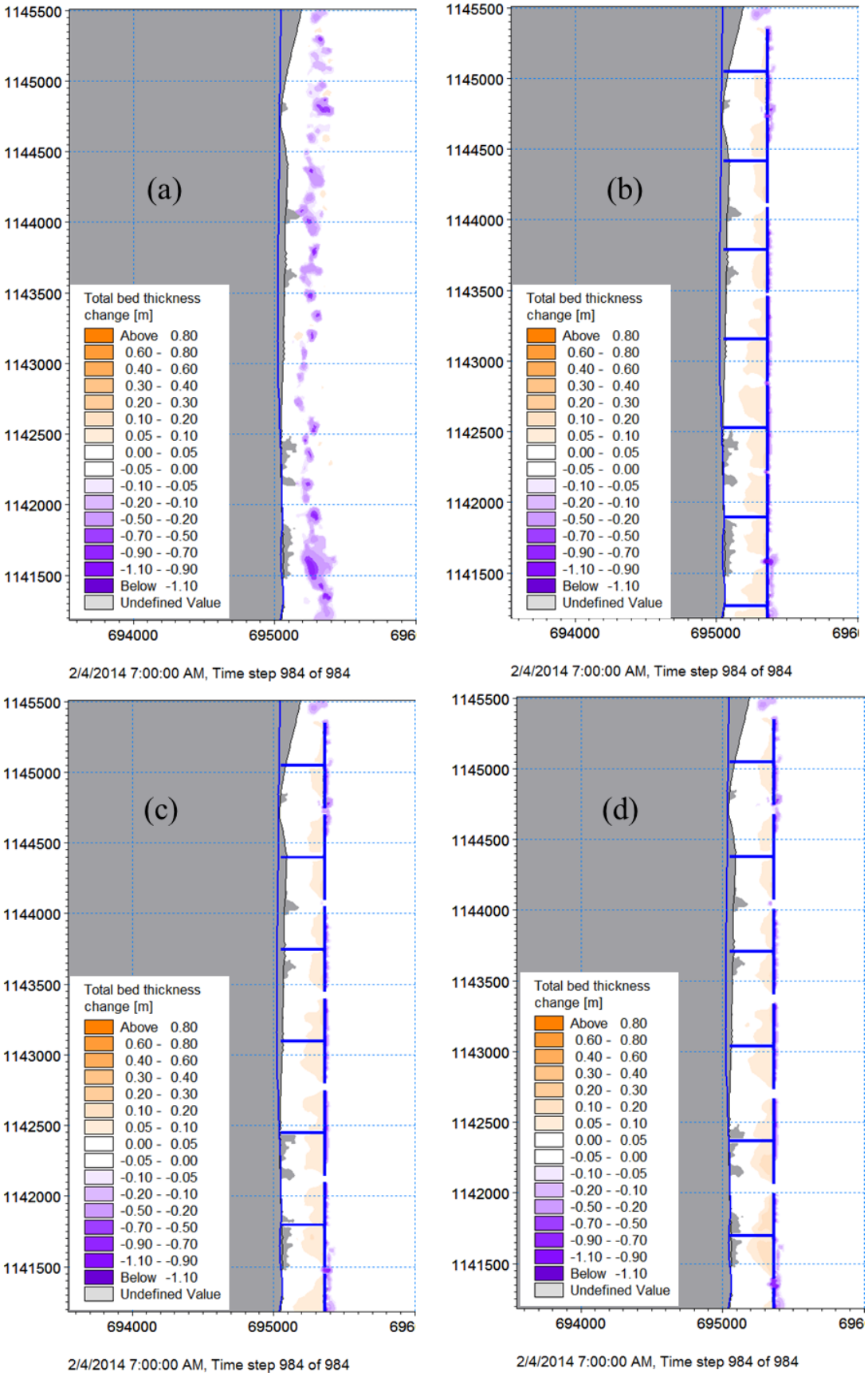

Figure 4-12 Distribution of erosion and accretion after one month of Northeast monsoon (January 2014) of scenarios (KB0 (a) KB1 (b), KB2 (c), KB3 (d)) – from Tieu River to Rach Bun sluice (middle of the shoreline)

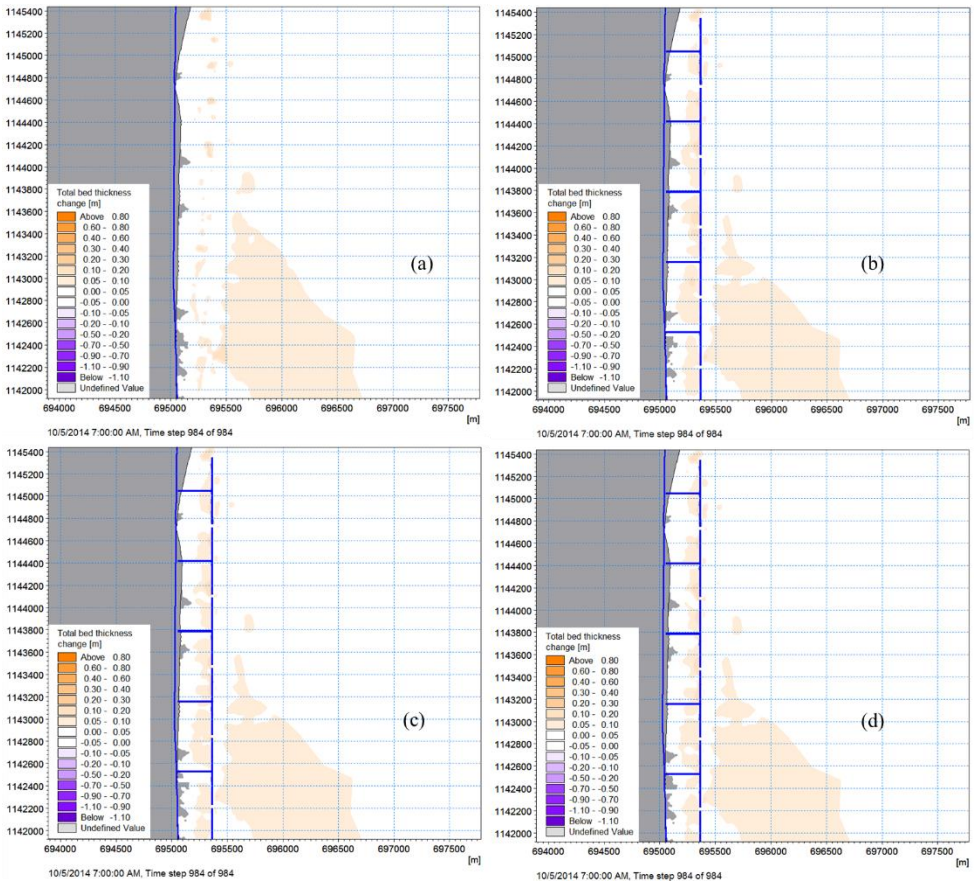

Figure 4-13 Distribution of erosion and accretion after one month of Southwest monsoon (September 2014) of scenarios (KB0 (a) KB1 (b), KB2 (c), KB3 (d)) - from Tieu River to Rach Bun sluice (middle of the shoreline)

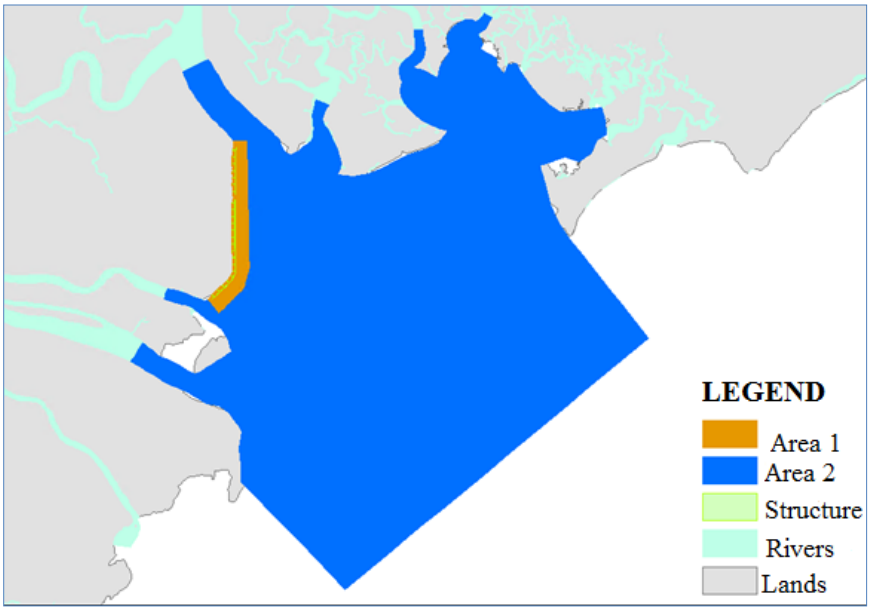

Figure 4-14 The zoning to calculate erosion and accretion volume in the study area

Table 4-3 Total accretion and erosion in study area after one month in the Northeast monsoon (25/12/2013 ÷ 5/2/2014) of scenarios

January 2014										
Scenarios	Area 2				Area 1				Net Vol. (Mm3)	Max Ero. THK (m)
	Vol. (10^6 m3)		Aveg THK (m)		Vol. (10^6 m3)		Aveg THK (m)			
	Accr.	Ero.	Accr.	Ero.	Accr.	Ero.	Accr.	Ero.		
KB0	11.062	-17.632	0.009	-0.013	0.3871	-1.0697	0.013	-0.037	-0.683	-0.196
G30(KB1)	11.337	-17.715	0.008	-0.013	0.4839	-0.8094	0.017	-0.028	-0.325	-0.653
G50(KB2)	12.242	-17.712	0.009	-0.013	0.4832	-0.8115	0.017	-0.028	-0.329	-0.618
G70(KB3)	11.339	-17.744	0.008	-0.013	0.4682	-0.7885	0.016	-0.027	-0.321	-0.566

Table 4-4 Total accretion and erosion in study area after one month in the SW monsoon (25/8/2014 ÷ 5/10/2014)

September 2014										
Scenarios	Area 2				Area 1				Net Vol. (Mm3)	Max Ero. THK (m)
	Vol. (10^6 m3)		Aveg THK (m)		Vol. (10^6 m3)		Aveg THK (m)			
	Accr.	Ero.	Accr.	Ero.	Accr.	Ero.	Accr.	Ero.		
KB0	34.4229	-11.7568	0.025	-0.008	0.7560	-0.16	0.027	-0.006	0.5960	0.000
G30(KB1)	34.4080	-11.7638	0.025	-0.008	0.7946	-0.17	0.028	-0.006	0.6246	-0.020
G50(KB2)	34.4075	-11.7641	0.025	-0.008	0.7881	-0.17	0.027	-0.006	0.6181	0.000
G70(KB3)	34.3827	-11.7644	0.025	-0.008	0.7823	-0.17	0.027	-0.006	0.6123	0.000

Table 4-5 Net volume (Mm3) and maximum erosion thickness (m) with various scenarios

Scenarios	Area 1				Combined January and September 2014		
	Jan.2014		Sep.2014		Vol. (Mm3)		Average thickness (m)
	Net Vol. (Mm3)	Max Ero. Thickness (m)	Net Vol. (Mm3)	Max Ero. Thickness (m)	Net Vol. (Mm3)	Max Ero. Thickness (m)	
KB0 (Baseline)	-0.683	-0.196	0.5960	0.000	-0.0870	-0.196	-0.003
G30(KB1)	-0.325	-0.653	0.6246	-0.020	0.2996	-0.653	0.010
G50(KB2)	-0.329	-0.618	0.6181	0.000	0.2891	-0.618	0.009
G70(KB3)	-0.321	-0.566	0.6123	0.000	0.2913	-0.566	0.009

e) Breakwaters impact on sediment reduction

In this part we assume the sediment reduction by 75% at all river mouths (due to damming upstream). Morphological variation for different scenarios of breakwater are expressed in Table 4-6 and

Table 4-7 for NE and SW monsoon months. This data can be used to compare to other protection measures. From the

Table 4-8 we can recognize that the G70 responded better to sediment deficit upstream.

Table 4-6 Accretion and erosion volume variation after one NE monsoon month (January 2014) (from 25/12/2013 ÷ 5/2/2014) with SSC reduction by 75%

January 2014				
Scenarios	Area 2		Area 1	
	(10^6 m3)		(10^6 m3)	
	V accretion	V erosion	V accretion	V erosion
KB0	11.0600	-17.6300	0.3900	-1.0700
KB0+ Reduce SSC 75%	7.9684	-17.8272	0.3113	-1.0704
G30 (KB1)	11.3400	-17.7100	0.4800	-0.8100
G30 (KB1) + Reduce SSC 75%	7.8855	-17.9202	0.3456	-0.8263
G50 (KB2)	12.2400	-17.7100	0.4800	-0.8100
G50 (KB2)+ Reduce SSC 75%	7.8958	-17.9556	0.3313	-0.8298
G70 (KB3)	11.3400	-17.7400	0.4700	-0.7900
G70 (KB3)+ Reduce SSC 75%	7.8867	-17.9490	0.3308	-0.8032

Table 4-7 Accretion and erosion volume variation after one SW monsoon month (September 2014) (from 25/8/2014 ÷ 5/10/2014) with SSC reduction by 75%

Scenarios	September 2014			
	Area 2 (10^6 m3)		Area 1 (10^6 m3)	
	V accretion	V erosion	V accretion	V erosion
KB0	34.4229	-11.7568	0.7560	-0.1640
KB0+ Reduce SSC 75%	15.0812	-12.5520	0.2824	-0.1949
G30 (KB1)	34.4080	-11.7638	0.7946	-0.1713
G30 (KB1) + Reduce SSC 75%	15.0708	-12.5581	0.3132	-0.2019
G50 (KB2)	34.4075	-11.7641	0.7881	-0.1678
G50 (KB2)+ Reduce SSC 75%	15.0702	-12.5582	0.3073	-0.1984
G70 (KB3)	34.3827	-11.7644	0.7823	-0.1676
G70 (KB3)+ Reduce SSC 75%	15.0702	-12.5578	0.3046	-0.1982

Table 4-8 Net volume (Mm3) and with various scenarios of gap and sediment reduction 75%

Scenarios	Combined January 2014 and September 2014				Net Vol. (Mm3)in Area1
	Area 2 (10^6 m3)		Area 1 (10^6 m3)		
	V accretion	V erosion	V accretion	V erosion	
KB0	45.483	-29.387	1.146	-1.234	-0.088
KB0+ Reduce SSC 75%	23.050	-30.379	0.594	-1.265	-0.672
G30 (KB1)	45.748	-29.474	1.275	-0.981	0.293
G30 (KB1) + Reduce SSC 75%	22.956	-30.478	0.659	-1.028	-0.369
G50 (KB2)	46.648	-29.474	1.268	-0.978	0.290
G50 (KB2)+ Reduce SSC 75%	22.966	-30.514	0.639	-1.028	-0.390
G70 (KB3)	45.723	-29.504	1.252	-0.958	0.295
G70 (KB3)+ Reduce SSC 75%	22.957	-30.507	0.635	-1.001	-0.366

f) Conclusion on the impact of breakwaters

- The breakwaters at the position of 300 m offshore, width of 600 m, gap between the two breakwaters of 30, 50 and 70 m, crest elevation of 2.2 m were simulated to study their impacts on flow, wave, morphology in the area of 2,000 m offshore from the shoreline and also with the sediment reduction by 75%.
- All of breakwaters can reduce flow, wave and increase accretion in the area, where the one with the gap of 70 m seemed better than others in term of trapping sediment and responding to the sediment reduction by 75%.

4.1.1.2 Sandbar impacts

Since the MIKE21 model cannot run cohesive and non-cohesive in one scenarios, we treated them in two steps.

The first step we run the model of sand transport assuming that the morphological changes in the area without sandbar are negligible, then only the sandbar deformation is considered. Fortunately the deformation of sandbar is not high so that we can go to the second step. Otherwise, the sandbar scenarios are not considered further.

The second step we run the model of mud transport, assuming that the average cross section of the deformation sandbar in the first step are unchanged. That means the sandbars now become "concrete" breakwater when morphological changes are considered the impact of sandbars.

a) Sandbar scenarios

There sandbar scenarios were studied as expressed in Table 4-9 and Figure 4-15.

Table 4-9 Sandbar configuration for Go Cong study area

No	Scenarios	Description	Sandbar configuration/dimensions (m)				
			Length	Distance of 2 units	Distance from shoreline	Width of sandbar	Top elevation
1	SB50	Sandbar at 500 m from the shoreline offshore	1000	200	500	50	-2.40
2	SB70	Sandbar at 500 m from the shoreline offshore	1000	200	500	70	-2.40
3	SB70(+0.0)	Sandbar at 500 m from the shoreline offshore	1000	200	500	70	+0.00

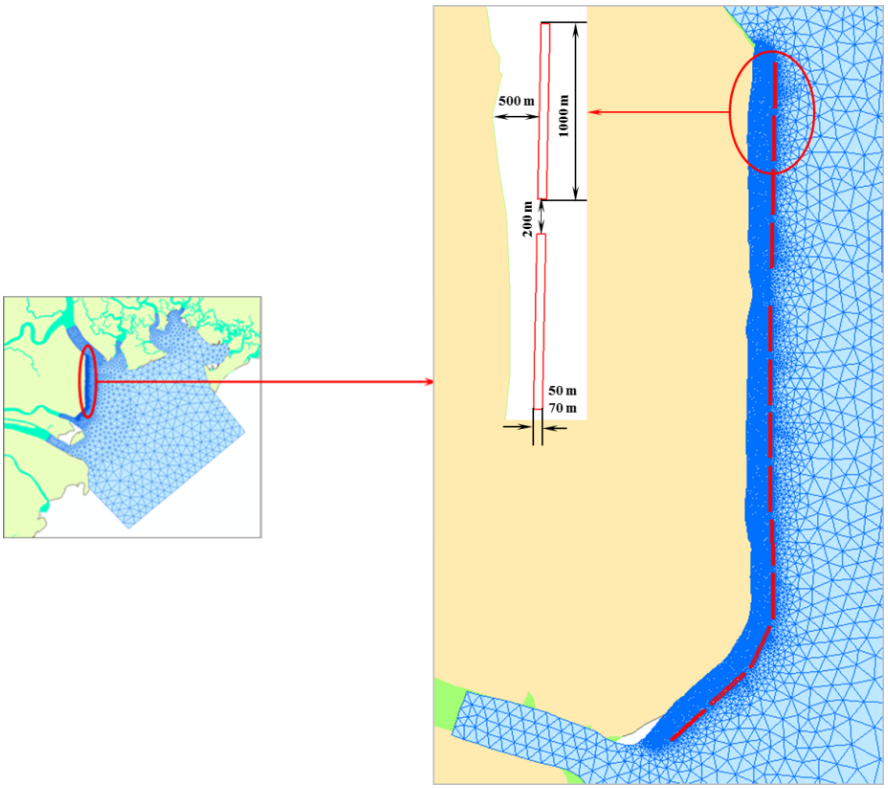

Figure 4-15 Sandbars in the study model at Go Cong, Tien Giang province

b) Calibrating the sandbar deformation by 21FM (HD&SW&ST) model

The deformation of sandbars in the physical models were presented in section Large-scale nourishment by near-shore sandbanks. In this section, numerical sand transport model is set up to calibrate sandbars deformation. Model set up is expressed in Figure 4-16 and Table 4-10. The smallest grid size is 2 m. In general, the deformation rates of the numerical model and physical model were similar. One scenario, for example presented in Table 4-10 and Figure 4-17.

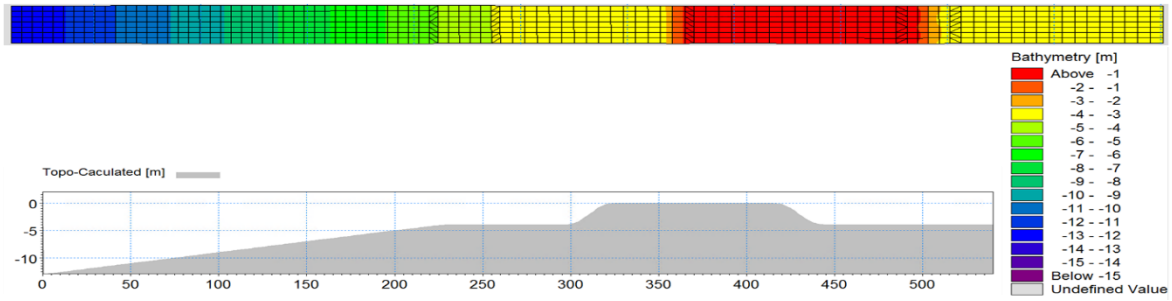

Figure 4-16 Numerical model 21FM (HD&SW&ST) set up for sandbar deformation calibration

Table 4-10 Typical scenario for 21FM (HD&SW&ST) model calibration

Tên kịch bản	MODEL					PROTOTYPE				
	B (m)	Rc (m)	Hm0 (m)	Tp (s)	Dura (min)	B (m)	Rc (m)	Hm0 (m)	Tp (s)	Dura (hrs)
WP6-NOU-B5-R15-JSW2	5	-0.15	0.1	1.53	80	100	-3	2	6.84	9.32

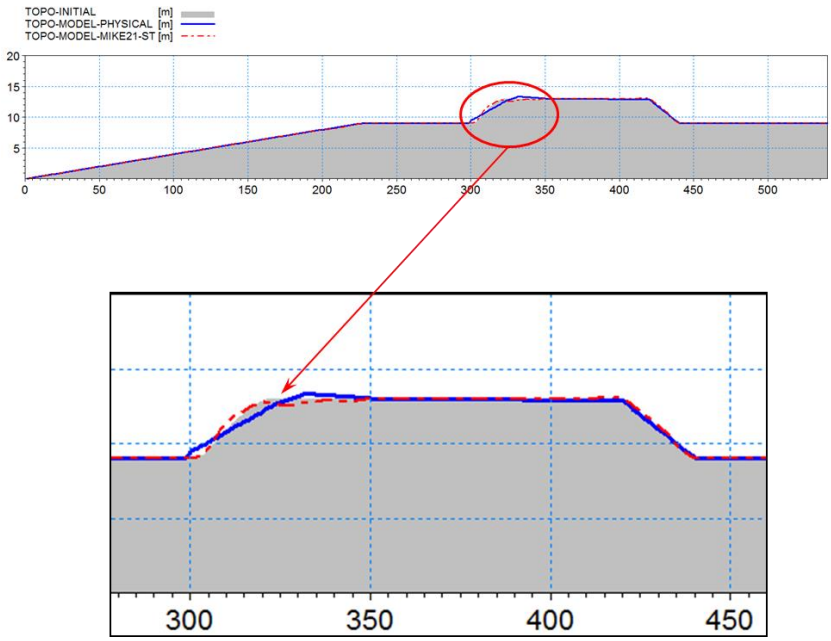

Figure 4-17 Calibration result of 21FM (HD&SW&ST) with typical scenario WP6-NOU-B5-R15-JSW2

c) *Morphological impact of sandbars*

This section we discuss the morphological changes of sandbars where sandbars are considered to be “concrete breakwater” and using MIK21FM-MT (as mentioned in part a)).

Table 4-11 and

Table 4-12 showed for the sandbar crest elevation of -2.4m (minimum sea level) there were insignificant impacts of sandbars (both B=50 m and B=70m) in NE and SW monsoon, since the erosion volume were nearly unchanged. Therefore, only sandbar of crest elevation of +0.0 m is considered later (see part 4.1.1.3)

Table 4-11 Morphological changes of sandbar impact after one month in the NE monsoon (January 2014)

January 2014									
Scenarios	Sand bar area				Shore area				Note
	Volume (10^6 m3)		Average thickness H(m)		Volume (10^6 m3)		Average thickness H(m)		Initial sand volume (10^6 m3)
	Acc.	Eros.	Accr.	Eros.	Acc.	Eros.	Accr.	Eros.	
KB0	0.3871	-1.07	0.02	-0.2					
SB50	0.390	-0.82	0.02	-0.2	11.06	-17.63	0.01	-0.12	0.346
SB70	0.472	-1.00	0.02	-0.2	10.52	-10.51	0.01	-0.10	0.466

Table 4-12 Morphological changes of sandbar impact after one month in the SW monsoon (September 2014)

September 2014									
Scenarios	Sand bar area				Shore area				Note
	Volume (10^6 m3)		Average thickness H(m)		Volume (10^6 m3)		Average thickness H(m)		Evaluation
	Acc.	Eros.	Accr.	Eros.	Acc.	Eros.	Accr.	Eros.	
KB0	0.76	-0.16	0.04	-0.03	34.42	-11.76	0.03	-0.03	
SB50	0.98	-0.18	0.05	-0.03	33.96	-8.66	0.03	-0.03	Good
SB70	0.98	-0.18	0.05	-0.03	33.96	-8.66	0.03	-0.03	Better

d) Sandbar deformation in 21FM (HD&SW&ST) model of the study area

The sandbars (of crest elevation of +0.0m and width of 70 m) lost volume after one month in the SW and NE monsoons were showed in Table 4-13. The lost volume happened mostly in the NE month (9.85 %) while in the SW month was very low (1.8%). For the both two months, the lost volume was about 12%.

The simulation area of sandbar lost is expressed in Figure 4-18. It can be seen the lost volume in the area near Soai Rap river mouth is higher than that in area near Cua Tieu mouth.

Table 4-13 Morphological changes of sandbars after one month in the NE monsoon (January 2014)

Calculation area of lost volume	Area 1	Area 2	Area 3	Total	Lost Percent
Initial Volume (Mm3)	1.183	0.959	0.418	2.560	0
Lost in Jan.2014 (Mm3)	-0.099	-0.09	-0.063	-0.252	-9.85
Lost in Sept.2014 (Mm3)	-0.023	-0.012	-0.01	-0.046	-1.80
Lost in Jan&Sept.2014 (Mm3)	-0.122	-0.103	-0.074	-0.299	-11.64

Figure 4-18 The simulation areas of sandbar lost volume in Go Cong

4.1.1.3 Comparison of breakwater and sandbar scenarios

This section discusses the different morphological impacts of the two scenarios of breakwaters and sandbars.

The breakwater BW-G70 (gap 70 m) was selected from the different gaps (G30, G50 and G70 m) when combining it's accretion impacts and response to the sediment deficit (-75%).

The sandbar scenarios of SB50 and SB70 with the crest elevation of -2.4 m did not have significant impacts on morphology, therefore the one of SB-70 and crest elevation of +0.0 m was considered and will be compared with breakwater BW-G70 scenario.

Figure 4-19 (Figure 4-20) and Figure 4-21 (Figure 4-22) presented the morphological variation after one month in the NE monsoon (Jan.2014) and in the SW monsoon (Sept. 2014) respectively.

Table 4-14 and Table 4-15 expressed the accretion and erosion volume after one month in the NE and SW monsoons. Table 4-16 combined the results of both NE and SW monsoon months.

It can be seen in Table 4-16 that the Sandbar scenario have higher impact on accretion in the area of 2 km from the shoreline offshore (accretion volume of 0.252 Mm3 for BW-G70 and 0.352 Mm3 for SB-70). It can be recognized that the sandbar width of 70 m and crest elevation of +0.0 m has maximum erosion depth of -0.19 m lower than the one of breakwater (BW-G70) of -0.62m.

For the case of sediment reduction by 75%, the response of the sandbar is better than breakwater as expressed in Table 4-17.

For detail comparison of breakwater and sandbar scenarios, the accretion volume and average thickness of additional areas from the shoreline to 300 m offshore (Area 300) for breakwater and to 500 m offshore for sandbar (Area 500) were calculated. Table 4-18 showed that breakwater for two typical months (NE and SW) can change the Area 300 from average erosion thickness of -0.04 m to accretion thickness of +0.04 m. The sandbar for two typical months (NE and SW) can change the Area 500 from average erosion thickness of -0.03 m to accretion thickness of +0.03 m. Again, in general, the sandbar scenario seems to be better than breakwater in term of trapping sediment in the large area.

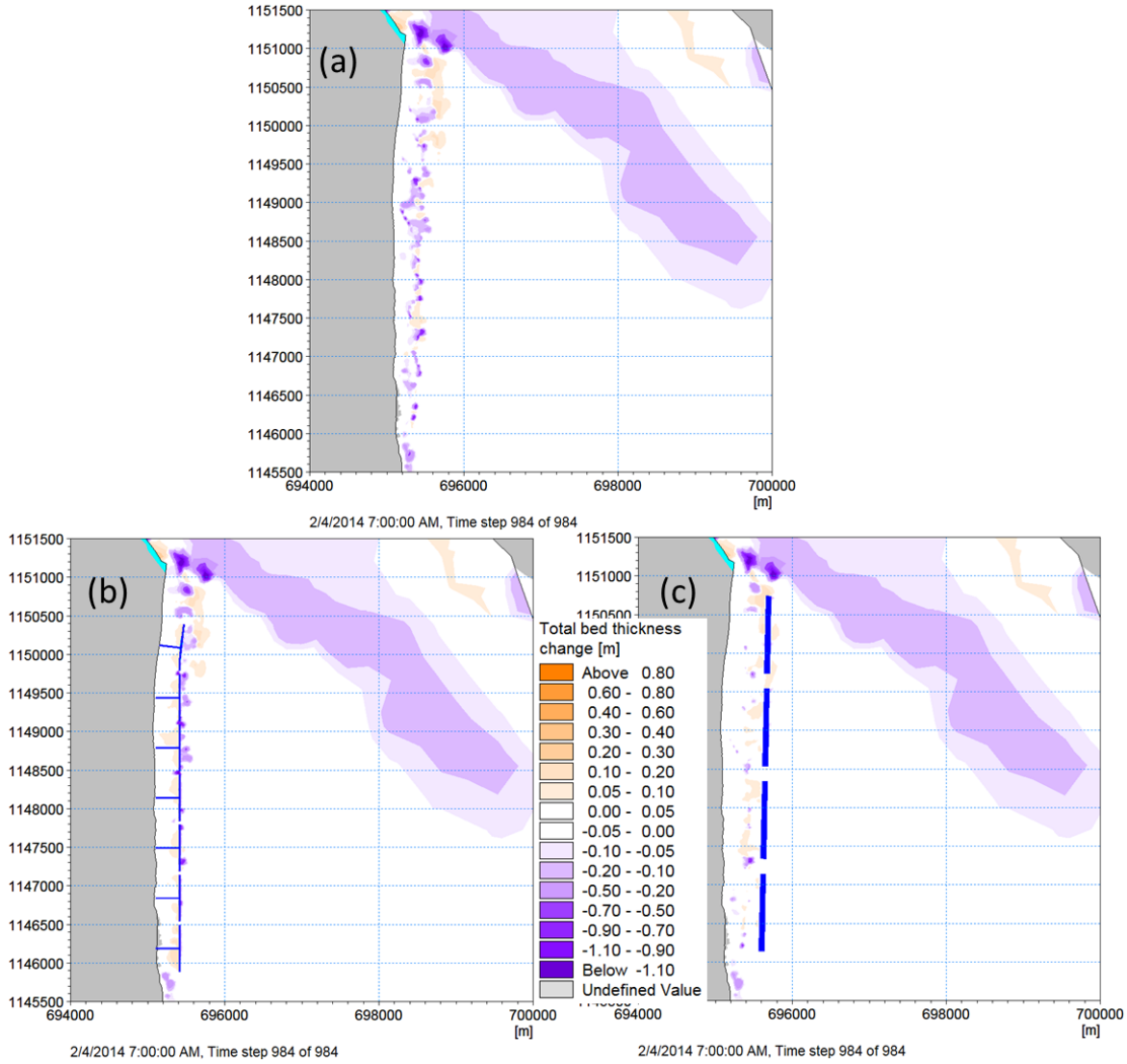

Figure 4-19 Distribution of erosion and accretion after one month of Northeast monsoon (January 2014) of scenarios (a)- Baseline, (b): BW G70, and (c): SB B70 (0.0) – from Soai Rap river to Rach Bun sluice

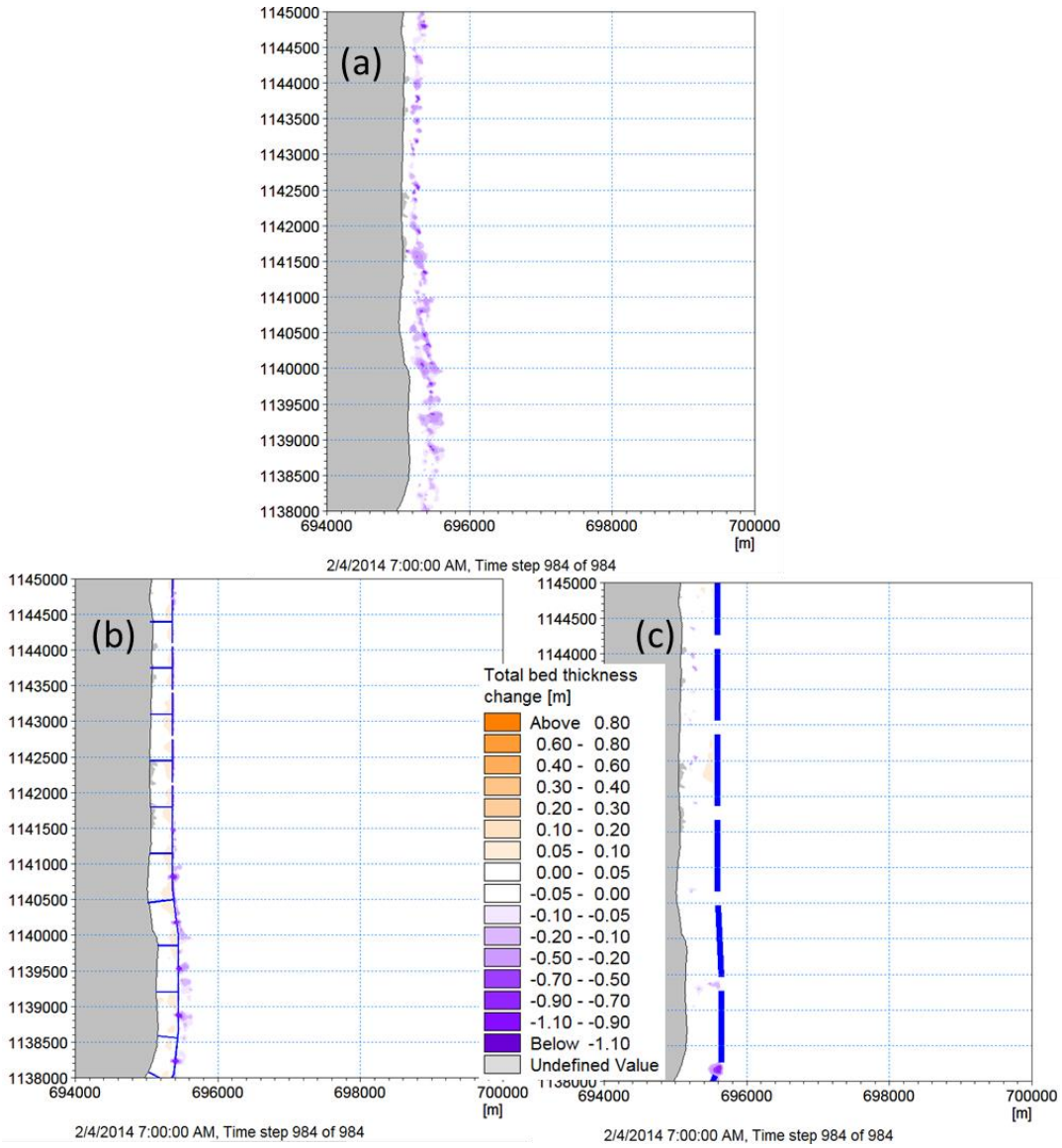

Figure 4-20 Distribution of erosion and accretion after one month of Northeast monsoon (January 2014) of scenarios (a): Baseline, (b): BW G70, (c): SB B70 – from Rach Bun sluice to Tieu River

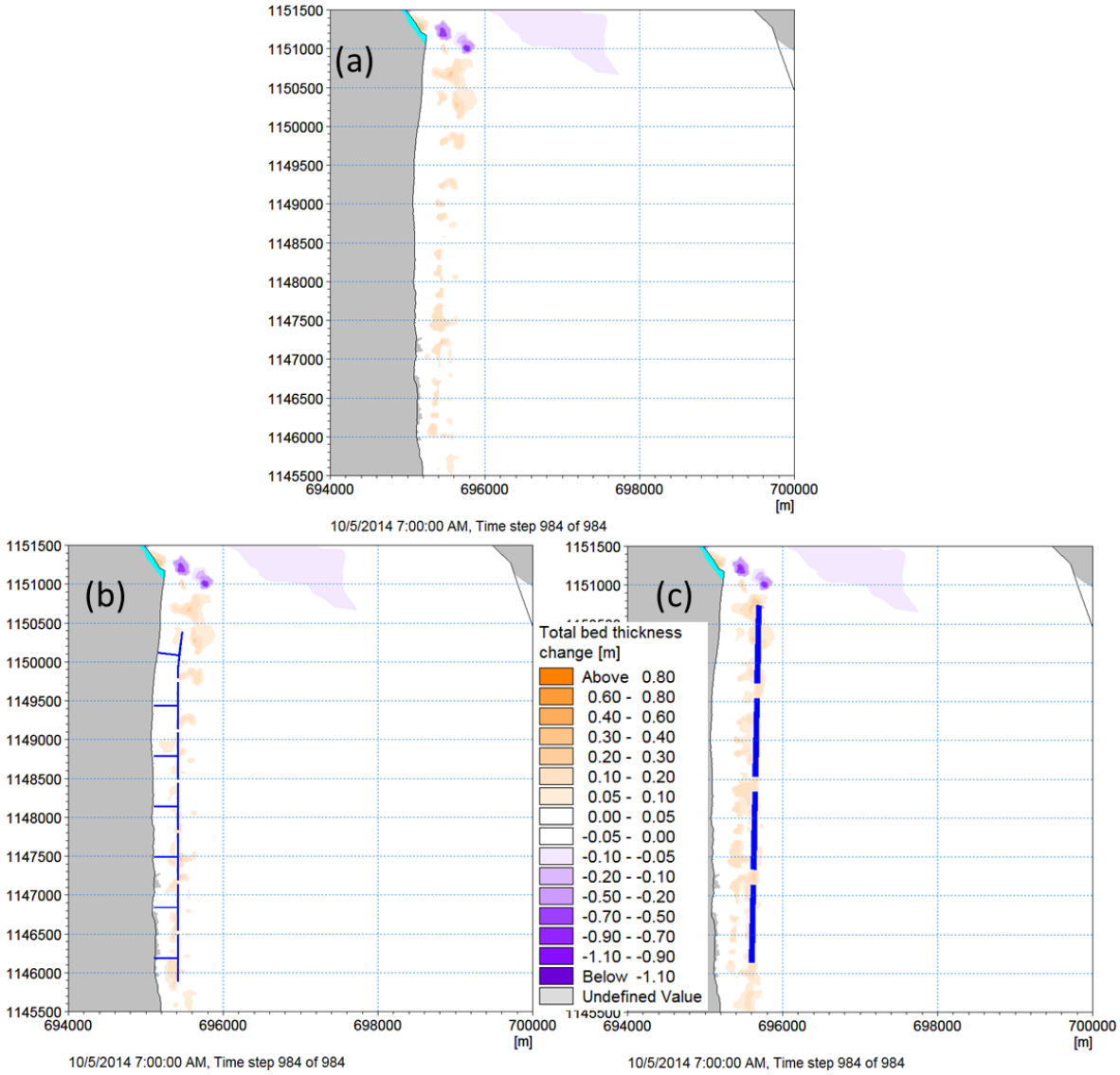

Figure 4-21 Distribution of erosion and accretion after one month of SW monsoon (September 2014) of scenarios (a)- Baseline, (b): BW- G70, and (c): SB- B70 (0.0) – from Soai Rap river to Rach Bun sluice

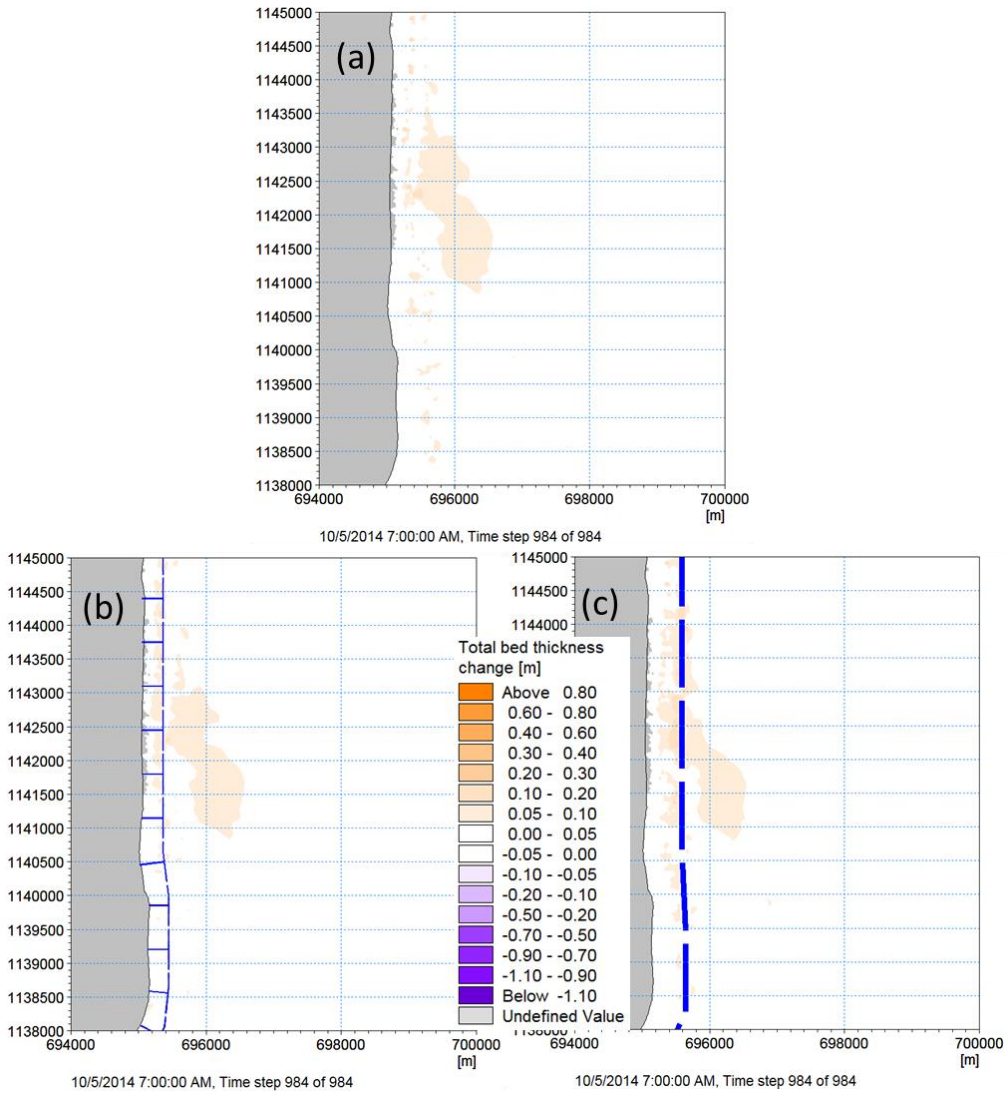

Figure 4-22 Distribution of erosion and accretion after one month of Southwest monsoon (September 2014) of scenarios (a): Baseline, (b): BW G70, (c): SB B70 – from Rach Bun sluice to Tieu River

Table 4-14 Accretion and erosion in Area 1 after one month in the NE monsoon (25/12/2013 ÷ 5/2/2014) of scenarios

January 2014						
Scenarios	Area 1					
	Vol. (10^6 m3)		Aveg THK (m)		Net Vol. (Mm3)	Max Ero. THK (m)
	Accr.	Ero.	Accr.	Ero.		
BASELINE	0.372	-0.714	0.013	-0.025	-0.341	
BW- G70(KB1)	0.377	-0.536	0.013	-0.019	-0.160	-0.615
SB B70(KB2)	0.328	-0.427	0.011	-0.015	-0.099	-0.194

Table 4-15 Accretion and erosion in Area 1 after one month in the SW monsoon (25/8/2014 ÷ 5/10/2014)

September 2014						
Scenarios	Area 1					
	Vol. (106 m3)		Aveg THK (m)		Net Vol. (Mm3)	Max Ero. THK (m)
	Accr.	Ero.	Accr.	Ero.		
BASELINE	0.567	-0.166	0.020	-0.006	0.401	
BW G50(KB1)	0.581	-0.169	0.020	-0.006	0.412	-0.007
SB B70(KB2)	0.617	-0.167	0.021	-0.006	0.451	-0.025

Table 4-16 Net volume (Mm3) and maximum erosion thickness (m) with various scenarios after one month in the NE and one month in the SW monsoon

Scenarios	Area 1				Combined Jan. and Sept. 2014		
	Jan.2014		Sep.2014		Net Vol. (Mm3)	Max Ero. THK (m)	Evaluation
	Net Vol. (Mm3)	Max Ero. THK (m)	Net Vol. (Mm3)	Max Ero. THK (m)			
BASELINE	-0.341	0.000	0.401		0.060		
BW-G50	-0.160	-0.615	0.412	-0.007	0.252	-0.615	Good
SB-B70(0.0)	-0.099	-0.194	0.451	-0.025	0.352	-0.194	Better

Table 4-17 Net sediment trapping volume (Mm3) and maximum erosion thickness (m) comparison of breakwater and sandbar in case of sediment reduction of 75%

Scenarios	Area 1				Combined January and September 2014		
	Jan.2014		Sep.2014		Vol. (Mm3)		Evaluation
	Net Vol. (Mm3)	Max Ero. Thickness (m)	Net Vol. (Mm3)	Max Ero. Thickness (m)	Net Vol. (Mm3)	Max Ero. Thickness (m)	
BASELINE	-0.341		0.401				
BASELINE+ REDUCE 75%	-0.470		0.082		-0.387		
G50(KB1)	-0.160	-0.615	0.412	-0.007	0.252	-0.615	
G70(KB1)+ REDUCE 75%	-0.295	-0.611	0.095	-0.007	-0.200	-0.611	Good
B70(KB2)	-0.099	-0.194	0.451	-0.025	0.352	-0.194	
B70(KB2) + REDUCE 75%	-0.202	-0.182	0.124	-0.025	-0.078	-0.182	Better

Table 4-18 Net volume (Mm3) and maximum erosion thickness (m) with various scenarios after one month in the NE and one month in the SW monsoon

Scenarios	Combined Jan. and Sept. 2014 - Area1 (2000)			Combined Jan. and Sept. 2014 - Area 300			Combined Jan. and Sept. 2014 - Area 500		
	Net Vol.	Max Ero. THK (m)	Ever. THK (m)	Net Vol.	Max Ero. THK (m)	Ever. THK (m)	Net Vol.	Max Ero. THK (m)	Ever. THK (m)

-75%									

4.1.2 Telemac2D models

With nesting approach, Telemac2D has been calibrated well from the Regional model (with 65,198 elements and minimum edge length is 733m) to Local Model (with 223,988 elements and minimum edge length is 16m) and study Model (with 101,216 elements and minimum edge length is 8m) (Figure 4-23) with water levels, discharges, tides, waves and currents, sediment transport and morphology especially the validation results based on the in-situ data of the LMDCZ project in October 2016 and February-March 2017, presented in WP5 Report.

This WP6 Report we discuss the efficiency and impacts of protection measures.

The mesh of the study area model is an unstructured mesh with the triangular element occupying most of the sea area but with the quadrilateral part in most of the rivers, with. To assess the impact of the protection measures in the area of Go Cong, the net areas are divided very smoothly with a grid step of about 8-10 m (Figure 4-23).

To study the impact of protection measures, various scenarios will be considered and expressed in Figure 4-23.

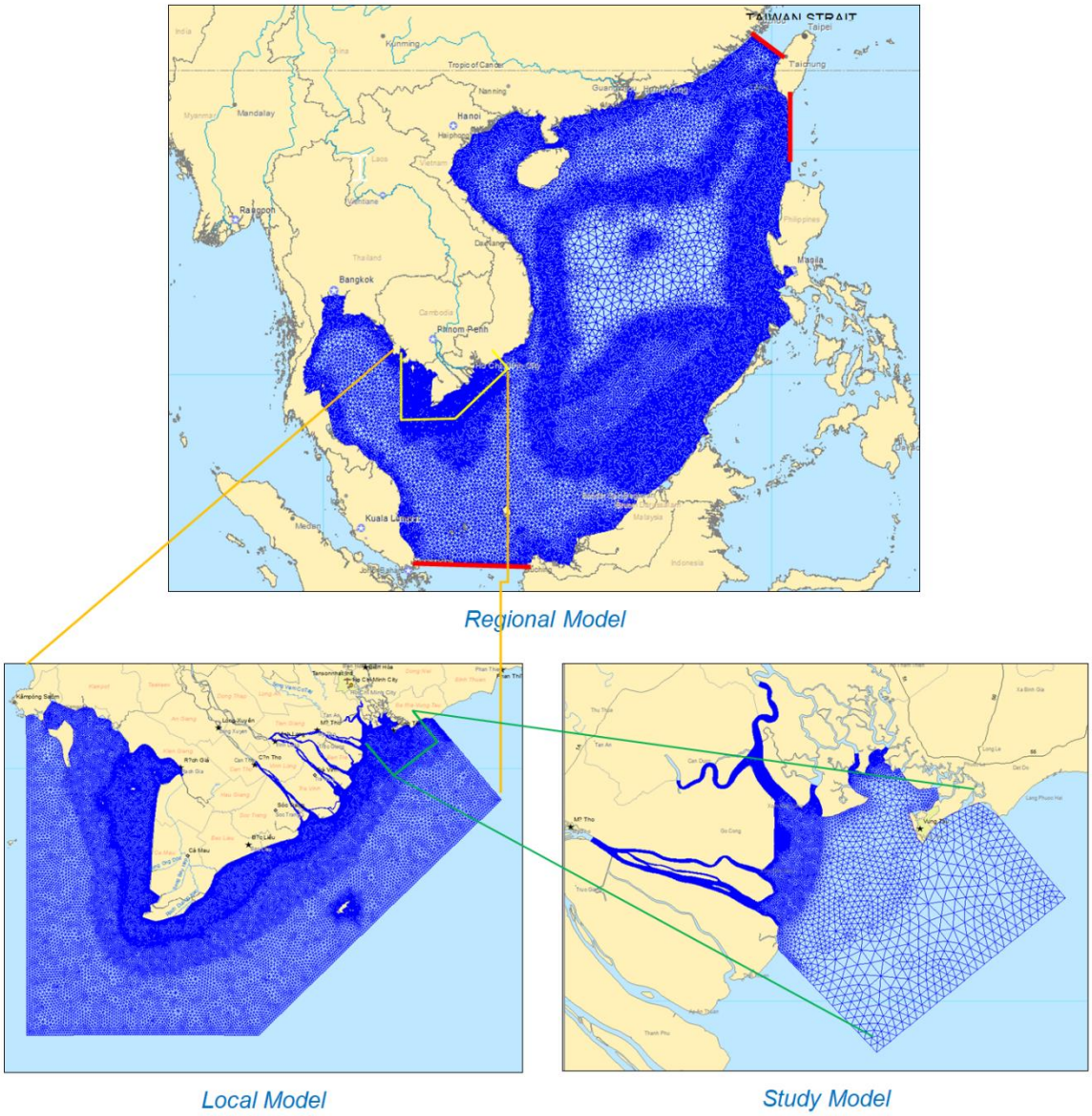

Figure 4-23 Nesting methodology for Telemac 2D models

The wave, flow and morphological changing between scenarios will be analyzed 3 cross sections (1,2,3) and 3 longitudinal sections (1',2',3') to the shoreline (Figure 4-24).

For more detailed analysis of erosion and accretion, 3 coastal zones are selected to extract data to compute the volumes (Figure 4-24).

- The zone 1: length of 14.5 km, width of 150 m and the area of 2.874.859 m^2.
- The zone 2: the length of 14.5 km, width of 300 m, and the area of 5.143.914 m^2. The zone 2 is the area from the hard breakwater to the shoreline.
- The zone 3 : length of 14.5 km, width of 1000 m and the area of 12.100.514 m^2.

Table 4-19 Scenarios for protection measures

No	SCENA-RIOS	Scenario description	BREAKWATER CONFIGURATION			
			Length (Ls)(m)	Distance from shoreline (Y)(m)	Gap between two breakwaters (Lg)(m)	Crest elevation (m)
1.	SC0	Baseline				
2.	SC1	T shape breakwaters	600	300	30	2.2

No	SCENA -RIOS	Scenario description	BREAKWATER CONFIGURATION			
			Length (Ls)(m)	Distance from shoreline (Y)(m)	Gap between two breakwaters (Lg)(m)	Crest elevation (m)
3.	SC2	T shape breakwaters	600	300	50	2.2
4.	SC3	T shape breakwaters	600	300	70	2.2
5.	SC4	Baseline + Sediment concentration at the upstream is reduced 75%				
6.	SC5	T shape breakwaters+ Sediment concentration at the upstream is reduced 75%	600	300	30	2.2
7.	SC6	T shape breakwaters+ Sediment concentration at the upstream is reduced 75%	600	300	50	2.2
8.	SC7	T shape breakwaters+ Sediment concentration at the upstream is reduced 75%	600	300	70	2.2
9.	SC8	Baseline + Sea Level Rise				
10.	SC9	T shape breakwaters + Sea Level Rise				
	SANDBARS CONFIGURATION					
			Length (Ls)(m)	Distance from shoreline	Width of sand-bar	Crest elevation
11.	SB1	Sand Bar	1000	500	50	-2.4
12.	SB2	Sand Bar	1000	500	70	0
13.	SB3	Sand Bar	1000	500	100	0

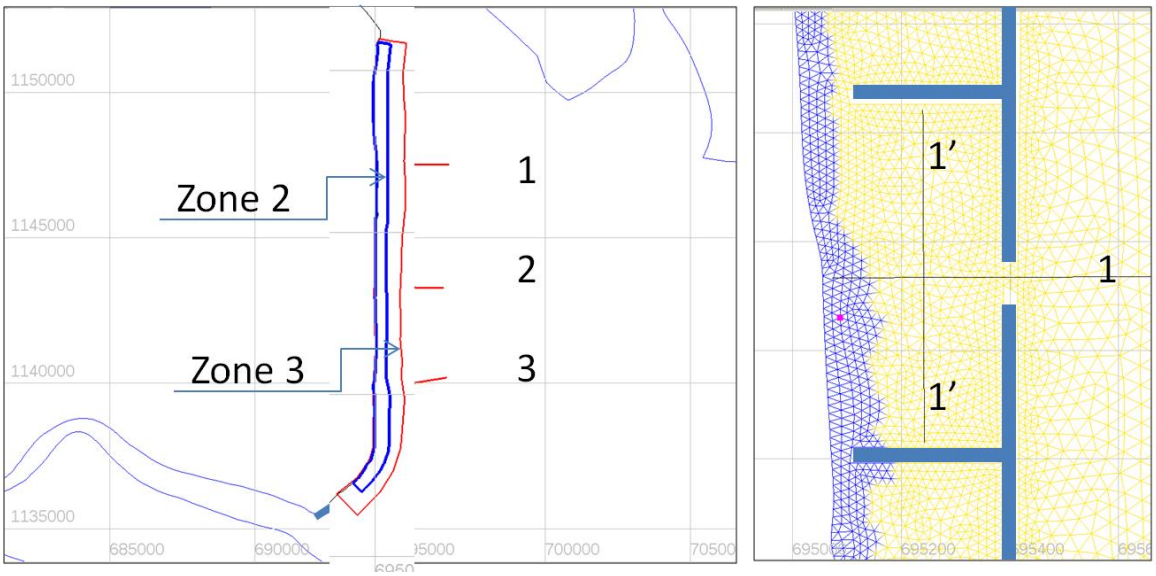

Figure 4-24 Cross-sections, longitudinal sections and zones for erosion and accretion analysis of various protection scenarios

4.1.2.1 T shape breakwater impacts

a) Wave impacts

The significant wave heights are compared of SC01 and SC02 in the NE monsoon month (January 2014) and SW monsoon month (September 2014) and presented in Figure 4-25 and Figure 4-26 respectively. In the plan view we can not see different impacts of different gaps. However, in the cross section (Figure 4-27) and longitudinal sections (Figure 4-28), it is easily to find out the less

the gap the more wave attenuation. That means in term of wave impacts, SC2 (gap=30 m) is better than others.

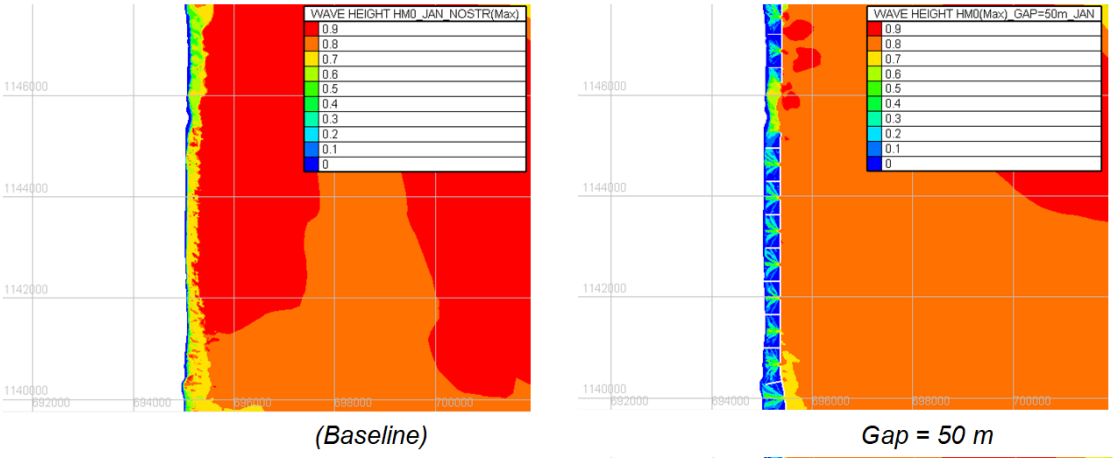

Figure 4-25 Significant wave height in January 2014 for SC1(baseline) and SC3 (Gap=50m) in January 2014

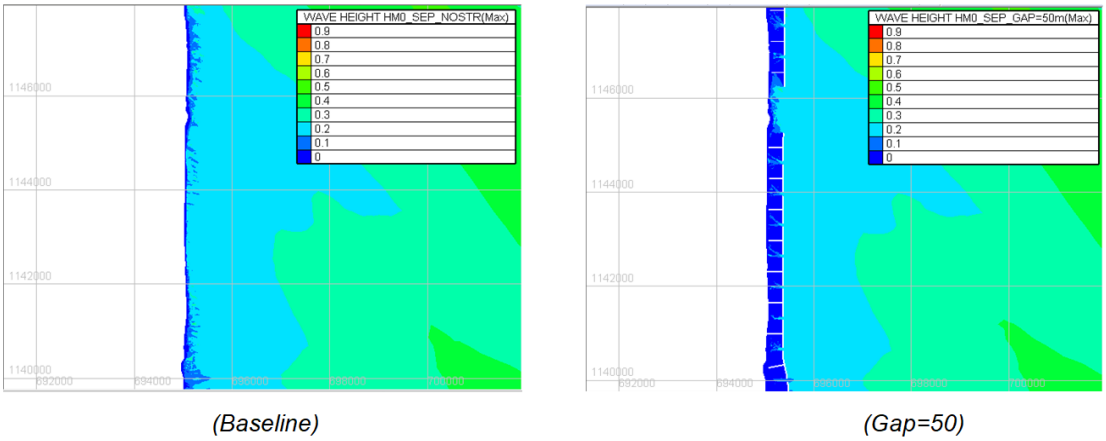

Figure 4-26 Significant wave height in January 2014 for SC1 (baseline) and SC3 (Gap=50m) in September 2014

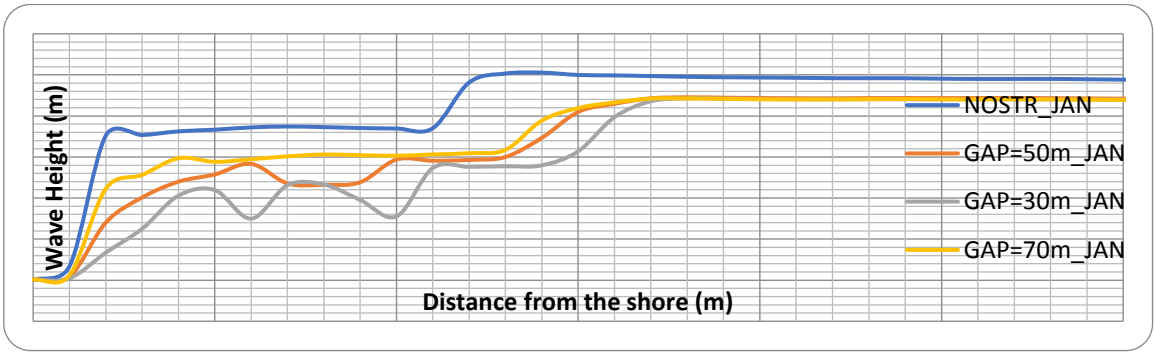

Figure 4-27 Significant wave height at profile 2 in January 2014 for baseline and different gaps

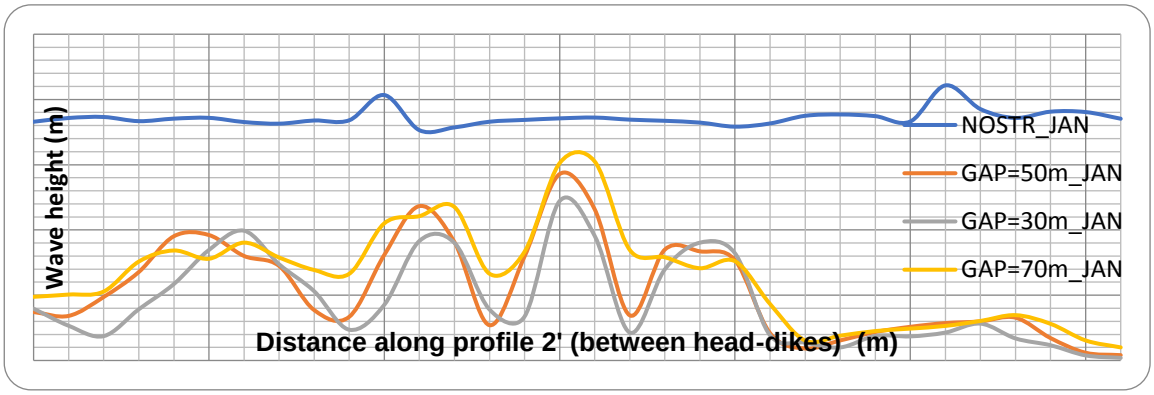

Figure 4-28 Significant wave height at longitudinal section 2' in January 2014 for baseline and different gaps

b) Impact on morphology

The morphological variations are compared of SC01 and SC03 in the NE monsoon month (January 2014) and SW monsoon month (September 2014) and presented in Figure 4-29 and Figure 4-30 respectively. In the plan view we cannot see different impacts of different gaps.

Considering the erosion and accretion in the cross sections, it can be seen that SC04 (gap=70m) is more effective in trapping sediment comparing to others scenarios (see Figure 4-31 and Figure 4-32).

The volumes of erosion and accretion in different areas after NE monsoon month (January 2014) and SW monsoon month (September 2014) presented in Table 4-20 and Table 4-21. Table 4-22 combined the for the two typical months of NE and SW monsoon.

In case of sediment reduction of 75%, the SC04 (Gap=70m) responded better than others (see Table 4-26).

In general, the SC04 (Gap=70m) is the most effective scenario in trapping sediment for the study area.

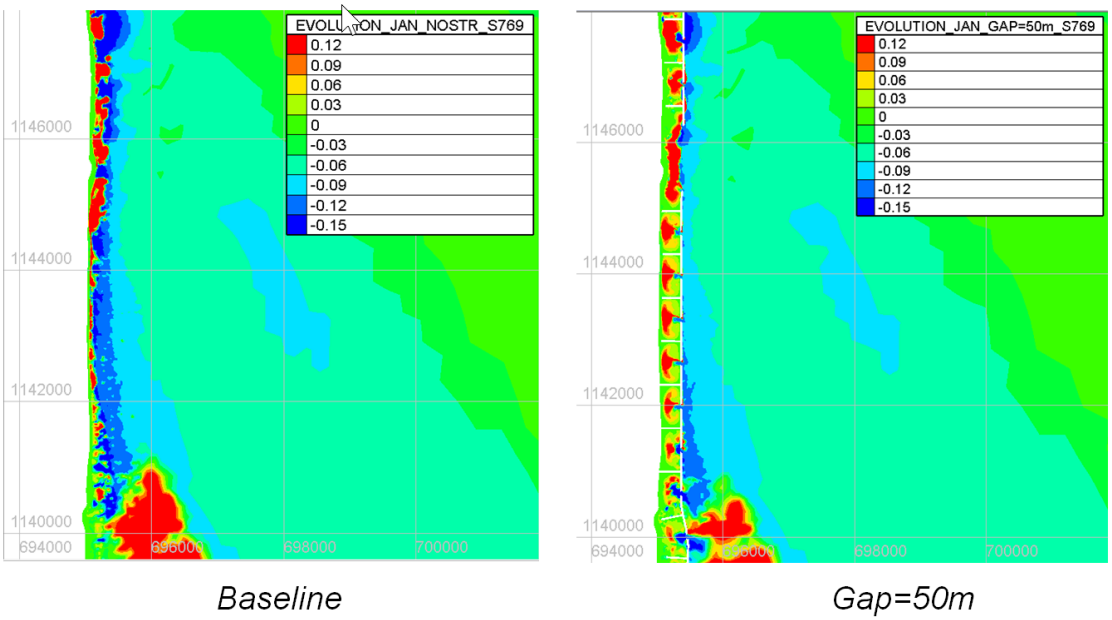

Baseline *Gap=50m*

Figure 4-29 Morphological changes after one month of NE monsoon (1/2014) for SC01 (baseline) and SC03 (Gap=50m)

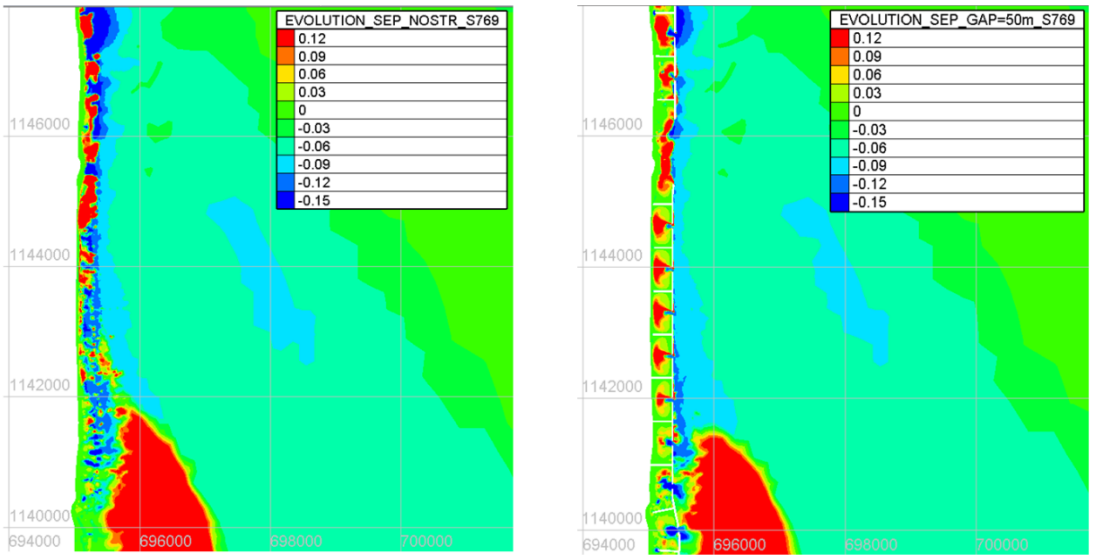

Figure 4-30 Morphological changes after one month of SW monsoon (9/2014) for SC01 (baseline) and SC03 (Gap=50m)

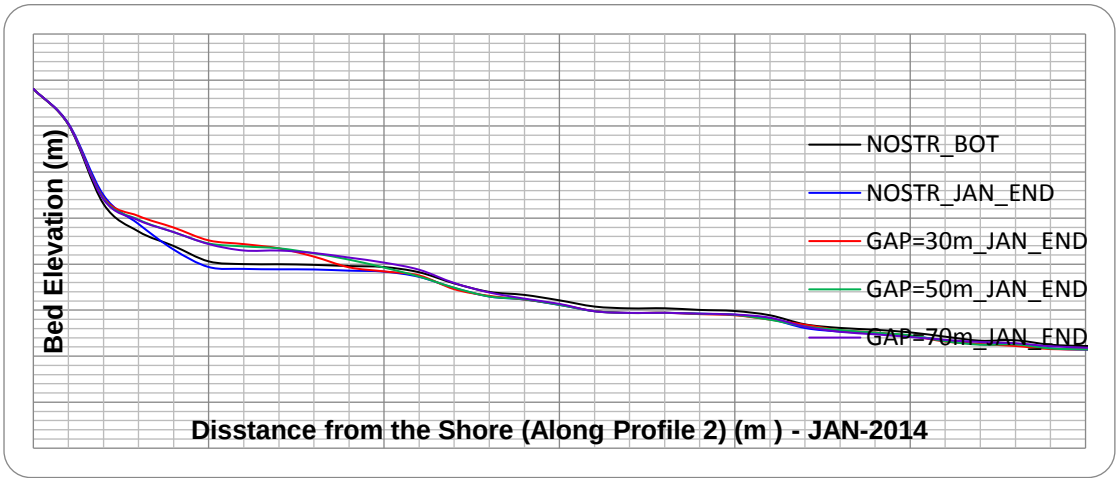

Figure 4-31 Morphological changes at Profile 2 after one month of NE monsoon (1/2014) for baseline and other scenarios

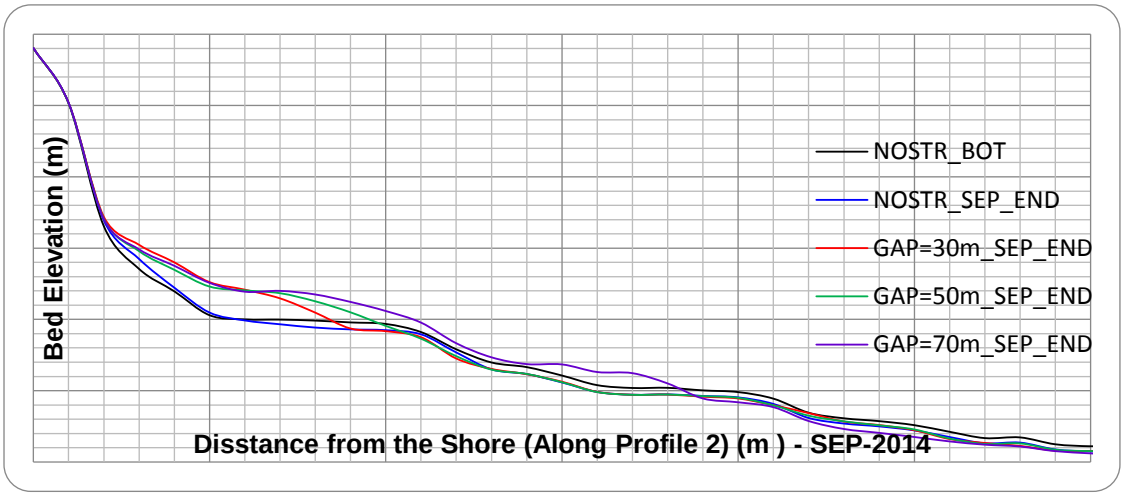

Figure 4-32 Morphological changes at Profile 2 after one month of SW monsoon (9/2014) for baseline and other scenarios

Table 4-20 Trapping sediment volumes of different breakwaters' scenarios in January 2014 (NE monsoon)

	Baseline Scenario		Br.W Gap=30m		Br.W Gap=50m		Br.W Gap=70m	
	Net Volume (m^3)	Accretion Thickness (m)	Net Volume (m^3)	Accretion Thickness (m)	Net Volume (m^3)	Accretion Thickness (m)	Net Volume (m^3)	Accretion Thickness (m)
Zone1	59,844	0.0208	168,656	0.0586	175,099	0.0609	170,419	0.0592
Zone2	(42,696)	-0.0083	302,671	0.0588	299,625	0.0582	298,711	0.058
Zone3	(164,806)	-0.0136	47,937	0.0039	48,285	0.0039	48,654	0.004

Table 4-21 Trapping sediment volumes and thickness of different breakwaters' scenarios in September 2014 (SW monsoon)

	Baseline Scenario		Br.W Gap=30m		Br.W Gap=50m		Br.W Gap=70m	
	Net Volume (m^3)	Accretion Thickness (m)	Net Volume (m^3)	Accretion Thickness (m)	Net Volume (m^3)	Accretion Thickness (m)	Net Volume (m^3)	Accretion Thickness (m)
Zone1	58,284	0.0202	132,083	0.0459	143,768	0.05	149,795	0.0521
Zone2	(23,460)	-0.0045	243,200	0.0472	245,186	0.0476	244,592	0.0475
Zone3	(149,912)	-0.0123	(10,968)	-0.0009	(8,564)	-0.0007	(714)	-0.0001

Table 4-22 Net trapping sediment volumes and thickness of different breakwaters' scenarios for one month in NE (January) and SW (September) monsoon of 2014

	Baseline Scenario		Br.W Gap=30m		Br.W Gap=50m		Br.W Gap=70m	
	Net Volume (m3)	Accretion Thickness (m)	Net Volume (m3)	Accretion Thickness (m)	Net Volume (m3)	Accretion Thickness (m)	Net Volume (m3)	Accretion Thickness (m)
Zone1	118,128	0.0411	300,739	0.1046	318,867	0.1109	320,214	0.1114
Zone2	(66,156)	-0.0129	545,871	0.1061	544,811	0.1059	543,303	0.1056
Zone3	(314,718)	-0.0260	36,969	0.0031	39,721	0.0033	47,940	0.0040

Table 4-23 Net trapping sediment volumes and accretion thickness of different breakwaters' scenarios for one month in NE (January) of 2014 in case of sediment reduction 75%

	Baseline Scenario		Br.W Gap=30m		Br.W Gap=50m		Br.W Gap=70m	
	Net Volume (m^3)	Accretion Thickness (m)	Net Volume (m^3)	Accretion Thickness (m)	Net Volume (m^3)	Accretion Thickness (m)	Net Volume (m^3)	Accretion Thickness (m)
Zone1	-5665	-0.0019	231613	0.0805	271927	0.0945	315938	0.1098
Zone2	-98589	-0.0191	464068	0.0902	467047	0.0907	522371	0.1015
Zone3	-273994	-0.0226	236830	0.0195	239386	0.0197	348961	0.0288

4.1.2.2 Sandbar impacts

a) Wave impacts

The significant wave heights are compared of Baseline, SB2 and SB03 in the NE monsoon month (January 2014) and SW monsoon month (September 2014) and presented in Figure 4-33 and Figure 4-34 respectively. In the plan view we can not see different impacts of different sandbar scenarios. However, in the cross sections (Figure 4-35 and Figure 4-36), it is easily to find out there is not much different of wave attenuation of the two different sandbar widths.

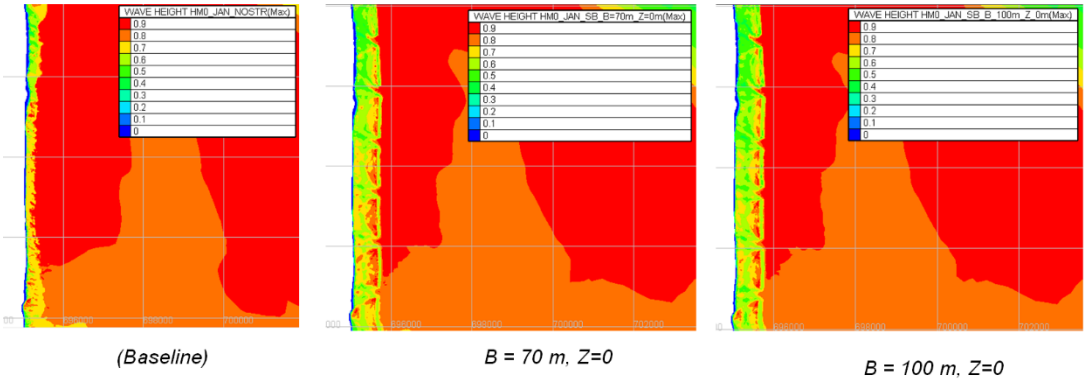

Figure 4-33 Significant wave height in January 2014 for SC1(baseline), SB2 (B=70m) and SB3 (B=100m) in January 2014

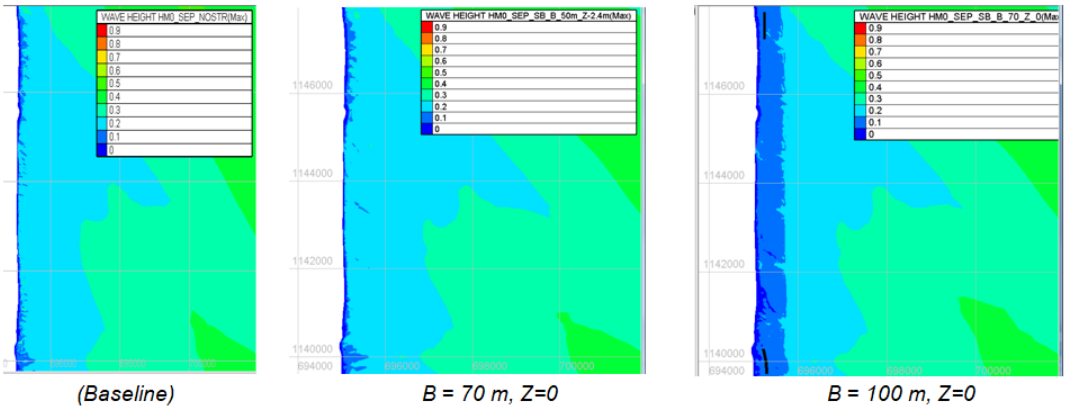

Figure 4-34 Significant wave height in January 2014 for SC1(baseline), SB2 (B=70m) and SB3 (B=100m) in September 2014

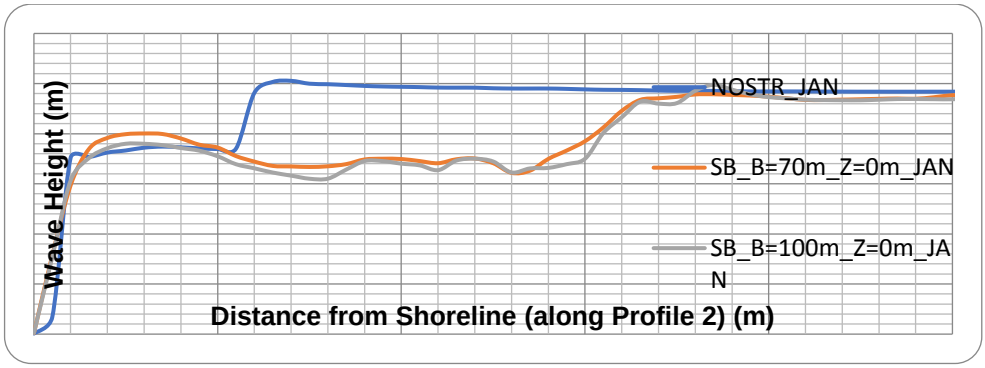

Figure 4-35 Significant wave height at cross section 2 in January 2014 for SB2 and SB3

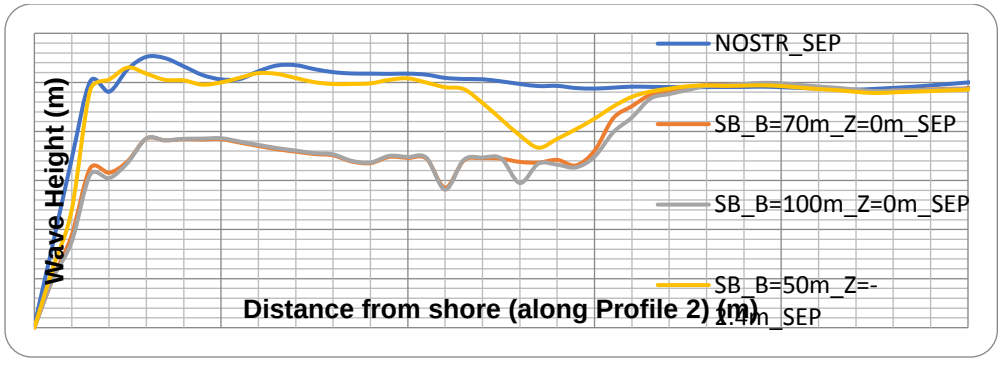

Figure 4-36 Significant wave height at cross section 2 in September 2014 for SB2, SB3 and SB4

b) Calibrate the sandbar deformation in Telemac2d (T2D&TOM&SIS) model

The deformation of sandbars in the physical models were presented the result of physical model test. In this section, numerical sand transport model is set up to calibrate sandbars deformation. Model set up is expressed in Figure 4-40. The smallest grid size is 2.3 m. In general, the deformation rates of the numerical model and physical model were similar. One scenario, for example presented in Table 4-24 and Figure 4-38.

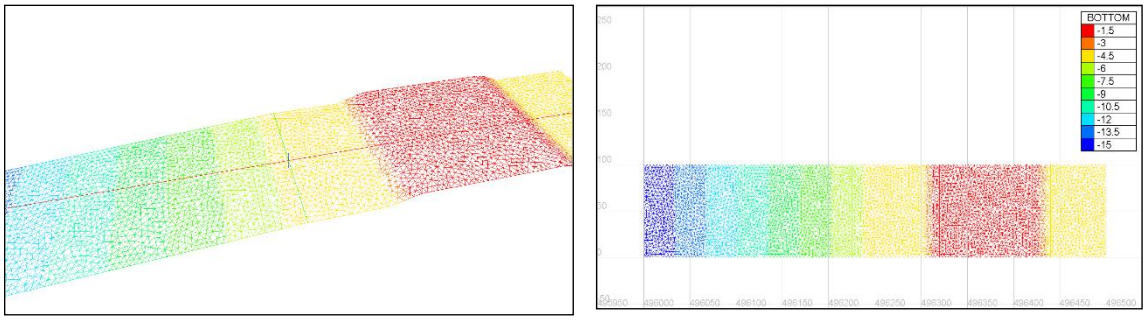

Figure 4-37 Numerical model T2D set up for sandbar deformation calibration

Table 4-24 Typical scenario for T2D model calibrate

Physical Model Scenario	Model					PROTOTYPE				
	B (m)	R_c(m)	Hm0 (m)	Tp (s)	Dur. (min)	B (m)	Rc (m)	Hm0 (m)	Tp (s)	Dur. (s)
WP6-NOU-B7-R10-JSW4	7.0	-0.1	0.14	1.69	141	140	-2.0	2.80	7.56	10.51

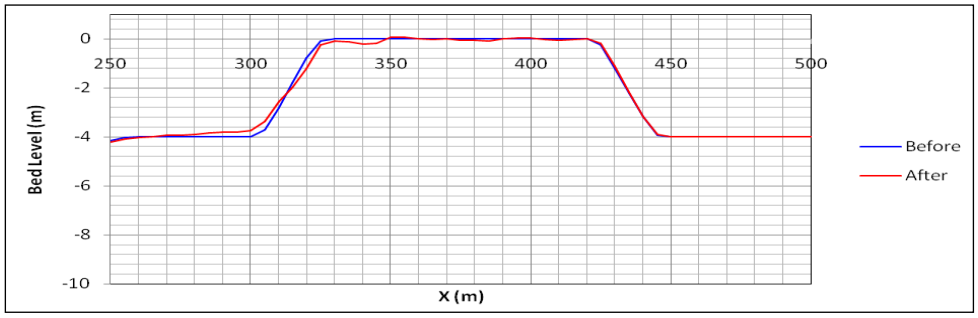

Figure 4-38 Calibration result of T2D with typical scenario WP6-NOU-B7-R10-JSW4

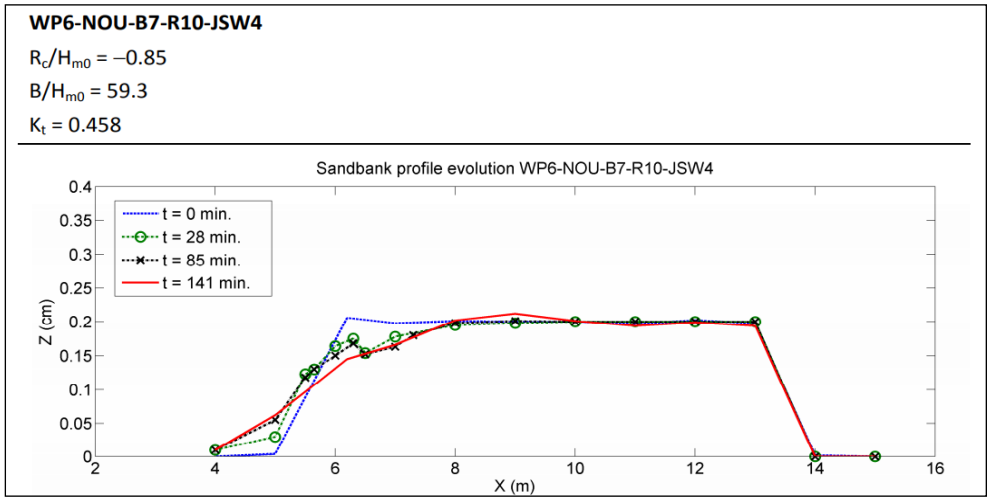

Figure 4-39 Physical Model result of scenario WP6-NOU-B7-R10-JSW4

c) *Morphological impacts of sandbars*

The morphological variations are compared of SC01, SB2 and SB3/SB1 in the NE monsoon month (January 2014) and SW monsoon month (September 2014) and presented in Figure 4-40and Figure 4-41 respectively. In the plan view we cannot see different impacts of different widths of sandbars. However, for the SB1 (B=50 m; Z=-2.4 m), less accretion in the study area can be seen clearly.

The volumes of erosion and accretion in different areas after NE monsoon month (January 2014) and SW monsoon month (September 2014) presented in Table 4-25 and Table 4-26. Table 4-27 combined the for the two typical months of NE and SW monsoon.

In general, the SB1 (B=50m, Z=-2.4 m) has not significant impact in trapping sediment for the study area comparing to SB2 and SB3 (see Table 4-26).

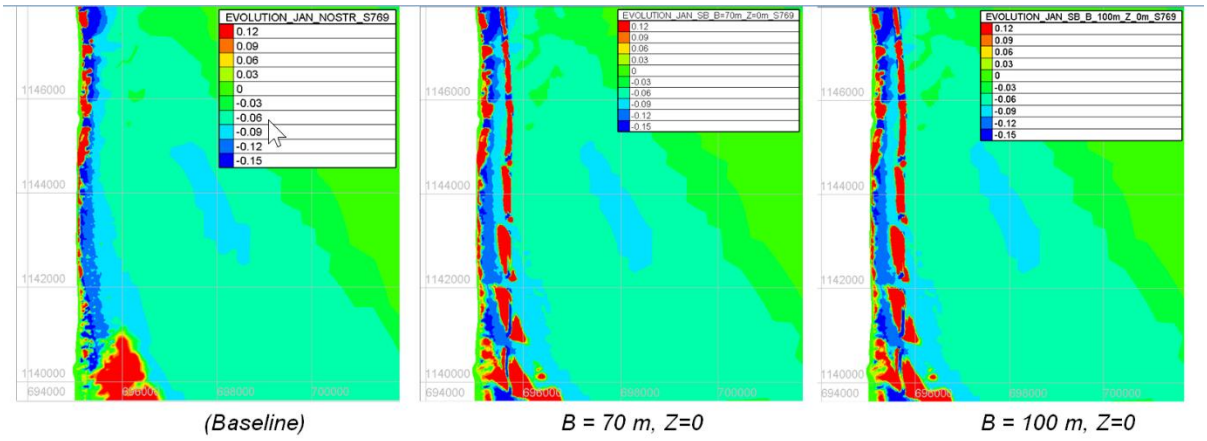

Figure 4-40 Morphological changes in January 2014 for baseline, SB2 (B=70m) and SB3 (B=100m)

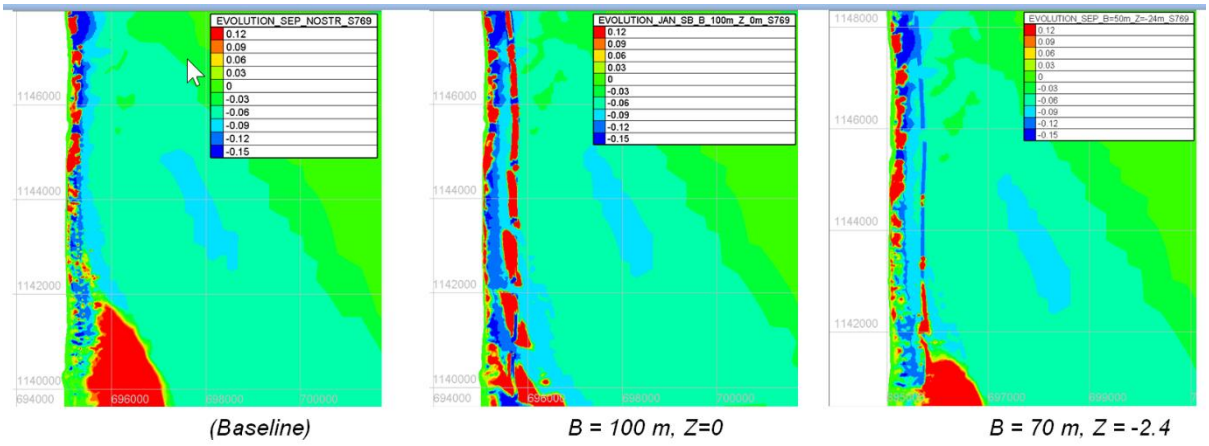

Figure 4-41 Morphological changes in September 2014 for SC1(baseline), SB3 (B=100m) and SB4 (B=70m, -2.4 m)

Table 4-25 Trapping sediment volumes and thickness of different sandbar' scenarios for one month in NE (January) monsoon of 2014

	Baseline Scenario		SB2: B=70m ; Z=0m		SB3: B=100m ; Z=0m	
	Net Volume (m^3)	Accretion Thickness (m)	Net Volume (m^3)	Accretion Thickness (m)	Net Volume (m^3)	Accretion Thickness (m)
Zone1	59,844	0.0208	87,760	0.0305	84,253	0.0293
Zone2	-42,696	-0.0083	30,498	0.0059	25,237	0.0049
Zone3	-164,806	-0.0136	280,104	0.0231	329,485	0.0272

Table 4-26 Trapping sediment volumes and thickness of different sandbar' scenarios for one month in SW (September) monsoon of 2014

	Baseline Scenario		SB1: B=50m ; Z= -2.4m		SB2: B=70m ; Z=0m		SB.3: B=100m ; Z=0m	
	Net Volume (m^3)	Accretion Thickness (m)	Net Volume (m^3)	Accretion Thickness (m)	Net Volume (m^3)	Accretion Thickness (m)	Net Volume (m^3)	Accretion Thickness (m)
Zone1	58,284	0.0203	88,469	0.0308	77,469	0.0269	74,693	0.026
Zone2	-23,460	-0.0045	37,824	0.0074	47,858	0.0093	43,024	0.0083
Zone3	-149,912	-0.0124	-129,525	-0.0107	69,695	0.0058	103,194	0.0085

Table 4-27 Net trapping sediment volumes and thickness of different sandbar' scenarios for one month in NE (January) and SW (September) monsoon of 2014

	Baseline Scenario		SB2: B=70m; Z=0m		SB.3: B=100m; Z=0m	
	Net Volume (m^3)	Accretion Thickness (m)	Net Volume (m^3)	Accretion Thickness (m)	Net Volume (m^3)	Accretion Thickness (m)
Zone1	118,128	0.0411	165,229	0.0575	158,946	0.0553
Zone2	-66,156	-0.0129	78,356	0.0152	68,261	0.0133
Zone3	-314,718	-0.0260-	349,799	0.0289	432,679	0.0358

d) Impacts comparison of the of T shape breakwater and sandbars

By Telemac 2D model, the impact analysis of hard breakwaters and sandbars are expressed in Table 4-28. It is clear that the hard breakwater can effectively trap sediment from the the breakwater onshore area (to the width of 300 m) where sandbars can trap sediment in the larger area (to the width of 1000 m).

Table 4-28 Net trapping sediment volumes and thickness in different area of Go Cong by hard breakwater and sandbars after one month in NE (January) and SW (September) monsoon of 2014

	Baseline Scenario		Br.W Gap=70m		SB2: B=70m ; Z=0m	
	Net Volume (m3)	Accretion Thickness (m)	Net Volume (m3)	Accretion Thickness (m)	Net Volume (m^3)	Accretion Thickness (m)
Zone1	118,128	0.0411	320,214	0.1114	165,229	0.0575
Zone2	-66,156	-0.0129	543,303	0.1056	78,356	0.0152
Zone3	-314,718	-0.0260	47,940	0.0040	349,799	0.0289

4.1.3 Comparison results from MIKE21 and Telemac 2D

Table 4-29 compared the results of MIKE21 and Telemac2D. It showed that the general trend of erosion and accretion is similar for both models. For the breakwater, the accretion impact simulation by Telemac2D is nearly double comparing to MIKE21 but for the sandbar, the accretion impact is half comparing to MIKE21.

Table 4-29 Net trapping sediment volumes and thickness by MIKE21 and Telemac2D in different area of Go Cong by breakwater and sandbars after one month in NE (January) and SW (September) monsoon of 2014

Model	Scenarios	Combined Jan. and Sept. 2014 - Area 300			Combined Jan. and Sept. 2014 - Area 500		
		Net Vol. (Mm3)	Max Ero. THK (m)	Everage THK (m)	Net Vol. (Mm3)	Max Ero. THK (m)	Aver. THK(m)
MIKE21	BASELINE	-0.194		-0.042	-0.214		-0.028
	BW-G70	0.184	-0.615	**0.040**	0.082	-0.615	**0.011**
	SB-B70(0.0)	0.046	-0.194	**0.010**	0.211	-0.194	**0.027**
Telemac2D	BASELINE	-0.066		-0.013	-0.202		-0.024
	BW-G70	0.543	-0.129	**0.106**	0.334	-0.129	**0.039**
	SB-B70(0.0)	0.784	-0.128	0.015	0.121	-0.128	**0.014**

4.2 At Phu Tan, Ca Mau province

4.2.1 MIKE21 models

4.2.1.1 Methodology

With nesting approach, MIKE21 has been calibrated well from the Regional model to Local Model (Figure 4-42) with water levels, discharges, tides, waves and currents, sediment transport and morphology especially the validation results based on the in-situ data of the LMDCZ project in October 2016 and February-March 2017, presented in WP5 Report.

This WP6 Report we discuss the efficiency and impacts of protection measures.

The mesh of the study area model is an unstructured mesh with the triangular element occupying most of the sea area but with the quadrilateral part in most of the rivers (31,702 elements). To assess the impact of the protection measures in the area of Phu Tan, the net areas are divided very smoothly with a grid step of about 10m ÷ 15m (Figure 4-42).

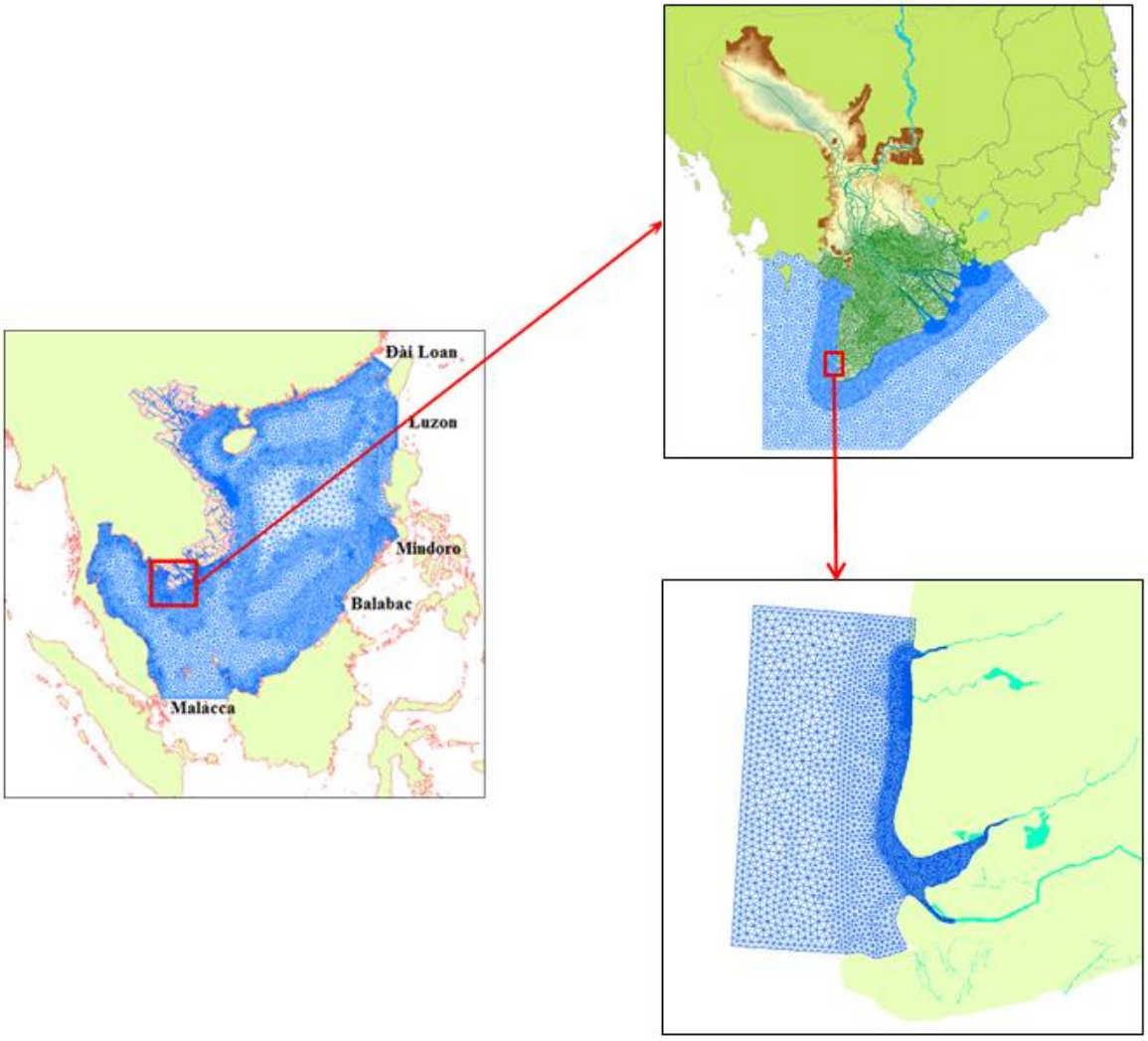

Figure 4-42 Nesting approach for studying protection measure at Phu Tan – Ca Mau

4.2.1.2 Calibration/validation

The model was calibrated/validated with in-situ data in the SW and NE monsoon with water levels, current/flow, waves both of fixed stations (Go Cong and U Minh) and mobile stations as presented in the report of WP6-Report_PhuTan-Mike21.

4.2.1.3 Hard breakwater impacts

a) Breakwater scenarios

The T breakwater and its configuration is presented in Table 4-30 and Figure 4-43. As lesson learned from the Go Cong study area, the different impacts of difference gaps of two breakwaters (Lg) are not much, therefore only KB2 is considered.

Table 4-30 Protection measure configurations

No	SCENARIOS	Senario description	BREAKWATER CONFIGURATION			
			Lengh (Ls) (m)	Distance from shoreline (Y)(m)	Gap between two breakwater (Lg) (m)	Crest elevation of breakwater (m)
1	KB0	Baseline				
2	KB2	Breakwaters	600	300	50	1.1

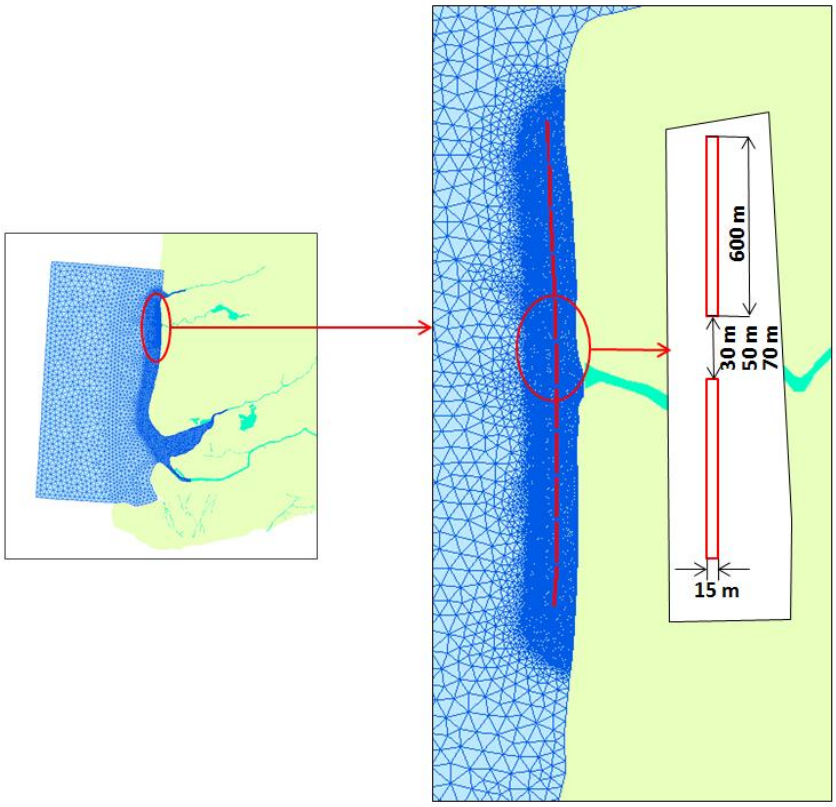

Figure 4-43 Detail meshes and protection measure of T shape breakwaters

b) Impact of breakwater on flows and waves

The beakwaters can reduce flow and wave in the same principle of the effect of breakwaters in Go Cong area and are not presented here (for detail impact of wave and current, refer to the W6_Report_Phu Tan_MIKE_13.1.2018).

c) Impact on morphology

The morphological change in KB0 and KB2 scenarios after 1 month of simulation of the NE monsoon (25/12/2013 ÷ 5/2/2014) and SW monsoon were presented in Figure 4-44 and Figure 4-45. Each month, the single simulation time is 54 hours with one server. Due to time and server number limited (3 of SIWRR and 3 of this project) only one month each monsoon can be simulated. During the NE monsoon, the breakwater impacts are not significant due to low wave as well as low SSC in the area. In the SW monsoon, due to high wave and high SSC, the impact of breakwaters are much more comparing to the NE monsoon.

To study the morphological impact in more detail, an area 1 from the shoreline to 2 km offshore and the length of 7 units of breakwater (length of 4.6 km) is considered the erosion and accretion volumes, maximum erosion depth (at gap site) and average erosion/accretion thickness.

The calculation results of erosion and accretion volume, after 1 month in the NE and SW monsoon are presented in Table 4-31 and Table 4-32 respectively. Table 4-4. Table 4-33 combined the NE and SW monsoon results. It can be seen from Table 4-33 that after 2 months of typical monsoon seasons, the breakwaters can reduce the average erosion depth in the area 1 (from the shoreline to 2 km offshore) from -1.8 cm to -1.1 cm. The breakwater also caused toe's erosion to the maximum of 0.5 m for 2 typical months. From the shoreline to 300 m offshore, the accretion effect is clearly (up to 0.1- 0.2 m).

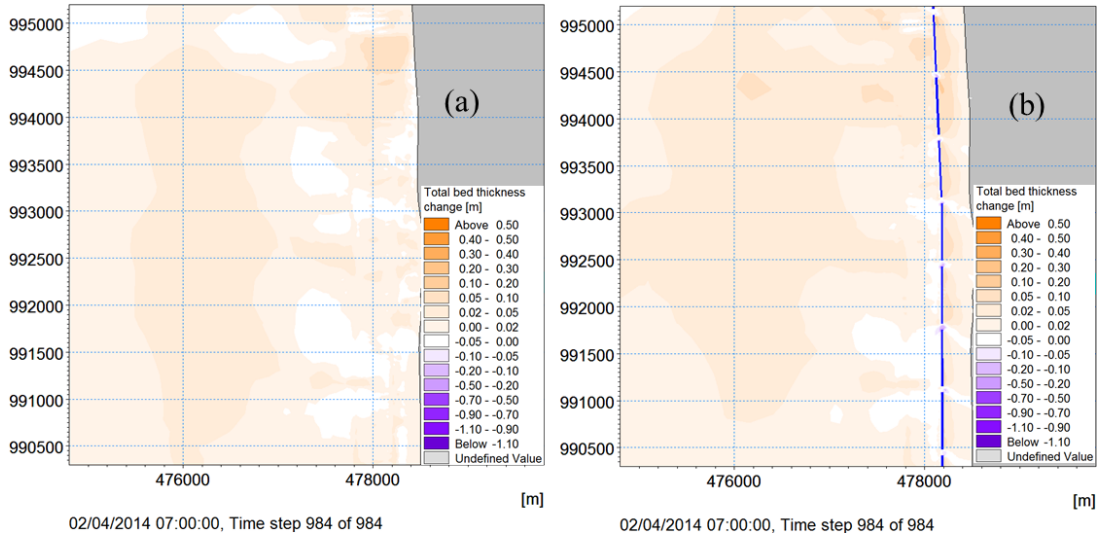

Figure 4-44 Distribution of erosion and accretion after one month of NE monsoon (January 2014)of scenarios (KB0 (a) KB2 (b))

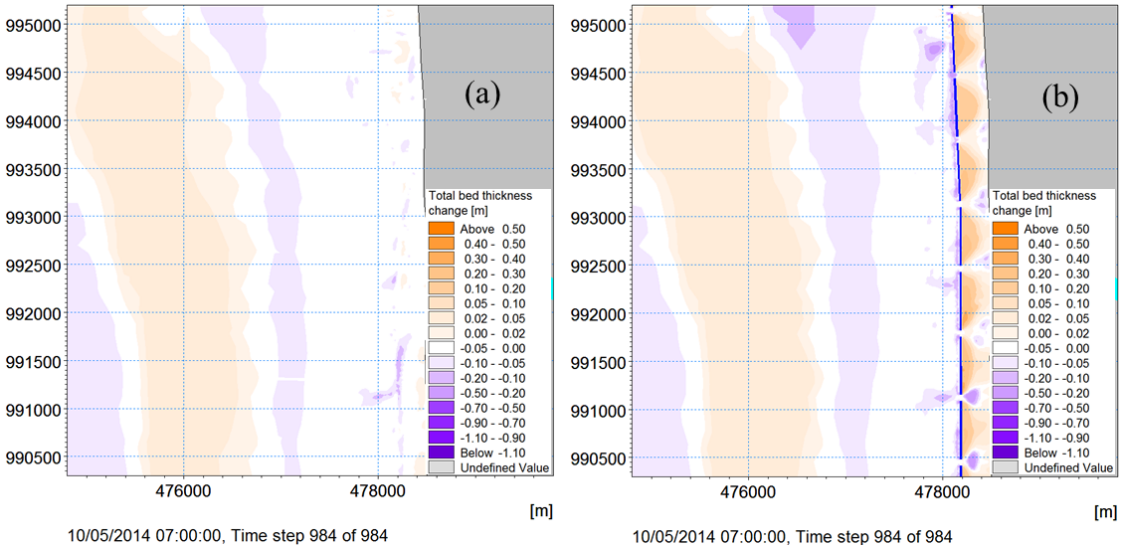

Figure 4-45 Distribution of erosion and accretion after one month of SW monsoon (September 2014) of scenarios (KB0 (a) KB3 (b))

Table 4-31 Total accretion and erosion in study area after one month in the NE monsoon (25/12/2013 ÷ 5/2/2014) of scenarios

January- 2014							
Scenarios	Area 1						
	Vol. (10^6 m3)		Aveg THK (m)		Net Vol. (Mm3)	Max Ero. depth (m)	Average thickness (m)
	Accr.	Ero.	Accr.	Ero.			
KB0	0.1285	-0.0195	0.0138	-0.0021	0.109	-0.062	0.0118
G70(KB3)	0.1728	-0.0165	0.0186	-0.0018	0.156	-0.497	0.0169

Table 4-32 Total accretion and erosion in study area after one month in the SW monsoon (25/8/2014 ÷ 5/10/2014)

September- 2014							
Scenarios	Area 1						
	Vol. (10^6 m3)		Aveg THK (m)		Net Vol. (Mm3)	Max Ero. THK (m)	Average thickness (m)
	Accr.	Ero.	Accr.	Ero.			
KB0	0.0161	-0.2920	0.0017	-0.031	-0.276	-0.289	-0.0298
G70(KB3)	0.1188	-0.3779	0.0128	-0.041	-0.259	-0.500	-0.0279

Table 4-33 Net volume (Mm3) and maximum erosion thickness (m) with various scenarios

Scenarios	Area 1				Combined January and September 2014 of Area 1		
	Jan.2014		Sep.2014		Vol. (Mm3)		Average thickness (m)
	Net Vol. (Mm3)	Max Ero. Thickness (m)	Net Vol. (Mm3)	Max Ero. Thickness (m)	Net Vol. (Mm3)	Max Ero. depth (m)	
KB0 (Baseline)	0.109	-0.062	-0.276	-0.289	-0.167	-0.289	-0.018
G70(KB3)	0.156	-0.497	-0.259	-0.500	-0.103	-0.500	-0.011

4.2.1.4 Sandbar impacts

a) Methodology

The methodology applied here is as the same as in Go Cong. That is due to the MIKE21 model cannot run cohesive and non-cohesive sediment in one scenarios, we treated them in two steps.

The first step we run the model of sand transport assuming that the morphological changes in the vicinity area are negligible, then only the sandbar deformation is considered. Fortunately the deformation of sandbar is not high so that we can go to the second step. Otherwise, the sandbar scenarios are not considered further.

The second step we run the model of mud transport, assuming that the average cross section of the deformation sandbar in the first step are unchanged. That means the sandbars now become "concrete" breakwater when morphological changes are considered the impact of sandbars.

b) Sandbar scenarios

Sandbar scenario was studied as expressed in Table 4-34 and Figure 4-46.

Table 4-34 Sandbar configuration for Phu Tan study area

No	Scenarios	Description	Sandbar configuration/dimensions (m)				
			Length	Distance of 2 units	Distance from shoreline	Width of sandbar	Top elevation
2	KB2	Sandbar at 500 m from the shoreline offshore	1000	200	500	120	0.0
3	KB3	Sandbar at 500 m from the shoreline offshore	1000	200	500	70	0.0

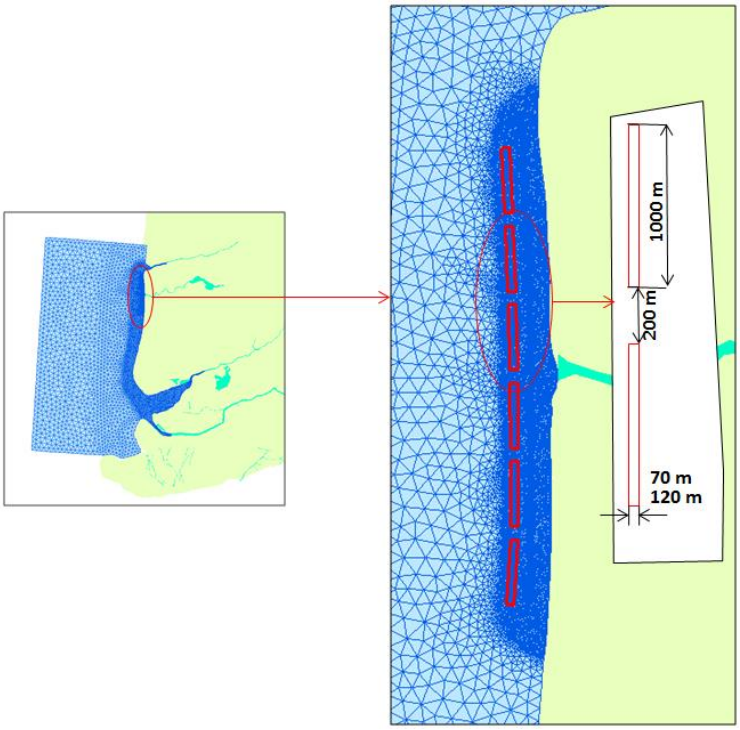

Figure 4-46 Sandbars in the study model at Phu Tan, Ca Mau province

c) *Current impacts*

Figure 4-47 and Figure 4-48 compared flow rose of the baseline and KB2 scenarios. It can be seen due to the sandbar installation, both flow in the NE and SW monsoon are significantly reduced.

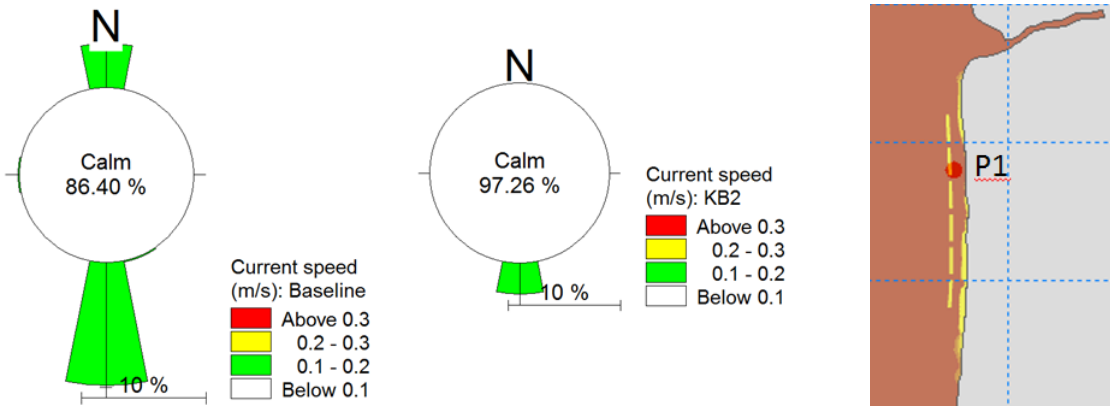

Figure 4-47 Comparison of flow rose at position P1 for baseline and KB2 scenario during NE monsoon (25/12/2013 ÷ 5/2/2014)

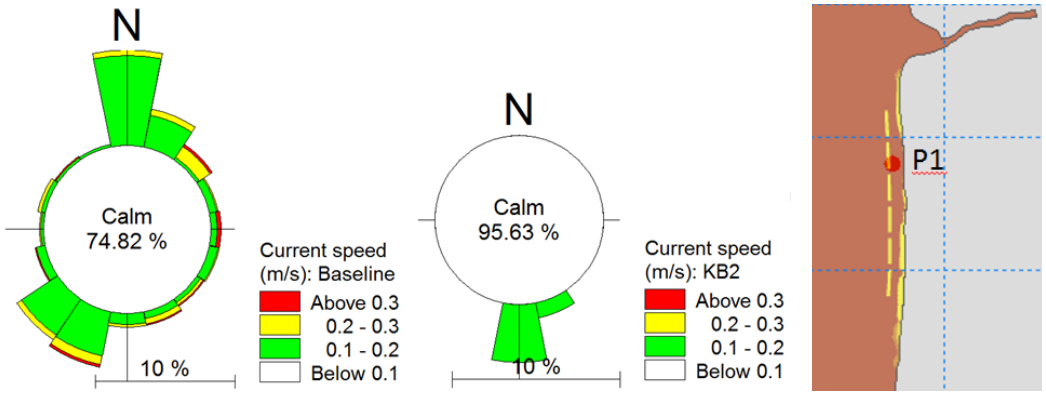

Figure 4-48 Comparison of flow rose at position P1 for baseline and KB2 scenario during SW monsoon (25/8/2014 ÷ 5/10/2014)

d) Wave impacts

Figure 4-49 and Figure 4-50 compared the wave roses of baseline and KB2 scenarios. It can be seen due to the sandbar installation, both wave in the NE and SW monsoon are significantly reduced.

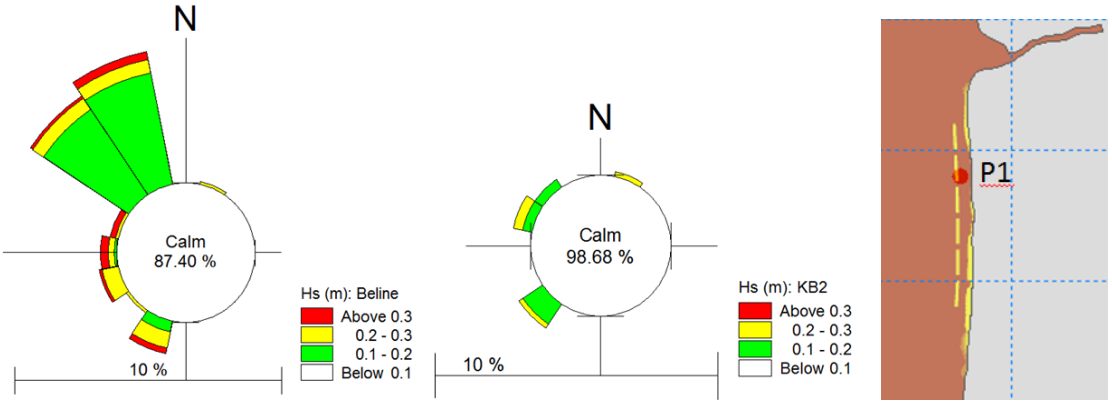

Figure 4-49 Comparison of wave rose at position P1 for baseline and KB2 scenario during NE monsoon

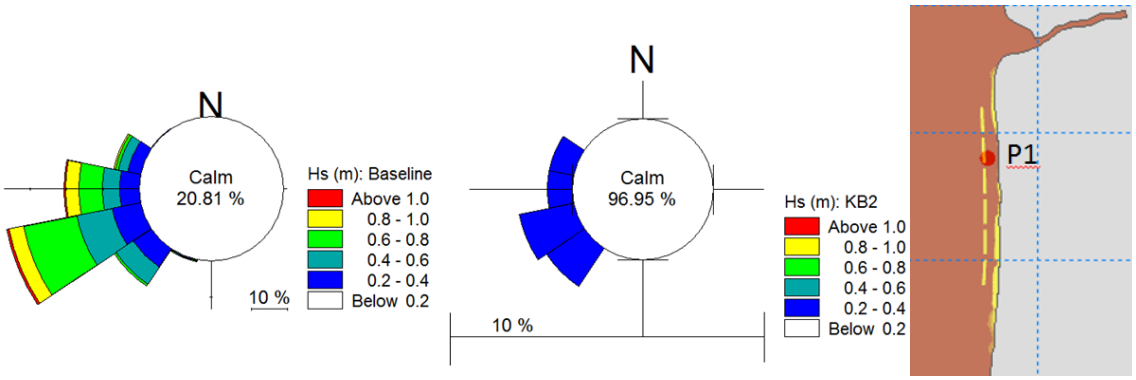

Figure 4-50 Comparison of wave rose at position P1 for baseline and KB2 scenario during SW monsoon

e) Morphological impacts

This section we discuss the morphological changes impact of sandbars where sandbars are considered to be “concrete breakwater” and using MIK21FM-MT (as mentioned in part a)).

Figure 4-51 and Figure 4-52 compared the morphological variation after one month in the NE monsoon (January 2014) and one month in the SW monsoon respectively.

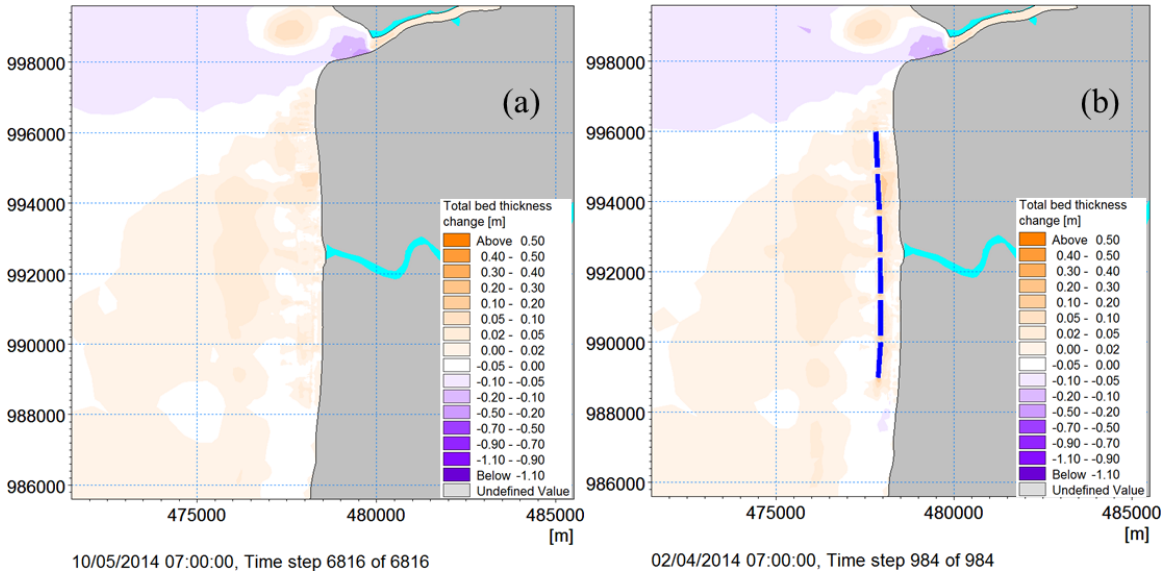

Figure 4-51 Distribution of erosion and accretion after one month of NE monsoon (January 2014) of scenarios (KB0 (a) KB2 (b))

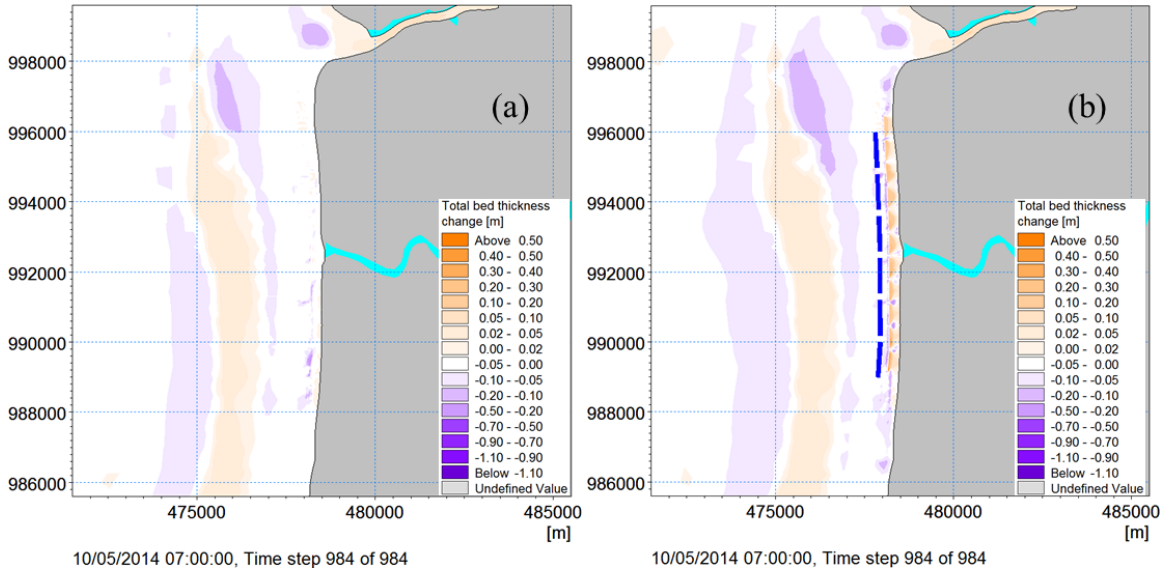

Figure 4-52 Distribution of erosion and accretion after one month of SW monsoon (September 2014) of scenarios (KB0 (a) KB2 (b))

To study the morphological impact in more detail, an area 1 from the shoreline to 2 km offshore and the length of 4 units of sandbars (length of 4.6 km) is considered the erosion and accretion volumes, maximum erosion depth (at gap site) and average erosion/accretion thickness.

Table 4-35 and Table 4-36 showed the impacts of sandbars (B=120m) in NE and SW monsoon.

Table 4-37 combined the NE and SW monsoon results. It can be seen the accretion trend in the NE monsoon and erosion in the SW monsoon (last column of the table). The sandbar (with of 120 m, crest level of 0.0 m) can trap sediment for 2 months in the NE and SW monsoon of the average thickness of about 0.001 m comparing with -0.018 m of non-measure.

Table 4-35 Morphological changes of sandbar impact after one month in the NE monsoon (January 2014)

Jan-2014							
Scenarios	Area 1						
	Vol. (10^6 m3)		Aveg THK (m)		Net Vol. (Mm3)	Max Ero. depth (m)	Average thickness (m)
	Accr.	Ero.	Accr.	Ero.			
KB0	0.128	-0.020	0.014	-0.0021	0.109	-0.062	0.0118
B120(KB2)	0.159	-0.029	0.017	-0.0031	0.130	-0.500	0.0141

Table 4-36 Morphological changes of sandbar impact after one month in the SW monsoon (September 2014)

Sep-2014							
Scenarios	Area 1						
	Vol. (10^6 m3)		Aveg THK (m)		Net Vol. (Mm3)	Max Ero. depth (m)	Average thickness (m)
	Accr.	Ero.	Accr.	Ero.			
KB0	0.0161	-0.2920	0.0017	-0.031	-0.276	-0.289	-0.0298
B120(KB2)	0.109	-0.147	0.0117	-0.016	-0.038	-0.500	-0.0041

Table 4-37 Net volume (Mm3) and maximum erosion thickness (m) with sandbar scenarios

Scenarios	Area 1				Combined January and September 2014 of Area 1		
	Jan.2014		Sep.2014		Vol. (Mm3)		Average thickness (m)
	Net Vol. (Mm3)	Max Ero. Thickness (m)	Net Vol. (Mm3)	Max Ero. Thickness (m)	Net Vol. (Mm3)	Max Ero. depth (m)	
KB0 (Baseline)	0.109	-0.062	-0.276	-0.289	-0.167	-0.289	-0.018
B120(KB2)	0.130	-0.500	-0.038	-0.500	0.091	-0.500	0.001

f) Lost (erosion) volume of sandbar

The losses of sandbar volume due to erosion were simulated and presented in Table 4-38. It can be seen that the lost volume in September 2014 was about 6.2% and in January was about 1%. Since sandbar lost volume happened mostly in the SW monsoon month, a duration of three months (August, September and October) was simulated and the sandbar lost volume for this three months was about 8.3%. The sandbar lost reduced with time was also proved in the physical model test (see the Report of physical Test). The estimation of sandbar lost is about 12-15%/year.

Table 4-38 Sandbar lost (erosion) volume after one month in the SW and NE monsoon and 3 months in the SW monsoon season

Duration	Initial Volume		Lost volume	
	(10^6 m3)	( )		(%)
Sept.	1.243	1 0 0		

2014				
Jan.2014	1.243	100		
Aug., Sept., Oct.2014	1.243	100		

4.2.1.5 Impact comparison of of breakwater and sandbars

Comparing with hard breakwater, the sandbar scenarios are higher effective with the accretion volume of 0.091 Mm3 whereas the hard breakwater can only reduce the erosion volume, from -0.167 Mm3 to -0.103 Mm3 for two typical NE and SW monsoon months of 2014 (see Table 4-39).

Three months in the SW monsoon (August, September and October 2014) were simulated to compare the accretion ability of breakwater and sandbar scenarios (simulation time was about 96 hours each scenario). It showed in Table 4-40 that the sandbar can reduced net erosion volume for 3 months in the SW monsoon from -0.363 Mm3 to -0.233 Mm3 and the positive impact of the sandbar is more than the breakwater.

For detail comparison of breakwater and sandbar scenarios, the accretion volume and average thickness of additional areas from the shoreline to 300 m offshore (Area 300) for breakwater and to 500 m offshore for sandbar (Area 500) were calculated. Table 4-41 showed the impacts for two typical months (NE and SW) and

Table 4-42 showed the impacts for 3 SW monsoon months (August, September and October 2014). Again, in general, the sandbar scenario seems to be better than breakwater in term of trapping sediment in the large area.

Table 4-39 Compare between sandbar and breakwater

Scenarios	Area 1	Combined January and September 2014

	Jan.2014		Sep.2014		Vol. (Mm3)		Average thickness (m)
	Net Vol. (Mm3)	Max Ero. Thickness (m)	Net Vol. (Mm3)	Max Ero. Thickness (m)	Net Vol. (Mm3)	Max Ero. Thickness (m)	
KB0 (Baseline)	0.109	-0.062	-0.276	-0.289	-0.167	-0.289	-0.018
Breakwater G70	0.156	-0.497	-0.259	-0.500	-0.103	-0.500	-0.011
Sandbar B120	0.130	-0.500	-0.038	-0.500	0.091	-0.500	0.001
Sandbar B70	0.128	-0.500	-0.203	-0.500	-0.075	-0.500	-0.008

Table 4-40 Compare between sandbar and breakwater after 3 month in the SW monsoon

Simulation in the SW months (8, 9, 10_2014)							
Scenarios	Area 1						
	Vol. (10^6 m3)		Aveg THK (m)		Net Vol. (Mm3)	Max Ero. Thckness (m)	Avarage thinkness (m)
	Accr.	Ero.	Accr.	Ero.			
KB0 (Baseline)	0.026	-0.389	0.0028	-0.042	-0.363	-0.499	-0.0398
Breakwater G70	0.147	-0.396	0.0159	-0.043	-0.248	-0.532	-0.0269
Sandbar B120	0.238	-0.471	0.0256	-0.051	-0.233	-0.501	-0.0251

Table 4-41 Compare between sandbar and breakwater

Scenarios	Combined Jan. and Sept. 2014 - Area1 (2000)			Combined Jan. and Sept. 2014 - Area 300			Combined Jan. and Sept. 2014 - Area 500		
	Net Vol. (Mm3)	Max Ero. THK (m)	Aver. THK (m)	Net Vol. (Mm3)	Max Ero. THK (m)	Aver. THK (m)	Net Vol. (Mm3)	Max Ero. THK (m)	Aver. THK (m)
BASELINE	-0.167	-0.289	-0.018	-0.013	-0.289	-0.0082	-0.001	-0.289	-0.0004
BASELINE-75%	-0.184	-0.294	-0.020	-0.014	-0.294	-0.0090	-0.024	-0.294	-0.0100
BW-G70	-0.103	-0.500	-0.011	0.121	-0.500	0.0796	0.085	-0.500	0.0357
BW-G70-75%	-0.073	-0.500	-0.008	0.053	-0.500	0.0346	0.064	-0.500	0.0267
SB-B120(0.0)	-0.040	-0.500	-0.004	0.029	-0.175	0.0193	0.214	-0.498	0.0897
SB-B120(0.0)-75%	-0.082	-0.500	-0.009	0.027	-0.175	0.0177	0.099	-0.500	0.0414
SB-B70(0.0)	-0.075	-0.500	-0.008	0.046	-0.175	0.030	0.226	-0.500	0.0940
SB-B70(0.0) -75%	-0.138	-0.500	-0.015	0.040	-0.175	0.026	0.105	-0.500	0.0440

Table 4-42 Compare between sandbar and breakwater

Scenarios	Aug, Sept, Oct. 2014 - Area1 (2000)			Aug, Sept, Oct. 2014 - Area 300			Aug, Sept, Oct. 2014 - Area 500		
	Net Vol. (Mm3)	Max Ero. THK (m)	Aver. THK (m)	Net Vol. (Mm3)	Max Ero. THK (m)	Aver. THK (m)	Net Vol. (Mm3)	Max Ero. THK (m)	Aver. THK (m)
BASELINE	-0.363	-0.499	-0.040	-0.080	-0.499	-0.053	-0.104	-0.499	-0.043
BASELINE-75%									
BW-G70	-0.248	-0.532	-0.027	0.097	-0.500	0.064	0.043	-0.500	0.018
BW-G70 -75%									
SB-B120(0.0)	-0.233	-0.501	-0.025	0.041	-0.364	0.027	0.179	-0.499	0.075
SB-B70(0.0)-75%									

4.2.1.6 Impact comparison of sandbars B=120 and B=70 m

Table 4-43 presented the impact of sandbars of 120 and 70 m width. In the area of 300 and 500 m from the shoreline, sandbars of 70 m width created higher accretion compared to sandbars of 120 width while in the area of 2000 m from the shoreline, the sandbars of 120 m width reduced the erosion volume better than 70 m width. The erosion thickness as a consequence is higher in the sandbar 70 m width scenario.

Table 4-43 Compare the impact of sandbar of widths 120m and 70m (combined Jan. and Sept. 2014)

Scenarios	Combined Jan. and Sept. 2014 - Area1 (2000)			Combined Jan. and Sept. 2014 - Area 300			Combined Jan. and Sept. 2014 - Area 500		
	Net Vol. (Mm3)	Max Ero. THK (m)	Aver. THK (m)	Net Vol. (Mm3)	Max Ero. THK (m)	Aver THK (m)	Net Vol. (Mm3)	Max Ero. THK (m)	Aver THK (m)
KB0	**-0.167**	-0.289	-0.018	-0.013	-0.289	-0.0082	-0.021	-0.289	-0.009
SB-B120(0.0)	**-0.040**	-0.500	-0.004	**0.029**	-0.175	0.0193	**0.214**	-0.498	0.090
SB-B70(0.0)	**-0.075**	-0.500	-0.008	**0.046**	-0.175	0.0303	**0.226**	-0.500	0.094

4.3 Summary the protection impacts at Go Cong and Phu Tan

The impact of different protection measures at Go Cong and Phu Tan are summaried in

Table 4-44 and Table 4-45 respectively.

Table 4-44 Summary the impacts of protection measures at Go Cong

Go Cong simulations	Baseline	Baseline -75% supply	Breakwater	Breakwater -75% supply	Sandbar	Sandbar -75% supply
Jan/Sep 2014 Sedimentation in 2-km coastal area (cm)	0.4	-1.2	**0.8**	-0.6	**1.1**	-0.3
Jan/Sep 2014 accretion inside structure (cm)	**-2.8**	**-3.6**	**4.0**	**3.7**	**2.7**	**1.6**
Comments			Scouring	Scouring	No scouring Small bar deformation	

Table 4-45 Summary the impacts of protection measures at Phu Tan

Phu Tan simulations	Baseline	Breakwater	Sandbar B=120 m	Sandbar B=70 m
Jan/Sep 2014 **Accretion** (cm) in 2-km nearshore area	-1.8	-1.1	-0.4	-0.8
Jan/Sep 2014 Accretion (cm) inside structure area	**-0.9**	**8.0**	**9.0**	**9.4**
Comments		Scouring, Wind contribution to trapping	Sandbar deformation Wind contribution to trapping	

5. Conclusions and Recommendations

- Protection measures have been selected from review of existing solutions applied worldwide and especially in the LMDCZ.

- Field survey have also been carried out to study the Concrete Pile breakwater implemented on the west coast of Ca Mau.
- Physical model tests were conducted for numerical models'calibration.
- Numerical models were validated by the in-situ survey data and results from physical models.
- Protection measures are proposed based on robust results.

Sandbar

For the sandbanks to work convincingly in Go Cong the relative freeboard Rc/Hm0 needs to be closer to -0.5; this means that we probably have to aim for a crest level of mean sea level + 0.0m;

The wider the better for long-term effect. As the deformation in the physical model test was for a relatively short duration, a width of 70 m seems appropriate.

The amount of sand needed in the order of 170 m3/m in the Go Cong area; if applied over the whole length around 2.56 Mm3.

The amount of sand needed in the order of 100 m3/m in the Phu Tan area; if applied over the whole length of 7 km, around 0.700 Mm3.

Porous breakwater

- At Phu Tan, the breakwater is I shape and porous type (see physical model test report) and location is 300 offshore; Length of 600 m; Gap between the two units of 70 m; Crest elevation: +1.10 m. At Phu Tan, the concrete pile breakwater (of Ca Mau) is considered as one option with the condition of it's porousity >= 20% to.
- At Go Cong, T shape breakwater and porous type (see physical model test report) and location is 300 offshore; Length of 600 m; Gap between the two units of 70 m; Crest elevation: +2.20 m;

The protection measure options for both Phu Tan (3 options) and Go Cong (2 options) are expressed in Table 5-1.

Table 5-1 Propose of protection measures at Phu Tan and Go Cong

Site	Options	Protection Measures	Crest level (m)	Width (m)	Y (m) Distance from the shoreline	Length of the unit (m)	Gap between units (m)	Estimation Initial Cost (USD/m)	Damage (%/year)
Phu Tan	1	Sandbars (100 m3/m; L=7km; V= 0.7 Mm3)	0	70	500	1000	200	500	15
		T fences (GIZ type)	Scale of fences is smaller than GIZ's					50	50
	2	Porous breakwaters	1.1	N/A	300	600	70	N/A	N/A
		T fences (GIZ type)	Scale of fences is smaller than GIZ's					50	50
	3	Concrete pile breakwater (CM) - porous >=20%	1.1	N/A	300	600	70	N/A	N/A
		T fences (GIZ type)	Scale of fences is smaller than GIZ's					50	50
Go Cong	1	Sandbars (170 m3/m; L=15.5km; V= 2.56 Mm3)	0	70	500	1000	200	800	20
		T fences (GIZ type)	Scale of fences is smaller than GIZ's					50	50
	2	Porous breakwaters	2.2	N/A	300	600	70	N/A	N/A
		T fences (GIZ type)	Scale of fences is smaller than GIZ's					50	50

Pilot experiment

We strongly recommend to carry out a limited but full-scale pilot experiment, testing both a section with T-groynes at Go Cong and I shape at Phu Tan and one with a sand bank with the total length of 2km each site.

REFERENCES

2. http://www.baobariavungtau.com.vn/khoa-hoc-cong-nghe/201607/cong-trinh-chong-xoi-lo-bo-bien-stabiplage-o-loc-an-bi-hu-hong-689726/index.htm
3. http://baotainguyenmoitruong.vn/moi-truong-va-phat-trien/bien-doi-khi-hau/201607/can-som-khac-phuc-cong-trinh-chong-xoi-lo-bo-bien-loc-an-2719194/
4. Dinh Cong San, Tang Duc Thang, Le Manh Hung (2017) "Existing shoreline, sea dyke, and shore protection works in the Lower Mekong Delta, Vietnam and oriented solutions for stability" International Water Technology Journal (IWTJ), Vol. 7–No.1, March 2017, pp 9-19.
5. Đặng Thị Linh và Thiều Quang Tuấn, 2015. Xây dựng quan hệ chu kỳ và chiều cao của sóng gió cho mùa vùng biển Bắc và Bắc Trung Bộ nước ta. Hội nghị khoa học thường niên năm 2015, Đại học Thủy lợi, Hà Nội, 407 – 409.
6. Monitoring of Shoreline Change Using Remote Sensing (WP3) – SIWRR interim report of LMDCZ project - September 2017
7. Report on the impacts of concrete pile breakwater in Ca Mau Province (WP6) – SIWRR interim report of LMDCZ project -October 2017.
8. Report on 2D laboratory study on protection measures for LMD (WP6), SIWRR interim report of LMDCZ project, July 2017.
9. Thorsten Albers and Nicole von Lieberman (2011). Current and Erosion Modelling Survey, Management of Natural Resources in the Coastal Zone of Soc Trang Province (available at: https://daln.gov.vn/r/files/ICMP-CCCEP/tai_lieu/Document/Soc-trang/2015/2011_Current-and-Erosion-Modelling-Survey-Soc-Trang.pdf)
10. Tuan, T.Q., Tien, N.V. and Verhagen, H.J., 2016. Wave transmission over submerged, smooth and impermeable breakwaters on a gentle and shallow foreshore. In: Proc. 9th PIANC-COPEDEC, pp. 897-905, Rio de Janeiro, BRAZIL.
11. Van der Meer, J. W., Briganti, R., Zanuttigh, B. and Wang, B., 2005. Wave transmission and reflection at low-crested structures: Design formulae, oblique wave attack and spectral change. Coastal Engineering, 52, 915 - 929.
12. Van der Meer, J.W. and Daemen, I.F.R. (1994) Stability and wave transmission at low crested rubble mound structures. Journal of Waterway, Port, Coastal and Ocean Engineering. 1. pp. 1-19.